

**Function of the CD74 receptor
in B cell pro-survival signaling
in the context of chronic lymphocytic leukemia**

In a u g u r a l - D i s s e r t a t i o n

zur

Erlangung des Doktorgrades
der Mathematisch-Naturwissenschaftlichen Fakultät
der Universität zu Köln

vorgelegt von

Romy Barthel

Köln, 2015

Berichterstatter/in: PD Dr. rer. nat. Frank Thomas Wunderlich
Prof. Dr. rer. nat. Thorsten Hoppe
Prof. Dr. med. Michael Hallek

Tag der mündlichen Prüfung: 19.01.2015

Table of contents

ZUSAMMENFASSUNG	1
ABSTRACT	2
1 INTRODUCTION	3
1.1 CHRONIC LYMPHOCYTIC LEUKEMIA.....	3
1.1.1 <i>Epidemiology and Etiology</i>	3
1.1.2 <i>Diagnosis</i>	3
1.1.3 <i>Pathophysiology</i>	4
1.1.4 <i>Therapy</i>	6
1.2 CLL ANIMAL MODELS.....	7
1.2.1 <i>Eμ-TCL1 mice</i>	7
1.3 CD74.....	9
1.3.1 <i>The invariant chain (Ii) part of the MHC class II complex</i>	10
1.3.2 <i>The surface receptor CD74</i>	11
1.3.2.1 CD74 receptor signaling.....	11
1.3.3 <i>CD74 physiology</i>	13
1.3.4 <i>CD74 pathophysiology</i>	14
1.3.4.1 CD74 during <i>Helicobacter pylori</i> infection.....	14
1.3.4.2 CD74 in B cell neoplasia.....	14
1.4 CD74 IN CHRONIC LYMPHOCYTIC LEUKEMIA.....	15
1.5 OBJECTIVE.....	17
2 RESULTS	18
2.1 CD74 EXPRESSION IN E μ -TCL1-TRANSGENIC MICE.....	18
2.2 CD74 IN THE DEVELOPMENT OF TCL1-INDUCED CLL.....	20
2.2.1 <i>Crossbreeding of Eμ-TCL1-transgenic mice with CD74^{ko} mice</i>	20
2.2.2 <i>Leukemia development in TCL1⁺ CD74^{ko} mice</i>	21
2.2.3 <i>BCR genetics in TCL1⁺ CD74^{ko} mice</i>	24
2.3 DISTRIBUTION OF MYELOID LINEAGE CELLS IN THE SPLEEN OF TCL1 ⁺ CD74 ^{ko} MICE.....	25
2.4 IMPACT OF CD74 DELETION ON APOPTOSIS AND PROLIFERATION OF MALIGNANT B CELLS.....	27
2.4.1 <i>Apoptosis of malignant B cells in TCL1⁺ CD74^{ko} mice</i>	27
2.4.2 <i>Proliferation of malignant B cells in TCL1⁺ CD74^{ko} mice</i>	29
2.5 OVERALL SURVIVAL OF TCL1 ⁺ CD74 ^{ko} MICE.....	31
2.6 SYNGENEIC TRANSPLANTATION OF MURINE CLL CELLS INTO CD74 ^{ko} MICE.....	32
2.7 CD74-DEPENDENT REGULATION OF PRO-SURVIVAL PATHWAYS.....	33
2.7.1 <i>Activation of pro-survival pathways in unstimulated murine CLL cells</i>	34
2.7.2 <i>Activation of pro-survival pathways in MIF-stimulated murine CLL cells</i>	35
2.7.3 <i>Signal transduction upon MIF stimulation in human CLL cells</i>	36
2.7.4 <i>CD74 receptor stimulation in murine CLL cells</i>	37
2.7.5 <i>MIF signaling involving CD74 co-receptors CXCR2, CXCR4 and CD44</i>	37

2.7.5.1	CD74 co-receptor expression levels in $TCL1^+$ $CD74^{ko}$ mice	38
2.7.5.2	MIF stimulation of murine CLL cells upon CXCR2- and CXCR4- or CD44 inhibition	39
2.8	B CELL DEVELOPMENT IN $TCL1^+$ $CD74^{ko}$ MICE	41
3	DISCUSSION	45
3.1	CD74 EXPRESSION IS UPREGULATED IN E_{μ} - <i>TCL1</i> -TRANSGENIC MICE	45
3.2	CD74 DELETION DOES NOT INFLUENCE DEVELOPMENT IN <i>TCL1</i> -INDUCED CLL	45
3.3	AKT KINASE ACTIVATION UPON MIF STIMULATION IS CD74-DEPENDENT	47
3.4	<i>TCL1</i> OVEREXPRESSION ALTERS B CELL DEVELOPMENT IN $CD74^{ko}$ MICE	49
3.5	CONCLUSION AND OUTLOOK	51
4	MATERIALS	52
4.1	INSTRUMENTS	52
4.2	CHEMICALS AND REAGENTS	53
4.3	SUBSTANCES	54
4.4	ANTIBODIES	55
4.4.1	<i>Antibodies for Immunoblotting</i>	55
4.4.2	<i>Antibodies for cell culture</i>	56
4.4.3	<i>Antibodies for flow cytometry</i>	56
4.5	MOUSE STRAINS	57
4.6	OLIGONUKLEOTIDES	57
4.7	SPECIAL REAGENTS AND KITS	57
4.8	PRIMARY PATIENT MATERIAL	58
4.9	SOFTWARE	58
5	METHODS	59
5.1	BREEDING	59
5.2	GENOTYPING	59
5.2.1	<i>DNA-Preparation</i>	59
5.2.2	<i>Polymerase-Chain-Reaction (PCR)</i>	59
5.2.3	<i>Agarose gel electrophoresis</i>	61
5.3	BLOOD ANALYSIS	61
5.3.1	<i>Blood sampling</i>	61
5.3.2	<i>Differential blood count</i>	61
5.4	EXTRACTION OF ORGANS	62
5.5	CELL CULTURE	62
5.5.1	<i>Culture conditions</i>	62
5.5.2	<i>Counting</i>	62
5.5.3	<i>Freezing and thawing of cells</i>	62
5.6	ISOLATION OF PRIMARY MURINE CELLS	63
5.6.1	<i>Isolation of primary murine splenocytes</i>	63
5.6.2	<i>Isolation of primary murine B cells</i>	63

5.6.2.1	Positive B cell selection	64
5.6.2.2	Negative B cell selection.....	64
5.7	ISOLATION OF PRIMARY HUMAN CLL CELLS.....	64
5.8	FLOW CYTOMETRY	65
5.8.1	<i>Staining of surface proteins</i>	65
5.8.2	<i>Staining of intracellular proteins</i>	65
5.9	STIMULATION EXPERIMENTS.....	65
5.10	PROTEIN BIOCHEMISTRY	66
5.10.1	<i>Preparation of cell lysates</i>	66
5.10.2	<i>Protein quantification</i>	66
5.10.3	<i>SDS Polyacrylamide gel electrophoresis (PAGE)</i>	67
5.10.4	<i>Protein transfer</i>	68
5.10.5	<i>Immunoblotting</i>	68
5.10.5.1	Detection by chemiluminescence.....	69
5.10.5.2	Detection by fluorescence	70
5.11	SYNGENEIC TRANSPLANTATION OF TCL1-CLL CELLS.....	70
5.12	QUANTIFICATION OF PROLIFERATING CELLS	70
5.13	QUANTIFICATION OF APOPTOSIS.....	71
5.14	IGVH STATUS	71
5.15	IMMUNOHISTOCHEMISTRY	71
	REFERENCES	73
	ABBREVIATIONS	I
	LIST OF FIGURES.....	III
	DANKSAGUNG	IV
	ERKLÄRUNG	V

Zusammenfassung

Das Oberflächenprotein CD74 wird auf der Membran von B-Zellen, Makrophagen und Epithelien exprimiert und kontrolliert viele Bereiche des Immunsystems. Von besonderem Interesse ist die Rezeptorfunktion von CD74 für das Chemokin MIF (macrophage migration inhibitory factor). Bei der Bindung von MIF an CD74 werden - unter anderem über den Korezeptor CD44 - die AKT, MAPK und NF- κ B Signalwege aktiviert, welche die Zellproliferation anregen und die Apoptose hemmen.

Bei vielen Tumorarten, wie z. B. Magenkarzinomen und B-Zell-Lymphomen, wird eine Überexpression von CD74 beobachtet. Die Funktion von CD74 in B-Zell-Lymphomen wurde im Fall der chronischen lymphatischen Leukämie (CLL) veranschaulicht, bei der nicht nur CD74 sondern auch MIF hoch reguliert sind. CLL tritt im hohen Lebensalter auf und ist die häufigste Leukämieform in Europa und Nordamerika. Das Tumormikromilieu spielt eine zentrale Rolle in der CLL und trägt maßgeblich zum Überleben der CLL-Zellen bei. Daher wird bei der Entwicklung von möglichen Therapien ein besonderes Augenmerk auf das Zusammenspiel der CLL-Zellen mit dem Tumormikromilieu gesetzt.

Die Rolle von CD74 in der CLL wurde meist in primären, humanen CLL-Zellen und Zelllinien *in vitro* untersucht ohne das Tumormikromilieu zu berücksichtigen. Um den Einfluss von CD74 auf die B-Zell-Onkogenese im Zusammenspiel mit dem Mikromilieu *in vivo* genauer zu untersuchen, wurden in dieser Arbeit das CLL Mausmodell (E μ -*TCL1*-transgen) mit dem CD74-defizienten Mausmodell gekreuzt. In den dadurch generierten $TCL1^+$ $CD74^{ko}$ Mäusen wurden dann die CLL-Entwicklung sowie die Veränderung der zellulären Signalwege untersucht und mit der Kontrollgruppe $TCL1^+$ $CD74^{wt}$ verglichen.

In $TCL1^+$ $CD74^{ko}$ Mäusen waren die gemessene Tumorlast im Blut, die Infiltration leukämischer Zellen in lymphatischen Organen und das Überleben der Tiere vergleichbar mit dem der Kontrollgruppe. Des Weiteren wurden Proliferation und Apoptose der CLL Zellen nicht von der CD74-Expression beeinflusst. Stimulationsexperimente mit leukämischen Zellen beider Modelle zeigten jedoch, dass die Aktivierung der AKT Kinase durch MIF nur in Gegenwart von CD74 stattfand, während die ERK und NF- κ B Signalwege CD74-unabhängig waren.

Anhand dieser Ergebnisse konnte in dieser Arbeit erstmals gezeigt werden, dass die Deletion von CD74, anders als MIF und CD44, die Entwicklung der CLL im Mausmodell nicht wesentlich beeinflusst. Zusammenfassend lässt sich somit auf eine untergeordnete Rolle der MIF vermittelten CD74 –Signalwege für das Wachstum und die Entwicklung von CLL Zellen schließen.

Abstract

CD74 is a surface protein expressed on B cells, macrophages and many epithelial cells and has been found to control several aspects of the immune system. One of them is its function as surface receptor for the chemokine macrophage migration inhibitory factor (MIF). Signaling through the CD74 receptor and its co-receptor CD44 upon MIF binding leads to activation of the AKT, MAPK and NF- κ B pathways, and thereby promotes cell proliferation and survival.

Elevated expression of CD74 has been observed in several human cancers e.g. gastric carcinoma and B cell neoplasia. The role of CD74 in B cell neoplasms has been suggested in the case of chronic lymphocytic leukemia (CLL), where both the receptor CD74 and its ligand MIF are upregulated. CLL is one of the most common leukemias found in adults in Europe and North America. The microenvironment plays a central role to CLL development and progression.

So far, studies on the role of CD74 in CLL were based on experiments with primary CLL cells or cell lines *in vitro*. However, the exact contribution of CD74 to the pathogenesis of CLL remained far from being understood.

To understand the role of CD74 for the pathogenesis of leukemia, this project aimed to determine the influence of the CD74 receptor during B cell lymphomagenesis and the mechanisms underlying CD74-dependent signaling in B cells by using the CLL mouse model (E μ -*TCL1*-transgenic). E μ -*TCL1* transgenic mice pro- and deficient for CD74 (TCL1⁺ CD74^{wt} and TCL1⁺ CD74^{ko}) were generated and monitored for CLL development and activation of pro-survival signaling upon MIF stimulation.

CLL development in TCL1⁺ CD74^{ko} mice was similar to control TCL1⁺ CD74^{wt} mice depicted by comparable growth of the leukemic load, development of hepatosplenomegaly and overall survival. Moreover, the apoptosis and proliferation rate of malignant cells from TCL1⁺ CD74^{ko} mice were similar to control mice. Experiments with MIF stimulation in CLL cells showed that MIF induced AKT activation in a CD74 dependent manner, whereas ERK and NF- κ B activation did not differ between TCL1⁺ CD74^{wt} and TCL1⁺ CD74^{ko} cells.

Taken together this study showed that targeted gene deletion of *Cd74* does not influence the development of CLL in E μ -*TCL1*-transgenic mice and suggested that the pathways mediated by MIF through CD74 are not sufficiently potent to promote growth of CLL cells.

1 Introduction

1.1 Chronic Lymphocytic Leukemia

Chronic lymphocytic leukemia (CLL) is one of the most common leukemias in Europe and North America. It mostly affects older individuals with an median age of 65 to 70 years and rarely under 50 years of age, with men being twice as often affected as women [1, 2]. The World Health Organization describes CLL as leukemic, lymphocytic lymphoma distinguishable from small lymphocytic leukemia (SLL) by its leukemic appearance [3]. Like other cancers, CLL is caused by genomic damage that alters distinct signaling pathways in B cells which leads to the induction of anti-apoptotic proteins and the downregulation of pro-apoptotic proteins [4]. Dysregulated expression and signaling of these cell death regulators then leads to a progressive accumulation of long-lived and apoptosis-resistant B cells in the peripheral blood, bone marrow and secondary lymphoid tissues [1].

1.1.1 Epidemiology and Etiology

The incidence of CLL lies at 3/100.000/year and varies with age and sex structure of the population [4, 5]. Rates of CLL in the population show also significant international variation, with the highest rates in the U.S. and Europe and the lowest rates in Asia [6]. The cause for CLL is still unsure. Large, population-based case-control and cohort studies have shown significant familial aggregation of CLL with first degree relatives being three times more likely to have CLL or other lymphoid neoplasms than the general population [6-8]. While there is evidence for a genetic disposition for CLL, attempts to link genetic aberrations to CLL have been unsuccessful [6]. Additionally, linking CLL incidences with environmental exposure to radiation or other chemicals showed no consistent evidence so far [4]. On the other hand, induction through viral infection, e.g. Epstein- Barr-Virus (EBV) and Merkel cell polyomavirus (MCPyV), is often discussed [9], but could not be proven so far [10].

1.1.2 Diagnosis

The World Health Organization and the guidelines from the international workshop on CLL defined a count of more than 5×10^9 monoclonal CD5-positive B cells per litre blood, which is consistent for more than 3 months, as a safe diagnosis for CLL [11]. To differentiate CLL cells from other B cell lymphomas, cell surface marker are used

which characterize the CLL cell phenotype. In flow cytometric analyses CLL cells are simultaneously positive for the surface marker CD19, low levels of CD20, CD23 and aberrant CD5 [12]. Often CLL is found during routine checkup, since many patients do not develop any symptoms [13]. Typical symptoms of CLL are lymphocytosis leading to enlargement of lymphoid organs (e.g. spleen and liver) and the swelling of lymph nodes, weight loss, abdominal pain, night sweat, susceptibility to infection and 30% of patients develop skin irritation. At a later stage defective haematopoiesis leads to anemia resulting in fatigue and weakness, while thrombocytopenia leads to bleeding [14]. Rai and colleagues developed a system of clinical staging CLL that could prospectively distinguish patients according to their overall outlook for survival [15-17]. Later Binet and colleagues added another prognostic classification [18]. Both methods of staging are recognized as simple, yet accurate predictors of survival and are still used in a modified version to group patients with CLL based on physical examination and complete blood counts [3, 11, 19].

In the last years molecular and cellular markers have been identified that also could predict disease progression. Especially the mutational profile of the immunoglobulin genes, cytogenetic abnormalities, serum-based markers like β 2-microglobulin and cellular marker like CD38 and ZAP-70 show strong prognostic value [4, 20].

1.1.3 Pathophysiology

One hallmark of CLL cells is the expression of the B cell receptor (BCR) [21]. The BCR is expressed on the plasma membrane of B cells as a disulfide-bonded complex of heavy and light immunoglobulin (Ig) chains associated with the $Ig\alpha$ and $Ig\beta$ (or CD79a/CD79b) heterodimer. The BCR is the key molecule for the signaling pathway involved in B cell proliferation, survival, differentiation, anergy and apoptosis [22]. The Ig component of the BCR has a unique molecular feature, which marks CLL cells and determines the indolent or aggressive nature of the disease. In this context CLL can be divided into two main subsets, based on whether the tumor arose from a B cell prior to initiation of somatic hypermutation in the Ig variable (V) region genes (unmutated CLL), or after this process had taken place and then stopped (mutated CLL) [23]. The unmutated cases show an aggressive disease progression which is often accompanied by high ZAP-70 expression, while mutated cases show a more indolent form with low ZAP-70 expression [24]. Furthermore, conventional cytogenetic analyses and fluorescent *in situ* hybridization (FISH) showed genetic aberrations in ~82% of CLL cases [25]. Among those aberrations, four are quite commonly found, del(17q13),

del(11q23), del(13q14) and trisomy 12 [20]. The 17p deletion (del17p) affects the tumor suppressor p53 protein and is associated with a poor prognosis [26], as well as the 11q deletion (del11q), which is mostly accompanied by a mutation in the ATM kinase leading to impaired DNA damage response in the cells [27, 28]. Deletion of 13q (del13q) is associated with a better prognosis and leads to the loss of the microRNA's miR15 and miR16 [29], which target the anti-apoptotic protein BCL-2 [30]. Despite the heterogeneity in the disease, CLL patients show a common gene expression signature differentiating them from other lymphoid cancers, which led to the conclusion that CLL patients share a common mechanism of transformation or cell of origin [31, 32]. Recently, studies were linking unmutated CLL to unmutated mature CD5-positive B cells and mutated CLL to a distinct CD5- and CD27-positive post-germinal center B cell subset [33].

Another hallmark of CLL is the accumulation of mature B cells that escape programmed cell death and undergo cell cycle arrest in the G0/G1 phase [34]. In accordance, CLL cells show a low proliferation rate and overexpression of the anti-apoptotic proteins of the BCL-2 family (BCL-XL, BAG1, MCL-1) while the pro-apoptotic proteins (BAX, BCL-XS) are under expressed [35]. Despite their apparent longevity *in vivo*, culturing of CLL cells *in vitro* results in spontaneous apoptosis, indicating a supporting role for the microenvironment in CLL cell survival [36]. Interestingly, first studies in the microenvironment of CLL revealed pseudo follicles and cell clusters in lymph nodes and the bone marrow. Those clusters consist of increased numbers of CD4-positive T cells and CLL cells. CD4-positive T cells express the CD40 ligand, which stimulates B cells and induces expression of anti-apoptotic proteins [37, 38]. T cells also secrete anti-apoptotic cytokines like Interleukine 4 (IL-4) providing further stimulus for B cells [39]. In fact, stimulation with CD40 ligand and IL-4 prevented CLL cells from apoptosis *in vitro* [37]. In addition stromal cells, nurse like cells and follicular dendritic cells are found in the microenvironment of CLL cells. Nurse like cells differentiate from CD14-positive monocytes through the interaction with CLL cells, which in turn protect CLL cells from apoptosis mediated through the production of B cell-activating factor of the TNF family (BAFF), the proliferation-inducing ligand (APRIL) [40] and the secretion of stromal-derived factor 1 (SDF-1) [41, 42]. Bone marrow derived stromal cells and follicular dendritic cells also provide a complex system of survival signals for CLL cells. For one they express integrins

interacting with CLL cells and secondly secrete cytokines like SDF-1 and VEGF (vascular endothelial growth factor) to further enhance CLL survival [43].

Another cytokine playing an important role in the maintenance of the CLL clone is the macrophage migration inhibitory factor (MIF). MIF is a proinflammatory and immunoregulatory cytokine ubiquitously expressed in cells of the mammalian system and has been shown to promote CLL development [44]. On B cells MIF binds to the surface receptors CD74, CXCR2 and CXCR4 and thereby stimulates pro-survival signaling. In CLL it has been shown that binding of MIF to the receptor CD74 leads to the production of Interleukin 8 (IL-8) and the upregulation of the anti-apoptotic protein BCL-2, which in turn promote CLL cell survival [45, 46] (this aspect will be further discussed under 1.4).

Taken together, CLL cells actively shape their microenvironment by producing cytokines and chemokines, and by subverting normal accessory cells to promote leukemia-cell survival, proliferation, and escape from immune surveillance [43].

1.1.4 Therapy

Chronic lymphocytic leukemia is a disease which is not curable. The only curative approach is allogeneic stem cell transplantation, which has a high lethality rate of 25% and therefore is only used on high-risk patient with good fitness [11, 47]. The management of CLL has changed a lot in the last decades due to a better understanding of the biology of the disease and the approval of new drugs. Treatment is chosen depending on the clinical stage of the disease, cytogenetics, patients fitness and treatment situation [48]. In 2008 the international workshop on CLL updated guidelines for the management of CLL [11]. Patients in clinical Binet stage A and B without active symptomatic disease are not treated but controlled after the “watch and wait”-principle. First-line treatment for patients in higher stages involves chemotherapy with differing regimes depending on the patient fitness. Patients with a 17p deletion have a very poor prognosis and often show resistance to chemotherapy [49]. First-line treatment for these high-risk patients so far were the purine analog Alemtuzumab in combination with steroids [50]. Since most patients eventually relapse alternative treatments within clinical trials are suggested [48]. Recently several novel drugs targeting kinases involved in the pro-survival signaling of B cells have been approved by regulatory agencies or are under evaluation. Among them being the BTK inhibitor Ibrutinib [51], the PI3K δ inhibitor Idealisib (GS1101) [52], which showed promising results in

refractory patients. This recent advances show the importance to dissect and understand the biology of the disease to provide the right approach to treat the disease.

1.2 CLL animal models

Mouse models recapitulating human malignancies are valuable tools for pre-clinical studies and to study pathological mechanisms. Several mouse models for CLL have been generated either through mimicking genetic aberrations, deregulated gene expression in CLL or driven by ectopic oncogene expression (reviewed in [53]).

The first mouse resembling human CLL was the E μ -*TCL1*-transgenic mouse generated in 2002 by Bichi and colleagues [54]. Since then several transgenic mice have been created that also lead to CLL-like disease. One of them is the APRIL-transgenic mouse, which resembles the elevated levels of the tumor necrosis factor (TNF) family member APRIL found in sera of CLL patients. At 9- to 12-month-old APRIL transgenic mice develop lymphoid tumors that originate from expansion of the peritoneal B-1 B cell population [55]. Another model is the BCL-2 \times traf2dn double transgenic mouse, studying the influence of both these molecules in CLL pathogenesis [56]. Both BCL-2 and the TNF-associated factor 2 (TRAF2) have been implicated in mediating CLL cell survival [35, 57]. The single BCL-2 or TRAF2 mutant mice develop lymphadenopathy and splenomegaly with age due to lymphoid cell expansion but only the BCL-2 \times traf2dn double transgenic mice develop an age-dependent B cell leukemia resembling human CLL [56]. Next to those, mice mimicking the deletion of 13q14 (e.g. *mir-15/16-1*^{-/-} and 14qC3 *minimal deleted region* (MDR)^{-/-} mice), the most frequent genetic lesion found in CLL [29], also develop CLL-like disease and provide evidence for the tumor suppressor function of a CLL-associated genetic lesion [58].

The most notable difference between those mouse models is the penetrance of the phenotype which is highest in the E μ -TCL1 mice (~100%), intermediate in 14qC3 MDR knock-out and APRIL-transgenic mice (40-50%) and lowest in the *mir-15/16-1* knock out mice [53]. Due to the complete disease penetrance and the similarities in the developed disease to human CLL, E μ -*TCL1* mice have become the most commonly used model in CLL research.

1.2.1 E μ -*TCL1* mice

TCL1 is a proto-oncogene highly expressed in most B cell and T cell tumors, e.g. CLL and T-PLL [59, 60]. Under physiological conditions *TCL1* is expressed during B cell development in pre-B cells, antigen-naïve IgM-positive, mantle zone and germinal

centre B cells [61, 62], and during T cell development in early T cells before the T cell receptor is expressed [63].

In CLL, *TCL1* expression correlates with aggressive clinical progression and the phenotypic features like unmutated *IgV_H* and *ZAP-70* expression [59]. In 2002, Bichi and colleagues used the human *TCL1* gene to establish a CLL mouse model. For that, a 350 bp sequence of the human *TCL1* gene was put under the control of the murine *IgV_H* promoter and the *E_μ* enhancer to ensure expression in immature and mature B cells. These mice spontaneously develop B cell hyperplasia first evident in the peritoneal cavity (~ 2 months) and later in the lymph nodes, spleen, bone marrow and blood (~ 3-8 months). Later at around 8-12 months these mice develop a CLL-like disease with an accumulation of CD5-positive B cells in the spleen, liver and lymph nodes [54]. Furthermore, the BCRs of *E_μ-TCL1*-transgenic mice resemble those from human CLL patients with the more aggressive form of the disease (unmutated *IgV_H* gene rearrangements) and exhibited stereotype in *IGHV*, *IGKV* and *IGLV* gene rearrangements [64]. Since its development, the *E_μ-TCL1*-transgenic mouse has been used by many laboratories to elucidate the functional role of specific molecules in the onset and progression of CLL in vivo (overview in Figure 1), providing new insights into the pathogenic role of those genes in the dysregulation of signaling, proliferation, and apoptosis, and in the aberrant cross-talk with the microenvironment [53].

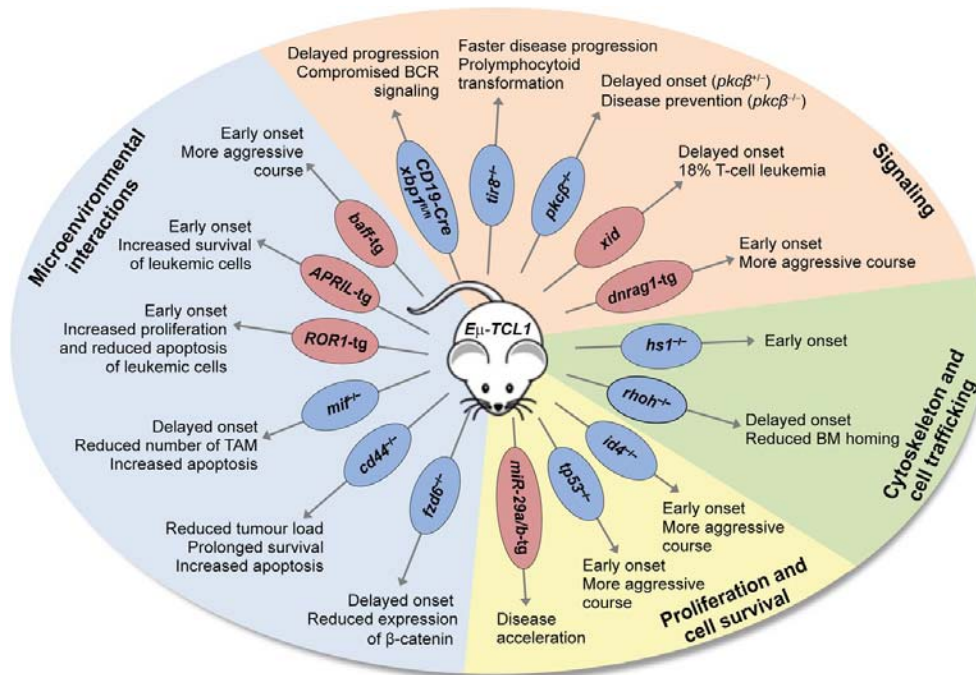


Figure 1: Study of novel pathogenic mechanisms in the *E_μ-TCL1*-transgenic mouse model
Deletion or overexpression (tg: transgenic) of molecules in the *E_μ-TCL1*-transgenic mouse model affecting disease phenotype. (bm: bone marrow; TAM: tumor associated macrophages) (from [53])

Functionally, TCL1 interacts with the protein kinase B (AKT) mediated by the PH domain of AKT. The interaction enhances the kinase activity and promotes the nuclear translocation of the AKT kinase, leading to the transduction of anti-apoptotic and proliferative signals [65]. However, the effects of TCL1 on AKT are not sufficient to explain TCL1 oncogenesis in E μ -*TCL1*-transgenic mice, since AKT activation itself does not cause B cell neoplasia [66, 67]. Studies on different transgenic mouse models (e.g. APRIL) showed the importance of the NF- κ B pathway in the development of a CLL-like disease suggesting a role of the NF- κ B pathway in the pathogenesis of CLL [68]. Interestingly, there are studies showing that TCL1 enhances NF- κ B activation independent of AKT through direct interaction with I κ B [67]. Studies on the oncogenic effect of TCL1 expression in B cells are still not completed and also suggest TCL1 as transcriptional regulator of the CREB binding protein p300 and the activating protein 1 (AP-1) [69].

1.3 CD74

The invariant chain (Ii, known as CD74 when expressed on the plasma membrane) is a type II membrane protein first identified as the MHC class II-associated chaperon [70]. It is expressed in HLA class II-positive cells like B cells, monocytes, macrophages, Langerhans cells, dendritic cells, thymic epithelial cells and gastric epithelial cells. CD74 controls several aspects of the immune system; e.g. B cell development, dendritic cell motility, thymic selection and has been associated with B cell neoplasia and solid tumor development, progression and metastasis [70].

The human *CD74* gene (chromosome 5, 9 exons) and the murine counterpart (chromosome 18, 8 exons) share much homology. Both have two main transcript variants (p31 and p41), with humans having two further transcripts (p35 and p43), resulting from an alternative translation start site [71, 72]. The human and the murine CD74 consist of a 29-46 amino acid NH₂-terminal intracytoplasmic domain, depending on which of two alternative initiation codons are translated, a 26-amino acid hydrophobic transmembrane region, and a 160-amino acid extracytoplasmic domain containing two N-linked carbohydrate chains [73] (Figure 2). In both species the shorter isoform of CD74 predominates with an estimated ratio of 9:1 [74]. The p33 and the p35 isoform regulate the MHC class II antigen presentation, while the p41 and p43 isoform encode a thyroglobulin type 1 domain that can bind cathepsins [75].

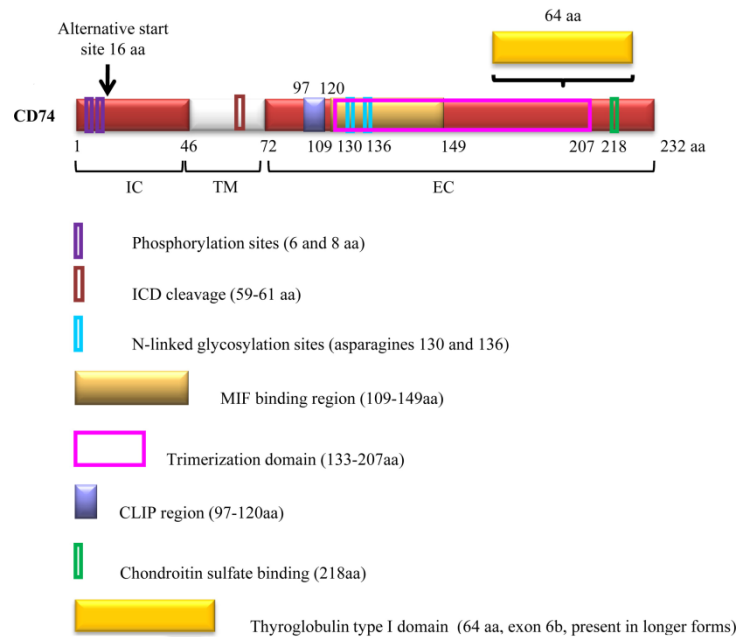


Figure 2: CD74 structure

The schema shows the intracytoplasmic (IC), transmembrane (TM) and extracellular (EC) domains of CD74. Amino acid numbers refer to the human p35 variant. CLIP: class II-associated invariant chain peptide. ICD: Intracellular domain.(from [73])

1.3.1 The invariant chain (Ii) part of the MHC class II complex

The first and best described function of the invariant chain (Ii) is its part in the major histocompatibility class II complex (MHC class II), which controls a major component of the immune system. The invariant chain functions as a chaperone helping with the proper folding of MHC class II proteins and protection from peptide binding during transit through the ER [76-78] (reviewed in [79]). In more detail, after synthesis in the endoplasmic reticulum (ER) the Ii combines with MHC class II heterodimers, where it assures proper folding and assembly of the MHC class II dimers [80-82]. This complex then exits the ER and travels through the golgi apparatus to the endosomal compartment. The cytoplasmic tail of Ii contains two di-leucin-based motifs, which are essential for efficient sorting [83]. During the transit to the endosomal compartment binding of the Ii to the MHC class II prevents the unspecific binding of peptides to the complex [84]. After the Ii-MHC class II complex reaches the endocytic compartment, the Ii is progressively degraded until only an Ii derived peptide called CLIP (class II associated invariant chain derived peptide) remains associated to MHC class II. CLIP then is exchanged for an antigenic peptide. The mature MHC class II-peptide complexes are then translocated to the cell surface for CD4⁺ T cell recognition [79].

In 2012 the group from Basha *et.al.* showed that the Ii also associates with MHC class I molecules in dendritic cells. There Ii directs a subset of MHC class I molecules to the endolysosomal pathway, where dissociation of the Ii and reassembly of MHC class I with antigenic peptides are carried out [85], showing that the Ii is also involved in the cross-presentation pathway of dendritic cells that has a major role in the generation of MHC class I-restricted, cytolytic T cell response to viral protein.

1.3.2 The surface receptor CD74

Several studies showed that 2-5% of the invariant chain (Ii) is found on the cell surface [86, 87]. A small subset of the Ii is modified by the addition of chondroitin sulfate and rapidly transported from the golgi apparatus to the cell surface [88], where it remains for a short time with an estimated surface half-life of ten minutes [89]. Expression of this cell surface protein, designated CD74, is independent from the expression of class II molecules [90, 91]. CD74 is expressed on several MHC class II positive cells (B cells, monocytes, macrophages, Langerhans cells, dendritic cells, thymic epithelium and gastric epithelial cells) but is also found on a number of cells without MHC class II (e.g. pulmonary alveolar epithelium, colon epithelium) [92, 93]. On the surface CD74 is a receptor for extracellular MIF, D-DT/MIF-2 and bacterial proteins [94-99].

1.3.2.1 CD74 receptor signaling

Studies on the signaling function of surface CD74 revealed several signaling pathways (overview Figure 3). The major part is the identification of CD74 as a high-affinity receptor for the macrophage migration inhibitory factor (MIF) [94]. MIF is a proinflammatory and immunoregulatory cytokine, which is ubiquitously expressed in mammals (reviewed in [100]). Extracellular MIF binds to CD74 and survival signals via the SYK, MAPK, AKT or the NF- κ B pathways are transmitted [94, 101, 102]. Those signaling events result in cell proliferation and inhibition of apoptosis [94, 103]. Although it was shown that phosphorylation of the serine residues takes place on the p35 variant of Ii [104], the short cytoplasmic sequence of CD74 does not appear to signal directly. It was demonstrated that MIF-induced extracellular signal-regulated kinase 1 and 2 (ERK1/2) MAP kinase activation is dependent on CD44 in fibroblast, monocytes, B cells (Raji cell line) and macrophages [105]. CD44 is a structurally diverse and multivalent co-receptor due to prominent alternative splicing and posttranslational modifications (e.g., glycosylation). It recruits several kinases (e.g.

receptor tyrosine kinases and non-receptor src family kinases), which eventually all evoke strong MAPK/ERK and PI3K/AKT responses [106].

Studies using a CD74 activating antibody show that activation of CD74 also results in the cleavage of the intracellular cytoplasmic domain of CD74 (CD74-ICD) in B cells [107, 108] by a process called regulated intermembrane proteolysis (RIP). In RIP cleavage of the membrane protein releases a new active peptide which migrates into the nucleus to regulate gene transcription (reviewed in [109, 110]). The RIP of the CD74-ICD is dependent on PI3K/AKT phosphorylation [111] and induces activation of the NF- κ B p65 and the B cell-enriched co-activator TAF_{II105} leading to cell proliferation and survival [112, 113].

MIF is also a non-cognate, high-affinity ligand for the chemokine receptors CXCR2 and CXCR4 [101, 114]. Both chemokine receptors belong to the family of seven helix-membrane-spanning G-protein coupled receptors. CXCR2 is the cognate receptor for CXC chemokines such as CXCL8, and CXCR4 is the cognate receptor for SDF1 α [115]. It has been shown that CD74 forms complexes with CXCR2 or CXCR4 on the surface of monocytes and T cells [101, 116], which has been suggested to amplify MIF triggered responses in monocytes [101].

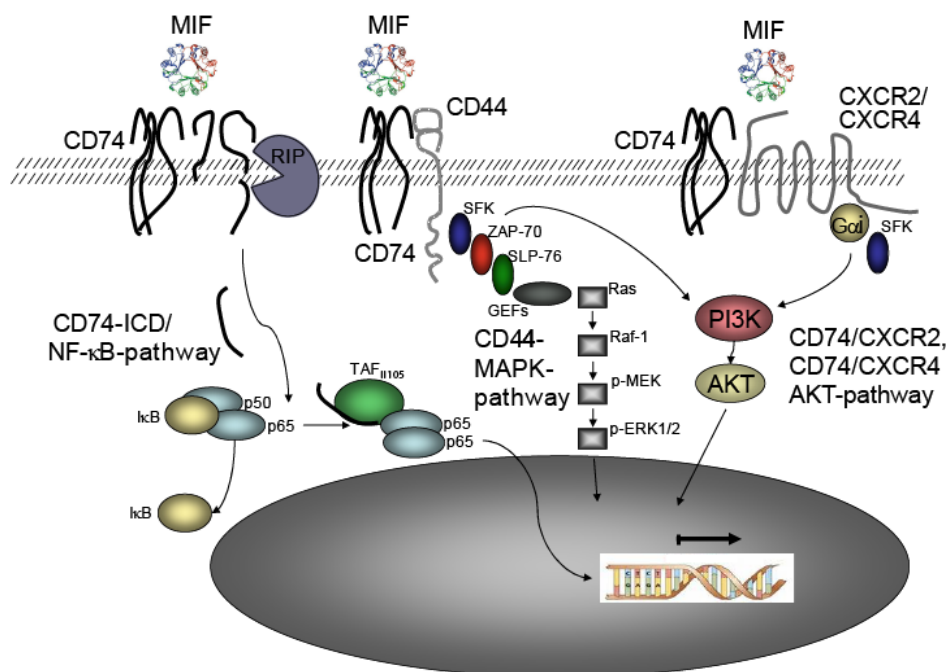


Figure 3: CD74- dependent MIF signaling

Schema of MIF induced CD74 signaling. 1: Binding of MIF leads to regulated intermembrane proteolysis (RIP) of the intracellular domain (ICD) of CD74, which then induces activation of the NF- κ B pathway. 2: MIF binding to CD74 leads to the recruitment of the co-receptor CD44, which induces activation of the PI3K/AKT and MAPK pathway. 3: CD74 and CXCR2 or CXCR4 form a complex leading to G-protein coupled (G α i) AKT activation upon MIF binding.

1.3.3 CD74 physiology

Development of the CD74-knockout mouse (CD74^{ko}) revealed the profound effect of CD74 on the MHC class II biology and the immune system [76]. Kept under controlled conditions, CD74 deletion generally did not change the health status of the mice, which was comparable to that of wild type mice [117], only occasional severe wasting was reported [76]. Studies on the CD74^{ko} mice revealed decreased levels of MHC class II surface expression on splenic B cells due to misfolding and dimerization of the MHC class II complex, which causes its retention in the endoplasmatic reticulum and vesicles [76, 77]. Since MHC class II plays a critical role in both thymic selection and peripheral expansion of CD4⁺ T lymphocytes [118], CD74^{ko} mice show decreased numbers of mature CD4⁺ T cells in the thymus and periphery.

Additionally, the loss of CD74 leads to a higher motility of dendritic cells due to an interaction of the motor protein myosin II with the cytoplasmic tail of CD74 in the endosomal compartment of dendritic cells. Upon degradation of CD74 through Cathepsin S the myosin II dissociates from the endosome and binds to actin leading to an enhanced motility of dendritic cells [119, 120].

Finally, studies with CD74^{ko} mice showed that CD74 is an essential cofactor for B cell maturation. Splenic B cells from mice lacking CD74 showed a developmental block in an immature state [121]. B cell development in mammals takes place in the primary lymphoid tissue (e.g. bone marrow, fetal liver) with the formation of immature B cells. Subsequently final differentiation into mature B cells, that are responsive to antigens, takes place in the secondary lymphoid tissue (e.g. lymph nodes and spleen) [122]. In CD74^{ko} mice the differentiation block is characterized by an accumulation of B cells in the transitional stage 1 (T1), marginal zone B cells and a decreased life span of follicular B cells [123] in the spleen. Mechanistically, activation of surface CD74 leads to regulated intermembrane proteolytic release (RIP) of the intracellular domain of CD74 (CD74-ICD) [107, 108] by Spp12a (Signal peptide peptidase-like 2a) [124]. The cleaved CD74-ICD then translocates to the nucleus and activates the NF- κ B p65 homodimer and the TAF_{II}105 B cell enriched co-activator [111, 113]. Insufficient NF- κ B activation in CD74 knockout mice then leads to a developmental block of B cell maturation [125].

1.3.4 CD74 pathophysiology

CD74 expression is increased in diverse tissue injury disorders, such as gastric epithelium during *Helicobacter pylori* infection [97], ulcerative colitis [126], heart-ischemia-reperfusion injury [127], toxin-induced liver fibrosis [128] and human atherosclerotic plaques [129]. Additionally, CD74 is expressed by a broad range of malignant cells, e.g. in more than 90% of B cell neoplasms [130] and solid tumors including clear renal carcinoma [131], intestinal adenomas [132], lung tumors [133] and breast cancers [73, 134]. Since CD74 is essential for initiating signaling cascades induced by MIF, leading to cell proliferation and cell survival, it is often involved in carcinogenesis and tumor progression, e.g. in gastric carcinoma [135] and B cell neoplasia [130].

1.3.4.1 CD74 during *Helicobacter pylori* infection

Expression of CD74 is increased in the gastric epithelium during *Helicobacter pylori* infection [97]. *Helicobacter pylori* binds directly to CD74 via urease, a common bacterial protein involved in the catalysis of urea [98], leading to increase of CD74 gene and protein expression in the gastric epithelium [97]. Additionally, binding of *Helicobacter pylori* to CD74 triggers signaling of the NF- κ B pathway causing the expression and secretion of Interleukin-8 [97]. Interleukine-8 (IL-8) is a pro-inflammatory cytokine and potent chemotactic factor for neutrophils, which increases the inflammatory response [70]. MIF is also highly expressed during *Helicobacter pylori* infection and binds to the abundant CD74 receptor leading to the activation of NF- κ B and ERK1/2 pathways [45, 105], which further promote the production of inflammatory cytokines and the increase of cell proliferation and survival [135, 136]. Together CD74 and MIF might contribute to carcinogenesis in chronic conditions through the upregulation of IL-8, which has its own mechanism leading to increased proliferation and tumor growth and angiogenesis [135].

1.3.4.2 CD74 in B cell neoplasia

CD74 expression is found on many B cell malignancies [130] and is also highly expressed on many cell lines used as models for hematological neoplasms [137].

Functionally, CD74 together with CD44 is essential for initiating signaling cascades induced by MIF in mature B cells [45]. MIF induces cell entry into S-phase by elevating cyclin E levels in a CD74-CD44-dependent manner, resulting in cell proliferation. The

same cascade leads to elevated expression of BCL-2, an anti-apoptotic protein supporting cell survival [45, 111]. Moreover, it was demonstrated that CD74 stimulation by MIF recruits the tyrosine kinase receptor, c-Met, to the CD74/CD44 complex and thereby enables the induction of its signaling cascade within the B cell. This signaling results in secretion of hepatocyte growth factor (HGF), which stimulates the survival of the mature B cell population in an autocrine manner [138].

Another axis inducing B cell survival involves the NF- κ B pathway. Binding of MIF to CD74 leads to activation of the p65 domain of the NF- κ B pathway which in turn increases the transcription and expression of TAp63 [139]. The p63 protein shows high sequence and structure homology to p53 [140] and plays a role in development regulation of limbs, skin, most epithelial tissue and epidermal differentiation [141]. In B cells TAp63 binds to the *Bcl-2* promotor and increases the expression of the anti-apoptotic protein BCL-2, which in turn leads to cell survival. Taken together, MIF binding to CD74 initiates pro-survival signaling, resulting in proliferation of the mature B-cell population, and their rescue from death [142].

The functional significance of this has especially been studied in Chronic Lymphocytic Leukemia (CLL) where it could be shown that CLL cells overexpress both CD74 and its ligand MIF in comparison to healthy B cells.

1.4 CD74 in Chronic Lymphocytic Leukemia

CD74 and its binding partner MIF are suggested to play a pivotal role in the regulation of malignant B cell survival in chronic lymphocytic leukemia (CLL) (reviewed in [142]). CLL cells show an upregulated expression of the surface receptor CD74 as well as MIF production [44, 46]. Studies using cell lines and CLL cells from patients show that MIF binding to CD74 on CLL cells leads to an increase in Interleukin-8 (IL-8) transcription and secretion [46]. IL-8 in turn induces BCL-2 expression, which then activates the anti-apoptotic pathway in CLL cells, though no effect on proliferation was observed [142]. IL-8 is a member of the CXC chemokine family, which is important in autoimmune, inflammatory and infectious diseases [143-145]. In addition, the chemokine IL-8 itself possesses tumorigenic and proangiogenic properties [146]. In CLL increased serum levels of IL-8 were shown to have negative prognostic significance [147]. Thus the signaling cascade induced by the MIF/CD74 axis results in an important CLL cell survival mechanism, which appears from the very early stages of the disease [46].

Also, CD74 plays an important role in the homing of CLL cells into the bone marrow. The bone marrow stroma plays an essential role in B lymphopoiesis by providing survival niches for both normal and leukemic mature B cells [148]. Adhesion of CLL cells to bone marrow stromal cells has been shown to rescue these lymphocytes from apoptosis [149]. With disease progression accumulation of CLL cells into the bone marrow increases, with advanced stage CLL cells showing a higher expression of the VLA-4 integrin compared to early stage cells [150, 151]. The VLA-4 integrin enables retention and survival of CLL cells in the bone marrow, an environment which is enriched with the VLA-4 ligands, VCAM-1, and fibronectin [151]. MIF and CD74 were demonstrated to play a significant role in the regulation of VLA-4 expression in CLL. Thus, MIF/CD74 and its target gene VLA-4 facilitate migration of CLL cells back to the bone marrow, where they interact with the supportive environment that rescues them from apoptosis [150].

Taken together these results suggest that blocking of CD74 or its ligand MIF, e.g. with an antagonistic anti-CD74 antibody, might inhibit survival of CLL cells and their homing to the bone marrow. In fact, Reinart *et al.* showed recently that deletion of MIF delays the development of CLL in the mouse model (E μ -*TCL1*-transgenic mice) by reducing the survival of CLL cells [44]. Additionally, Fedorchenko *et al.* showed that deletion of the CD74 co-receptor CD44 reduced the tumor-burden in the CLL mouse model and led to prolonged survival [152]. At the moment the expression of CD74 on B cells is being exploited to develop novel strategies for the therapy of B cell lymphoma. Labelling of anti-CD74 monoclonal antibodies with radioactivity or cytostatic drugs, to enhance targeting of the malignant cells, was demonstrated to effectively kill malignant B cells *in vitro* and *in vivo* [153-157].

1.5 Objective

The surface receptor CD74 has been shown to be an important regulator of B cell survival. Binding of the macrophage migration inhibitory factor (MIF) to CD74 regulates the activity of several pro-survival pathways such as PI3K/AKT, MAPK or NF- κ B in normal and malignant B cells.

Studies on MIF, the high-affinity ligand of CD74, and the CD74 co-receptor CD44 have shown that both molecules promote disease development in the CLL mouse model. Since CD74 is known to be the mediator of MIF-induced and CD44-mediated intracellular signaling transduction, we postulated a central role for CD74 in CLL development and CLL survival signaling.

So far, studies on the role of CD74 in CLL are based on experiments with primary CLL cells or human cell lines *in vitro*. Given the strong dependence of CLL cells on the tumor microenvironment, the exact contribution of CD74 to the pathogenesis of CLL is far from being understood. Thus, the CD74 knock out mouse was crossed with the murine CLL-model (E μ -*TCL1*-transgenic). Using this model, this project aimed to clarify the influence of the CD74 receptor during B cell oncogenesis and the mechanisms underlying CD74-dependent signaling in B cells.

In detail, the resulting $TCL1^+$ CD74^{wt} and $TCL1^+$ CD74^{ko} mice were analyzed comparing the leukemic load, overall survival and biology of the malignant B cells. Furthermore, the mechanism of CD74-dependent regulation of pro-survival signaling was studied using murine malignant B cells from the established mice.

2 Results

2.1 CD74 expression in E μ -*TCL1*-transgenic mice

Studies on CLL showed a significantly higher expression of the surface protein CD74 in human CLL cells compared to healthy B cells [46]. The aim of this project was to study the role of the CD74 in CLL development by using the E μ -*TCL1*-transgenic CLL mouse model. Therefore, the expression of CD74 in malignant B cells was examined during the development of CLL in the E μ -*TCL1*-transgenic mouse model (Figure 4). Splenic B cells from E μ -*TCL1*-transgenic mice (TCL1⁺) at different leukemic stages (ranging from 22% - 94% CD5⁺/CD19⁺ cells) were isolated. CD74 protein expression was analyzed by immunoblotting. In this experiment the CD74 protein expression did not differ in E μ -*TCL1*-transgenic mice compared to wild type control mice (TCL1^{wt}).

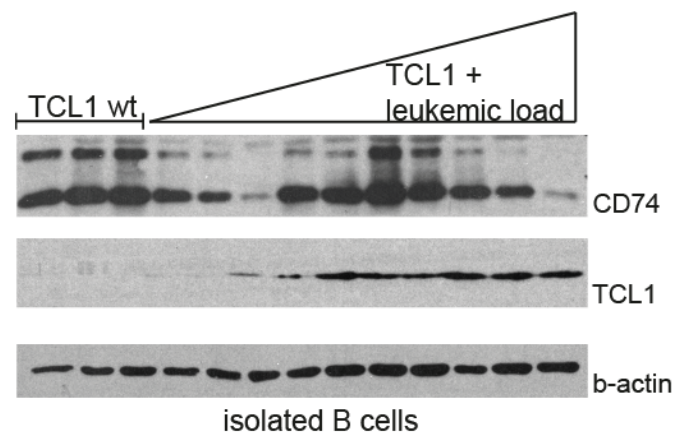


Figure 4: CD74 expression in splenic B cells from wild type and TCL1⁺ mice

Splenic B cells of wild type (TCL1^{wt}) and TCL1-transgenic (TCL1⁺) mice, with different leukemic load, were isolated and lysed. Protein lysates were separated using SDS-PAGE and transferred on to a nitrocellulose membrane. Immunodetection was performed using ECL detection. Leukemic load was measured using flow cytometry (percentage of CD5⁺ B cells in the spleen).

In parallel, blood from TCL1⁺ mice was taken every 3 months and CD74 expression measured in CD5-expressing B cells by flow cytometry (Figure 5). Here, a significant increase in the mean fluorescence of the CD74 signal was observed in highly leukemic TCL1⁺ mice compared to TCL1^{wt} mice (3 months: TCL1^{wt} 43.58±10.4 vs. TCL1⁺ 32.44±5.5; 6 months: TCL1^{wt} 35.56±7.6 vs. TCL1⁺ 56.58±17.6; 9 months: TCL1^{wt} 52.54±3.3 vs. TCL1⁺ 69.83±11.8; 12 months: TCL1^{wt} 43.99±8.8 vs. TCL1⁺ 93.6±6.6 ΔMFI).

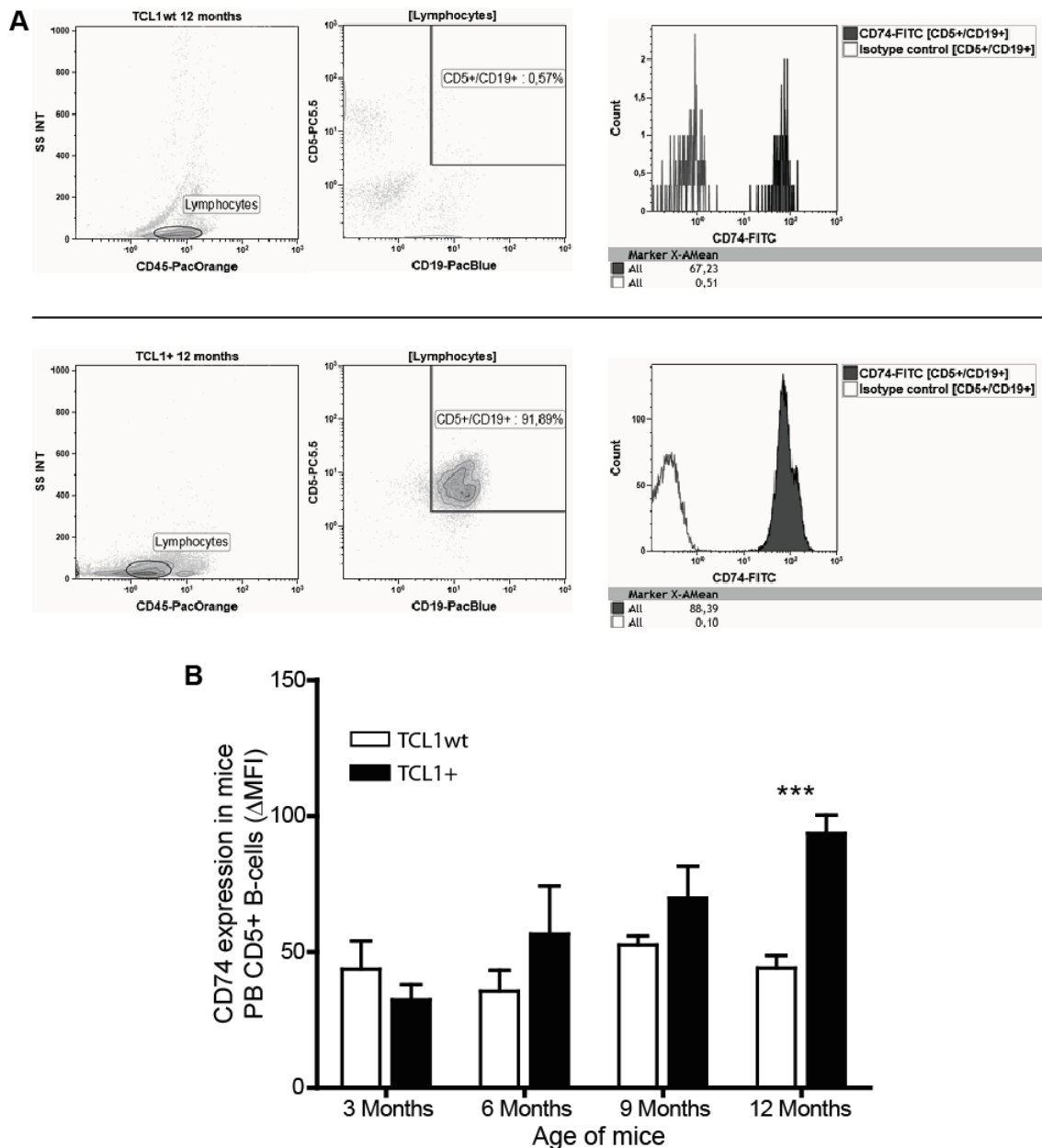


Figure 5: Flow cytometric analyses of CD74 expression in malignant B cells from murine blood samples

A: Flow cytometric analysis of CD74 expression in CD5-expressing B cells from murine blood samples in TCL1^{wt} and TCL1⁺ mice. Blood samples were stained with CD5, CD19, CD45 and CD74 antibodies. After gating on lymphocytes using the CD45 expression and the side scatter (SS INT), malignant B cells were gated on using both CD5 and CD19 expression. Using the CD5⁺/CD19⁺-gate, mean fluorescent intensity (MFI; here depicted as X-A-Mean) of CD74-FITC signal was measured. The appropriate isotype control was used as control. **B:** Blood samples of TCL1^{wt} and TCL1⁺ mice were taken from different age groups and CD74 expression in CD5⁺ B cells was measured via flow cytometry. (PB: peripheral blood) [t-test, *** p<0.0005, bars show SEM; TCL1^{wt} n=5; TCL1⁺ 3 months n=7, 6 months n=4, 9 months n=5, 12 months n=7]

2.2 CD74 in the development of TCL1-induced CLL

Studies on CD74 and its role in the malignant transformation of B cells were mostly carried out in primary human samples and human cell lines. Given the strong dependence of CLL cells on the tumor microenvironment [39, 43, 158, 159], the functional contribution of CD74 to the pathogenesis of CLL within this niche is far from being understood. Thus, the CD74-knockout mouse ($CD74^{ko}$) was crossed with the murine CLL model ($E\mu$ -*TCL1*-transgenic) to study the functional influence of CD74 in the pathogenesis of TCL-1-induced CLL.

2.2.1 Crossbreeding of $E\mu$ -*TCL1*-transgenic mice with $CD74^{ko}$ mice

Breeding of the $CD74^{ko}$ mouse with the $E\mu$ -*TCL1*-transgenic mouse was done in the animal facility of the Experimental Medicine at the University Hospital of Cologne. Since a homozygous state of the transgene *TCL1* might cause artificial phenotypes, special care in the breeding strategy was taken to avoid a homozygous state of *TCL1* in the F2 generation. Animals of the F2 generation with the genotypes $TCL1^{+/wt} Cd74^{-/-}$ and $TCL1^{+/wt} Cd74^{wt/wt}$ (from now on called $TCL1^+ CD74^{ko}$, $TCL1^+ CD74^{wt}$ respectively) were used for the analyses of leukemic development and survival.

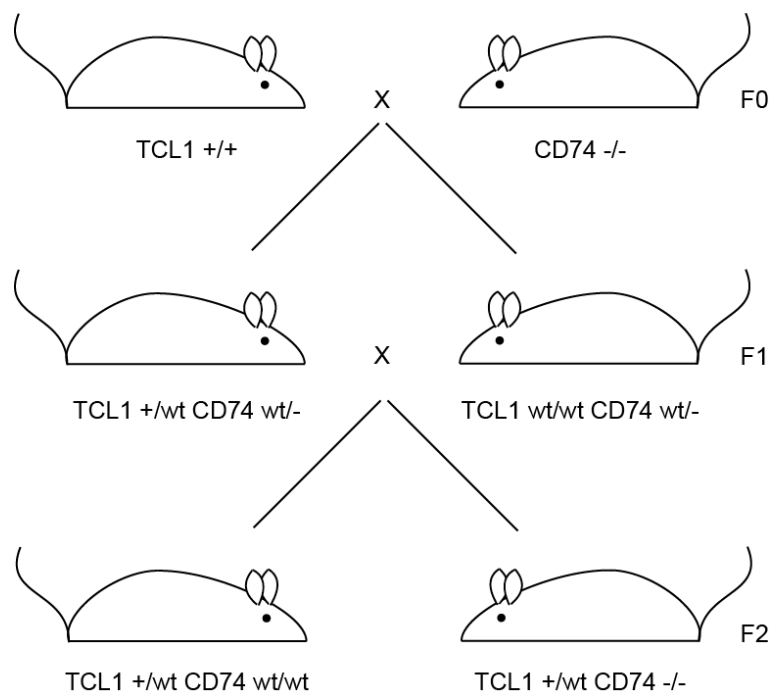


Figure 6: Breeding strategy for $TCL1^+$ with $CD74^{ko}$ mice

B6C3H $E\mu$ -*TCL1* mice homozygous for *TCL1* were crossed with C57Bl/6J $CD74^{-/-}$ mice. To avoid homozygosity for *TCL1* in experimental animals, F1 generations were crossed using $TCL1^+$ mice with $TCL1^{wt}$ mice leading to F2 generations with the preferred genotype.

Littermates with $TCL1^{wt/wt} Cd74^{wt/wt}$ and $TCL1^{wt/wt} Cd74^{-/-}$ genotypes (from now on called $TCL1^{wt} CD74^{wt}$, $TCL1^{wt} CD74^{ko}$ respectively) were used as controls.

The genotypes of the mice were controlled by polymerase chain reaction (PCR) using tail tissue from the mice. Genomic DNA was extracted from the tissue samples and used as templates in the PCR with suitable primer pairs. For *Cd74*, one primer pair is binding to the exon 1 and exon 4 in the gene and another primer pair binds to the neomycin cassette inserted into the genome to delete *Cd74*. Figure 7 shows a schema of the PCR strategy to analyze *Cd74* expression. Similarly, the *TCL1* status was analyzed by using a *TCL1*-specific primer pair (data not shown).

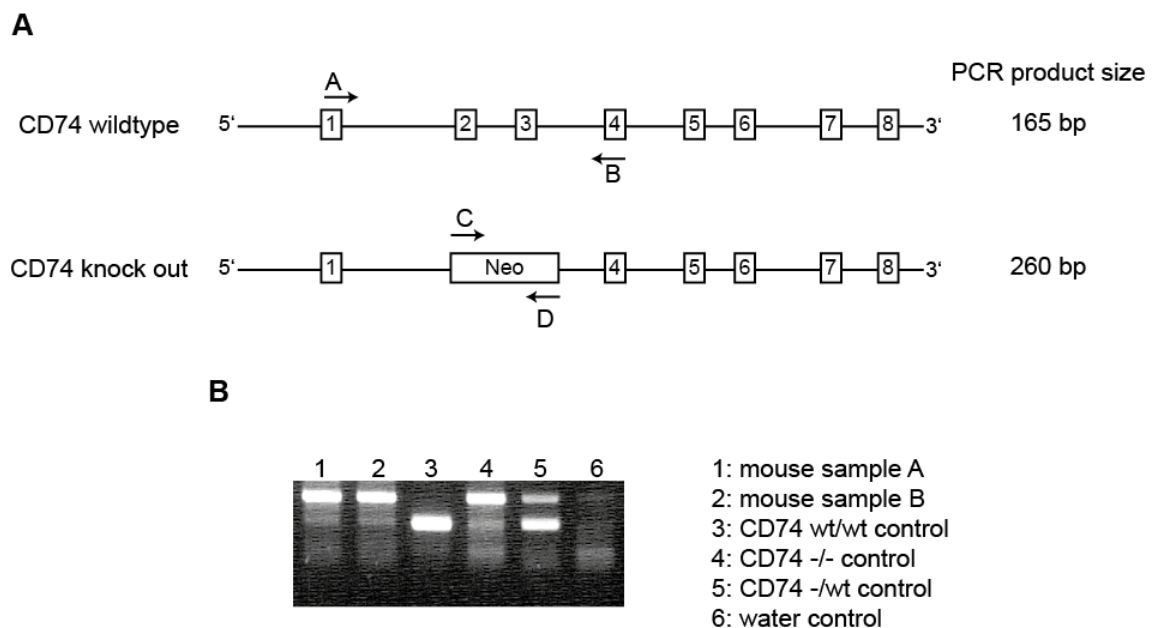


Figure 7: Genotyping PCR for CD74 status

Genomic DNA was extracted from mice tails and then used for PCR. **A:** Primer pairs were binding to either exon 1 and 4 (165 bp) or to the neomycin cassette (260 bp). **B:** Example of PCR products separated by agarose gel electrophoresis.

2.2.2 Leukemia development in $TCL1^{+} CD74^{ko}$ mice

The $E\mu$ -*TCL1*-transgenic mouse model develops a CLL-like disease with an accumulation of CD5-positive B cells in the peripheral blood, spleen, liver and lymph nodes [54]. Therefore, leukemic load and hepatosplenomegaly in $TCL1^{+} CD74^{wt}$ and $TCL1^{+} CD74^{ko}$ mice was measured in order to monitor the development of leukemia.

The leukemic load in the blood of $TCL1^{+} CD74^{wt}$ and $TCL1^{+} CD74^{ko}$ mice was compared at months 3, 6, 9 and 12 by measuring the leukocyte number (WBC) and amount of malignant B cells ($CD5^{+}/CD19^{+}$). The leukocyte count of both strains

showed similar levels in the course of disease development from 6 to 12 months (6 months: $TCL1^+ CD74^{wt}$ 14080 ± 583.7 vs. $TCL1^+ CD74^{ko}$ 12370 ± 744.6 ; 9 months: $TCL1^+ CD74^{wt}$ 14740 ± 891.7 vs. $TCL1^+ CD74^{ko}$ 23190 ± 6005 ; 12 months: $TCL1^+ CD74^{wt}$ 28830 ± 3443 vs. $TCL1^+ CD74^{ko}$ 37560 ± 7812 cells/ μ l) (Figure 8). The $TCL1^+ CD74^{ko}$ group showed a significantly lower leukocyte count at 3 months ($TCL1^+ CD74^{wt}$ 14730 ± 367.5 vs. $TCL1^+ CD74^{ko}$ 9488 ± 250.1 cells/ μ l), which was in agreement with published data, that $CD74^{ko}$ mice show a lower leukocyte count due to a lower number of mature B cells in the periphery [160].

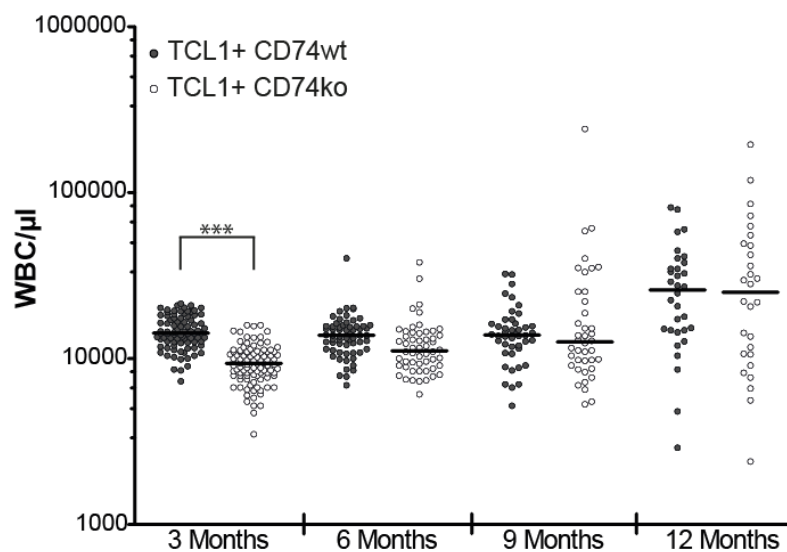


Figure 8: White blood cell count in $TCL1^+ CD74^{wt}$ and $TCL1^+ CD74^{ko}$ mice

Blood samples of $TCL1^+ CD74^{wt}$ and $TCL1^+ CD74^{ko}$ mice were taken every 3 months and the white blood count (WBC) measured using the XE-5000 hematology-analyzer. [t-test, *** $p < 0.0001$, bars show median]

Additionally to the leukocyte count, the amount of malignant CD5-expressing B cells was measured using flow cytometry (Figure 9A). The analysis of CD5-expressing B cells also revealed no significant difference in the number of malignant B cells in $TCL1^+ CD74^{ko}$ mice compared to $TCL1^+ CD74^{wt}$ mice (3 months: $TCL1^+ CD74^{wt}$ 270.2 ± 29.4 vs. $TCL1^+ CD74^{ko}$ 354.1 ± 59 ; 6 months: $TCL1^+ CD74^{wt}$ 1512 ± 674.6 vs. $TCL1^+ CD74^{ko}$ 2696 ± 496.7 ; 9 months: $TCL1^+ CD74^{wt}$ 3187 ± 660.6 vs. $TCL1^+ CD74^{ko}$ 5617 ± 1292 ; 12 months: $TCL1^+ CD74^{wt}$ 7691 ± 1936 vs. $TCL1^+ CD74^{ko}$ 7201 ± 1983 cells/ μ l) (Figure 9B).

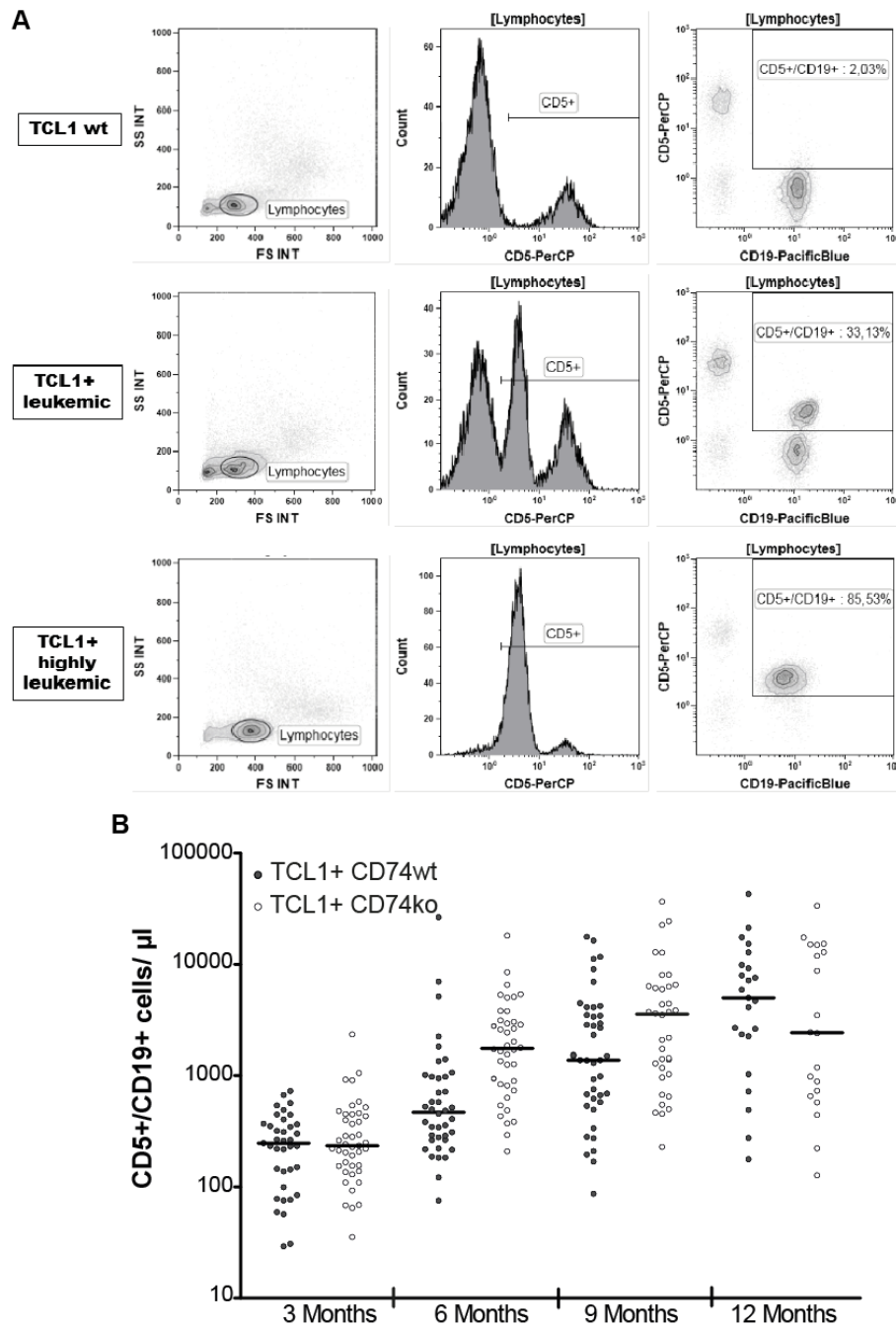


Figure 9: Absolute numbers of CD5-expressing B cells in $TCL1^+$ $CD74^{wt}$ and $TCL1^+$ $CD74^{ko}$ mice

A: Flow cytometric analysis of malignant B cells in murine blood samples from $TCL1^+$ mice in the course of leukemia development. Blood samples were stained with CD5, CD19 and CD45 antibodies. After gating on lymphocytes using the CD45 expression and the side scatter (SS INT) malignant B cells were gated on using both CD5 and CD19 expression. Malignant B cells show a medium CD5 expression, which is clearly distinguished from T cells with a high CD5 expression (middle panel). **B:** Blood samples of $TCL1^+$ $CD74^{wt}$ and $TCL1^+$ $CD74^{ko}$ mice were taken every 3 months and used for flow cytometric analyses of CD5-expressing, malignant B cells. Absolute numbers were calculated using the white blood count from Figure 8. [bars show median].

Furthermore, splenomegaly and hepatomegaly were analyzed in both groups, since E μ -*TCL1*-transgenic mice, like CLL-patients, show increased infiltration of malignant cells into the lymphoid tissues [54]. As shown in Figure 10, both mouse models developed similar hepatosplenomegaly (liver weight: $TCL1^+ CD74^{wt}$ $3.46 \pm 0.4g$ vs. $TCL1^+ CD74^{ko}$ $3.63 \pm 0.3g$; spleen weight: $TCL1^+ CD74^{wt}$ $1.34 \pm 0.3g$ vs. $TCL1^+ CD74^{ko}$ $1.48 \pm 0.1g$).

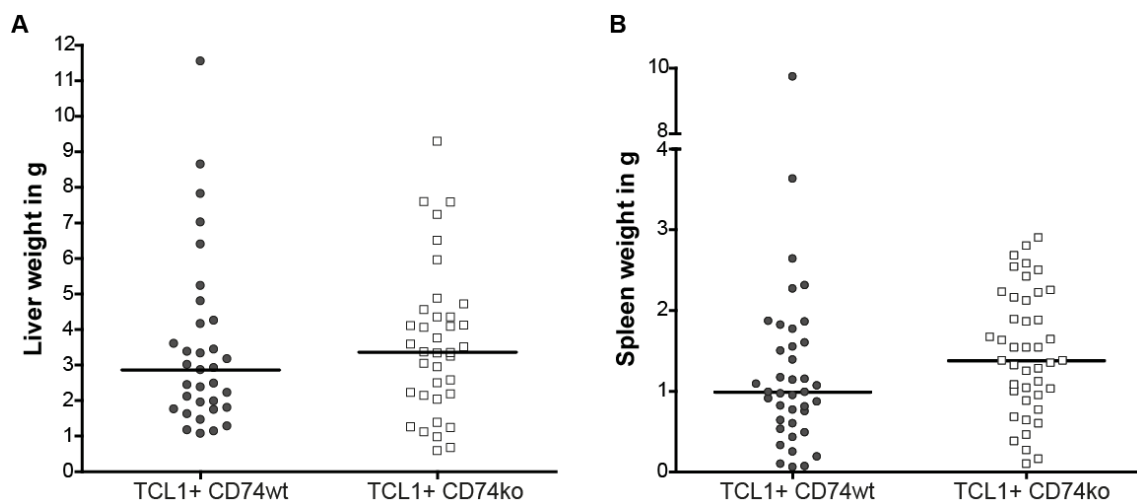


Figure 10: Hepatosplenomegaly in $TCL1^+ CD74^{wt}$ and $TCL1^+ CD74^{ko}$ mice

A: Analysis of liver weight at time of death in $TCL1^+ CD74^{wt}$ (n=33) and $TCL1^+ CD74^{ko}$ (n=37) mice.

B: Analysis of spleen weight at time of death in $TCL1^+ CD74^{wt}$ (n=33) and $TCL1^+ CD74^{ko}$ (n=37). [bars show median]

2.2.3 BCR genetics in $TCL1^+ CD74^{ko}$ mice

The status of heavy chain gene somatic hyper mutations in the B cell receptor is one of the prognostic markers for CLL. The E μ -*TCL1*-transgenic mouse was described to develop leukemia resembling the aggressive, unmutated IgV_H CLL cases [54]. The status of heavy-chain gene somatic hyper-mutations and the immunoglobulin heavy and light chain usage was analyzed in leukemic, murine samples. Table 1 shows that both $TCL1^+ CD74^{wt}$ and $TCL1^+ CD74^{ko}$ mice developed an IgV_H unmutated B cell clone.

Table 1: BCR-genetics in TCL1⁺ CD74^{wt} and TCL1⁺ CD74^{ko} mice

Genotype	IGHV	IGHD	IGHJ	Mutation status
TCL1 ⁺ CD74 ^{wt}	1-26	1-1	1	unmutated; in-frame; no stop-codon,
TCL1 ⁺ CD74 ^{wt}	11-2	2-1	1	unmutated; in-frame; no stop-codon,
TCL1 ⁺ CD74 ^{wt}	12-3	3-1	1	unmutated; in-frame; no stop-codon
TCL1 ⁺ CD74 ^{wt}	7-3	2-3	1	unmutated; in-frame; no stop-codon
TCL1 ⁺ CD74 ^{ko}	3-8	1-1	1	unmutated; in-frame; no stop-codon
TCL1 ⁺ CD74 ^{ko}	12-3	3-3	1	unmutated; in-frame; no stop-codon
TCL1 ⁺ CD74 ^{ko}	12-3	3-2	1	unmutated; in-frame; no stop-codon
TCL1 ⁺ CD74 ^{ko}	12-3	2-3	1	unmutated; in-frame; no stop-codon
TCL1 ⁺ CD74 ^{ko}	6-6	4-1	3	unmutated; in-frame; no stop-codon

2.3 Distribution of myeloid lineage cells in the spleen of TCL1⁺ CD74^{ko} mice

As mentioned before, the microenvironment with its different stimuli is important for the survival of CLL cells. The study from Reinart *et al.* showed that deletion of the CD74 receptor ligand MIF led to a decreased migration of macrophages into the spleen [44]. To further dissect the role of CD74 in the migration of microenvironmental cells to the spleen, different cells of the myeloid lineage were analyzed in the spleen of TCL1⁺ CD74^{wt} mice and compared to the TCL1⁺ CD74^{ko} spleens (Figure 11). Using flow cytometry with antigens specifically expressed on monocytes/macrophages (CD11b⁺/CD18⁺) [161], dendritic cells (CD11c⁺) [162], granulocytes (Gr-1⁺) [163] and macrophages (F4/80⁺) allowed to quantify the amount of these myeloid cells found in the spleen. Aged mice of control groups, not transgenic for *TCL1*, were included in the analysis to compare wild type and CD74^{ko} mice. As shown in Figure 11 both TCL1^{wt} groups showed similar levels of the tested myeloid lineage cell populations (TCL1^{wt} CD74^{wt} CD11b⁺/CD18⁺: 15.47±8%, CD11c⁺: 32.29±19.1%, Gr-1⁺: 21.57±7.9%, F4/80⁺:8.46±4.7%; TCL1^{wt} CD74^{ko} CD11b⁺/CD18⁺: 17.3±6.5%, CD11c⁺: 19.47±1.1%, Gr-1⁺: 38.23±6.4%; F4/80⁺:3.58±0.7%). However, a significant increase of monocytes and granulocytes was observed in the spleen of TCL1⁺ CD74^{ko} mice (CD11b⁺/CD18⁺: 2.1±0.4% TCL1⁺ CD74^{wt} vs. 8.57±2.3% TCL1⁺ CD74^{ko}; Gr-1⁺: 7.1±1.4% TCL1⁺ CD74^{wt} vs. 18.68±4.9% TCL1⁺ CD74^{ko}). Dendritic cells were found equally in the spleens of TCL1⁺ CD74^{wt} and TCL1⁺ CD74^{ko} mice (9.69±1.2% TCL1⁺ CD74^{wt} vs.

15.33±3.7% $TCL1^+ CD74^{ko}$). Additionally, $F4/80^+$ macrophages were also found in similar amounts (1.34±0.7% $TCL1^+ CD74^{wt}$ vs. 3.4±2.1% $TCL1^+ CD74^{ko}$).

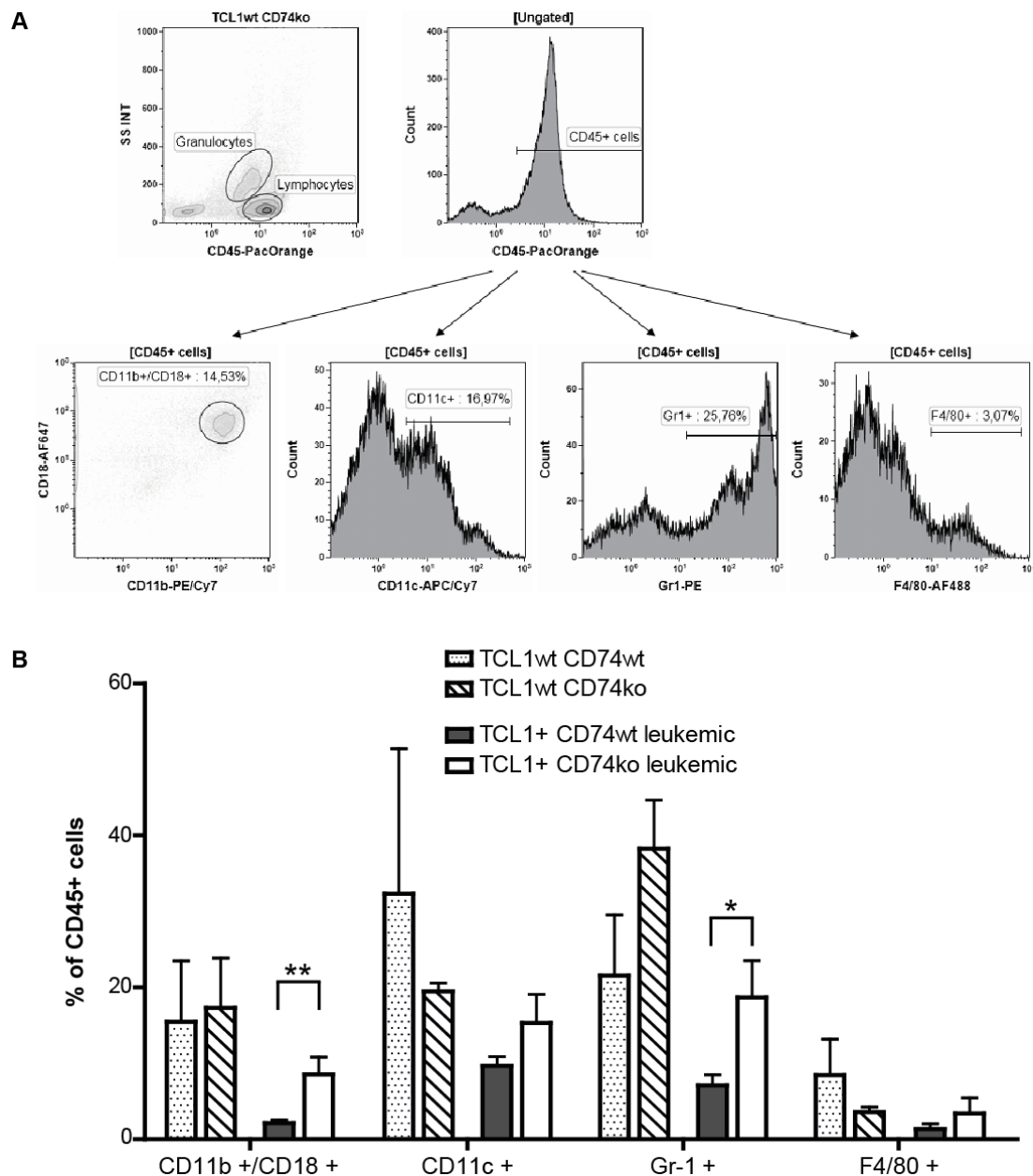


Figure 11: Flow cytometric analyses of myeloid cells in the spleen of $TCL1^+ CD74^{ko}$ mice

A: Flow cytometric analysis of myeloid cells in isolated splenocytes from a $TCL1^{wt} CD74^{ko}$ mouse. Splenocytes were stained with CD11b, CD11c, CD18, CD45, F4/80 and Gr-1 antibodies. After gating on $CD45^+$ -cells, expression of other antigens was analyzed. **B:** Splenocytes from aged mice (~12 months) were isolated and used for flow cytometric analyses. Different myeloid cell types were distinguished within the $CD45^+$ cell population. [t-test, * $p < 0.05$, ** $p < 0.005$, bars show SEM; $TCL1^{wt} CD74^{wt}$ n=3 (n=5 for $CD11b^+/CD18^+$ and n=7 for $F4/80^+$), $TCL1^{wt} CD74^{ko}$ n=3 (n=7 for $CD11b^+/CD18^+$ and $F4/80^+$), $TCL1^+ CD74^{wt}$ n=8, $TCL1^+ CD74^{ko}$ n=4 (n=6 for $CD11b^+/CD18^+$ and $F4/80^+$)]

To further analyze the number of macrophages in the spleen of leukemic mice, spleen sections were stained with a CD68 antibody specific for macrophages. After staining, slides were scanned and red stained cells were counted at 40-fold magnification (Figure 12). The staining showed similar amounts of macrophages between leukemic $TCL1^+$ $CD74^{wt}$ and $TCL1^+$ $CD74^{ko}$ mice (14.3 ± 3.8 vs. 20 ± 6.1 of $CD68^+$ cells).

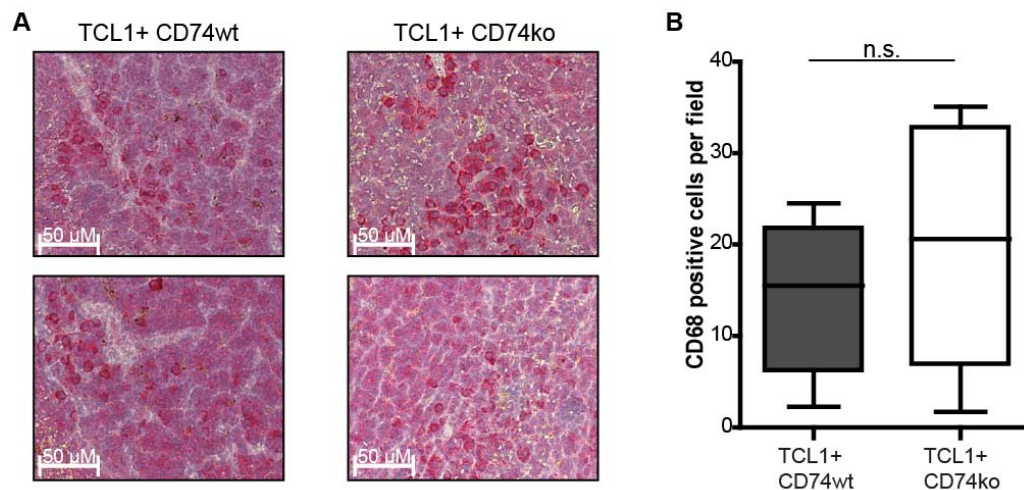


Figure 12: Macrophages in the spleen of $TCL1^+$ $CD74^{ko}$ mice

Spleen sections of leukemic mice were stained for CD68 by immunohistochemistry. **A:** Two examples of the staining (40-fold magnification) per genotype are shown (CD68 positive cells are dark red). **B:** 10 high power fields per mice were counted and the mean depicted in the box plot. [t-test, n.s. $p > 0.05$, bars show SEM; $n = 5$ per group]

2.4 Impact of CD74 deletion on apoptosis and proliferation of malignant B cells

CD74 as a receptor has been shown to regulate the activity of several pro-survival pathways such as PI3K/AKT, MAPK or NF- κ B in normal and malignant B cells [94]. To study the effect of CD74 on the apoptosis and the proliferation, both parameters were measured in malignant B cells from the spleen of $TCL1^+$ $CD74^{ko}$ mice and compared to $TCL1^+$ $CD74^{wt}$ mice.

2.4.1 Apoptosis of malignant B cells in $TCL1^+$ $CD74^{ko}$ mice

Since CD74 plays a pivotal role in the proliferation and survival signaling in B cells [46], apoptosis rate was analyzed in malignant B cells from $TCL1^+$ $CD74^{wt}$ and $TCL1^+$ $CD74^{ko}$ mice *in situ* via immunohistochemistry and *ex vivo* by culturing. First spleen sections of leukemic mice were stained for cleaved Caspase 3, a critical molecular effector of apoptosis, which is responsible for the proteolytic cleavage of many key

proteins [164]. After staining, slides were scanned and brown stained cells were counted at 40-fold magnification (Figure 13).

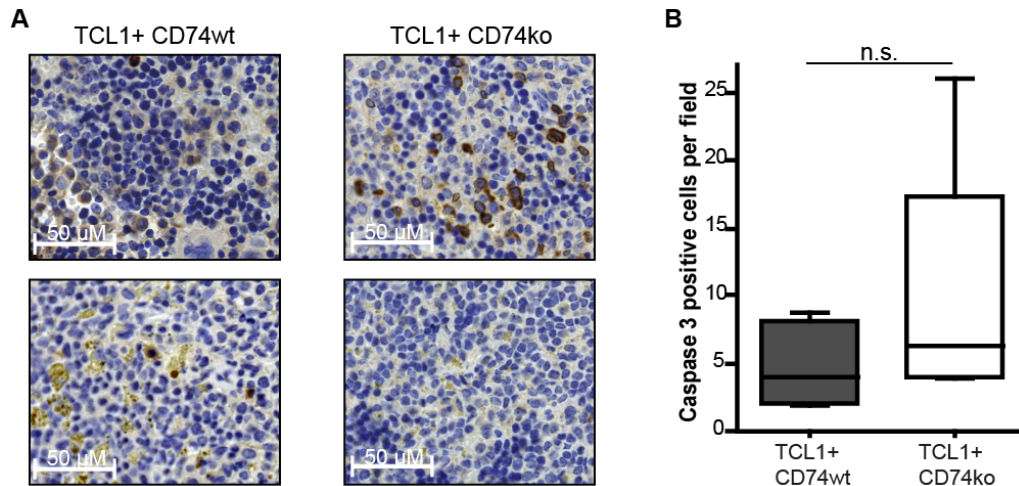


Figure 13: Apoptosis rate in the spleens of $TCL1^+$ $CD74^{wt}$ and $TCL1^+$ $CD74^{ko}$ mice
Spleen sections of leukemic mice were stained for cleaved Caspase 3 by immunohistochemistry. **A:** Two examples of the staining (40-fold magnification) per genotype are shown (cleaved Caspase 3⁺ cells are brown). **B:** 10 high power fields per mice were counted and the mean depicted in the box plot. [t-test, n.s. $p > 0.05$, bars show SEM; $TCL1^+$ $CD74^{wt}$ $n=6$; $TCL1^+$ $CD74^{ko}$ $n=4$]

Staining of cleaved Caspase 3 in spleens of leukemic mice showed no significant difference in the number of stained cells, representing apoptotic cells, between $TCL1^+$ $CD74^{wt}$ and $TCL1^+$ $CD74^{ko}$. Quantification of 10 bright fields per mouse showed insignificantly more apoptotic cells in the spleens of $TCL1^+$ $CD74^{ko}$ mice [$TCL1^+$ $CD74^{wt}$ 4.71 ± 1.2 vs. $TCL1^+$ $CD74^{ko}$ 10.63 ± 5.2 cleaved Caspase 3-positive cells].

To have a closer look at the survival of $TCL1$ -induced leukemic cells after deletion of $CD74$, *ex vivo* analyses of apoptosis was carried out. Splenocytes from leukemic mice were cultured in cell culture medium. Spontaneous apoptosis of unstimulated splenocytes was then measured by staining for Annexin V and 7-AAD using flow cytometry. Figure 14 shows the percentage of viable cells (Annexin V and 7-AAD negative) after *ex vivo* culturing for 24 h. Cells from leukemic $TCL1^+$ $CD74^{ko}$ mice showed an insignificant higher amount of viable cells after unstimulated culturing [Figure 14A; $TCL1^+$ $CD74^{wt}$ $54 \pm 8\%$ vs. $TCL1^+$ $CD74^{ko}$ $85 \pm 1\%$ viable cells].

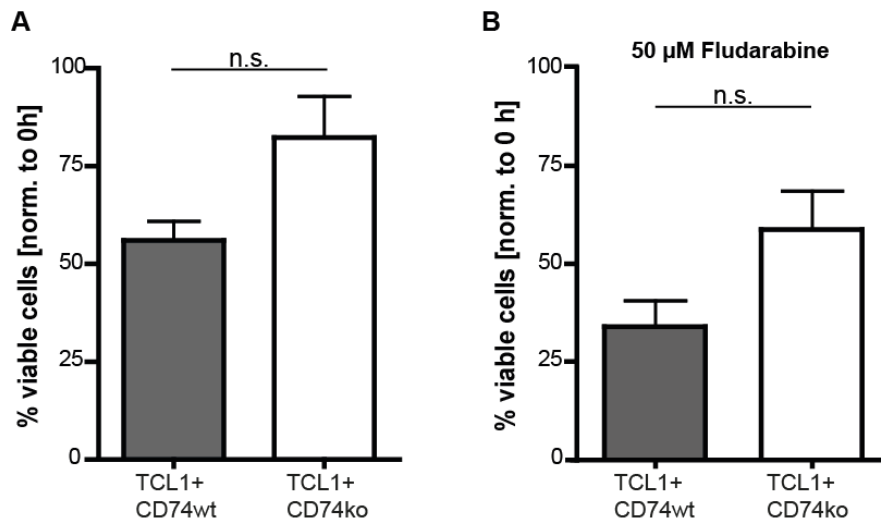


Figure 14: In vitro apoptosis analyses of leukemic mice

Splenocytes from leukemic $TCL1^+$ $CD74^{wt}$ and $TCL1^+$ $CD74^{ko}$ mice were isolated and analyzed for viability by staining for Annexin V and 7-AAD after 24h in culture **A**: without additional stimuli [Mann Whitney test, n.s. $p > 0.05$, bars show SEM; $n = 6$ per group] **B**: with Fludarabine (50 μM) treatment. [Mann Whitney test, n.s. $p > 0.05$, bars show SEM; $n = 4$ per group]

Furthermore apoptosis was tested after treatment with Fludarabine, a purine nucleoside analog and the major choice for CLL chemotherapy. The drug is cytotoxic against both dividing and resting cells [165, 166]. In dividing cells, fludarabine inhibits ribonucleotide reductase and DNA synthesis [167] whereas in quiescent cells the main mechanism of cytotoxicity appears to be inhibition of cellular DNA repair processes leading to the induction of apoptosis [168]. Cells from both groups showed a similar reduction of viability after treatment with Fludarabine (Figure 14B; $TCL1^+$ $CD74^{wt}$ $34 \pm 7\%$ vs $TCL1^+$ $CD74^{ko}$ $59 \pm 10\%$ viable cells).

2.4.2 Proliferation of malignant B cells in $TCL1^+$ $CD74^{ko}$ mice

Besides apoptosis, proliferation of malignant B cells was measured in both mouse models. Two different methods were used to analyze the proliferation capacity of B cells *in vivo*. The first one was measuring the BrdU incorporation. Bromodeoxyuridine (BrdU) is an analog of the DNA precursor thymidine and is incorporated into newly synthesized DNA by cells entering and progressing through the S phase of the cell cycle [169]. The incorporated BrdU can be stained with a specific BrdU antibody. Here leukemic mice (~9 months) were injected with BrdU intraperitoneally and sacrificed for splenocyte isolation after 24h.

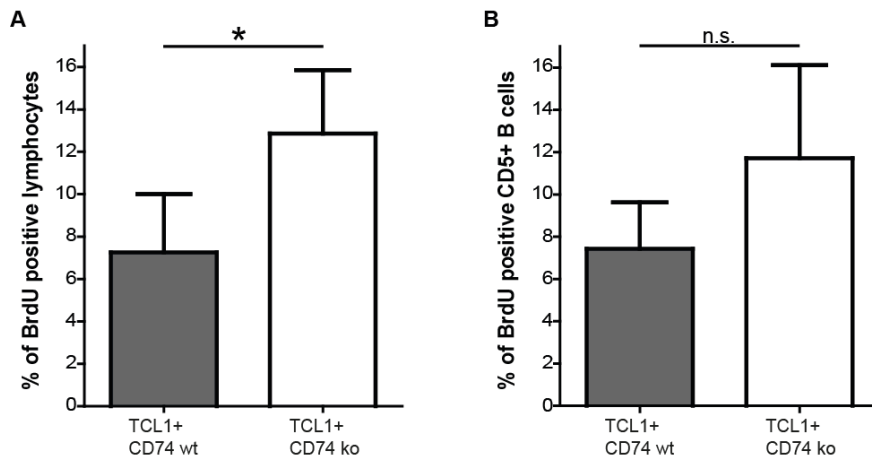


Figure 15: Proliferation capacity of lymphocytes from TCL1⁺ CD74^{wt} and TCL1⁺ CD74^{ko} mice

Mice were injected with BrdU (2 mg) intraperitoneally and splenocytes were isolated after 24h. The cells were stained with CD45, CD5, CD19 and a BrdU antibody. BrdU uptake then was measured via flow cytometry in **A:** lymphocytes (CD45⁺) and **B:** malignant B cells (CD5⁺/CD19⁺). [t-test *p<0.05, bars show SEM; n=5 per group]

Flow cytometric analyses gating on lymphocytes showed a higher amount of proliferating lymphocytes in TCL1⁺ CD74^{ko} spleens compared to TCL1⁺ CD74^{wt} mice (Figure 15A; TCL1⁺ CD74^{wt} 7.3±1.2 % vs. TCL1⁺ CD74^{ko} 12.9±1.3% of lymphocytes). On the other hand, gating on CD5⁺ B cells showed no differences in the proliferation capacity of malignant B cells between both groups (Figure 15B; TCL1⁺ CD74^{wt} 7.4±0.9 % vs. TCL1⁺ CD74^{ko} 11.7±1.9% of CD5⁺ B cells).

Second, proliferation was quantified using immunohistochemistry. Spleen sections of leukemic mice were stained for Ki-67 expression. Ki-67 is a nuclear protein that is present at low levels in quiescent cells but is increased in proliferating cells [170]. After staining, slides were scanned and brown stained cells were counted at 40-fold magnification. Quantification of Ki-67 positive cells in the spleen sections showed that both genotypes display equal amounts of proliferating cells (Figure 16; TCL1⁺ CD74^{wt} 324±79.1 vs. TCL1⁺ CD74^{ko} 332.8±24.2 Ki-67 positive cells).

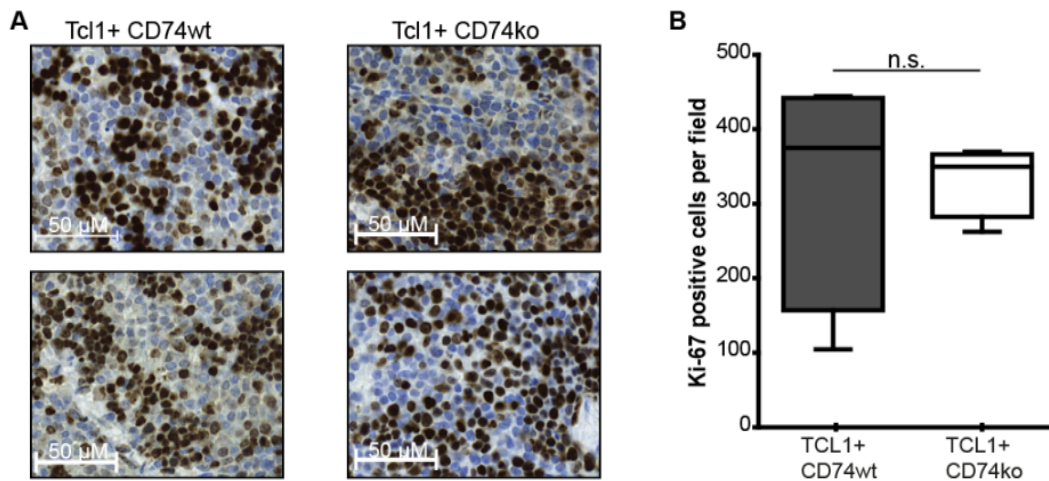


Figure 16: Proliferation in the spleen of $TCL1^+$ $CD74^{wt}$ and $TCL1^+$ $CD74^{ko}$ mice

Spleen sections from leukemic $TCL1^+$ $CD74^{wt}$ and $TCL1^+$ $CD74^{ko}$ mice were immunohistochemically stained with Ki-67 antibody. **A:** Two examples of the staining (40-fold magnification) per genotype are shown (Ki-67⁺ cells are brown). **B:** 10 high power fields per mice were counted and the mean depicted in the box plot. [t-test; n.s. $p > 0.05$, bars show SEM; $n = 4$ per group]

2.5 Overall survival of $TCL1^+$ $CD74^{ko}$ mice

To compare CLL pathogenesis between the two mouse models, overall survival of both groups was monitored. Around 40 mice per group were included in the survival experiment. Observation was carried out until mice became moribund (weight loss $< 10\%$, apathy, swollen abdomen or lymph nodes). Sick animals, not caused by CLL, were euthanized and censored in the Kaplan-Meier curve. Parallel the mice were analyzed for the leukemic load by a 3-month blood examination as described previously (2.2.2). Survival observation was carried out for 700 days. A median survival of 414 days for $TCL1^+$ $CD74^{wt}$ mice was observed, which is in accordance with data within our research group. Mice from the $TCL1^+$ $CD74^{ko}$ group showed a median survival of 430 days, which is not significantly different to the control group.

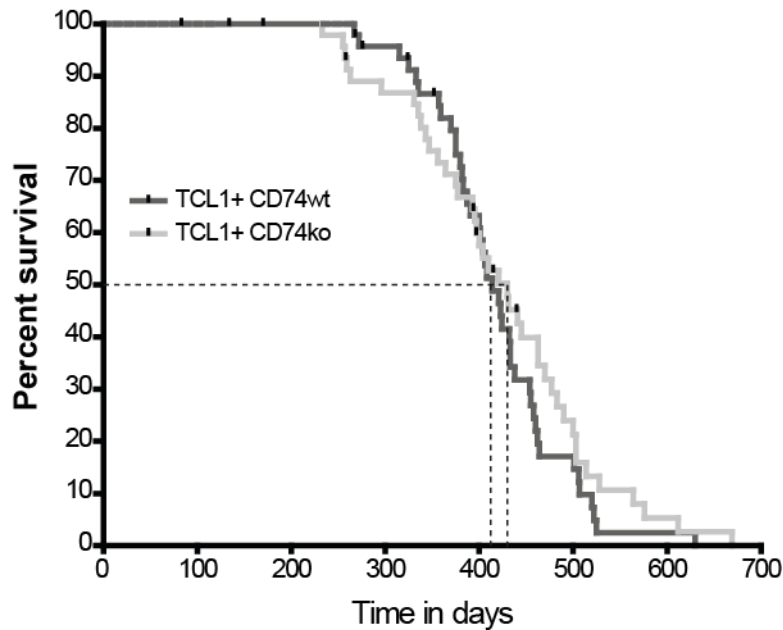


Figure 17: Overall survival of TCL1⁺ CD74^{ko} mice

Overall survival of TCL1⁺ CD74^{wt} and TCL1⁺ CD74^{ko} mice was observed for up to 700 days. [Mantel-Cox test, $p > 0.05$; ticks show censored events; TCL1⁺ CD74^{wt} $n = 47$; TCL1⁺ CD74^{ko} $n = 48$]

2.6 Syngeneic transplantation of murine CLL cells into CD74^{ko} mice

In 2001 the group of Hofbauer *et al.* described the syngeneic transplantation of CLL-like cells from E μ -*TCL1*-transgenic mice into wild type mice [171]. Since CLL cells highly depend on the microenvironment to survive and proliferate, this model is a good tool to analyze the role of the microenvironment in the engraftment of an established malignant clone.

In this project, this method was used to further analyze the influence of CD74 in the microenvironmental cells (e.g. dendritic cells or monocytes) on the development of the CLL-like disease. For this purpose, the spleen of highly leukemic C57BL/6 E μ -*TCL1* mice (TCL1^{+/+}) were removed and the malignant B cells isolated as described under 5.11. Cells were injected into young (~3 months) wild type and CD74^{ko} mice (C57BL/6 and C57BL/6 CD74^{ko}) intraperitoneally. The engraftment of the CLL-like cells was observed through blood sampling every week. Both groups, CD74^{wt} and CD74^{ko} mice, showed an engraftment of the malignant TCL1⁺ B cells after 2 weeks of injection. Measurement of CD5-expressing B cells in the peripheral blood over 6 weeks showed similar growth of the malignant cells in both CD74^{wt} and CD74^{ko} mice (Figure 18A). Additionally, both groups presented splenomegaly at the time of death with a similar spleen weight (CD74^{wt} 1.16 ± 0.1 g vs CD74^{ko} 1.17 ± 0.2 g) (Figure 18B). The median

survival of both groups was reached after 6 weeks with a insignificant longer survival of CD74^{ko} mice, 44 days, compared to CD74^{wt} mice, 36.5 days (Figure 18C).

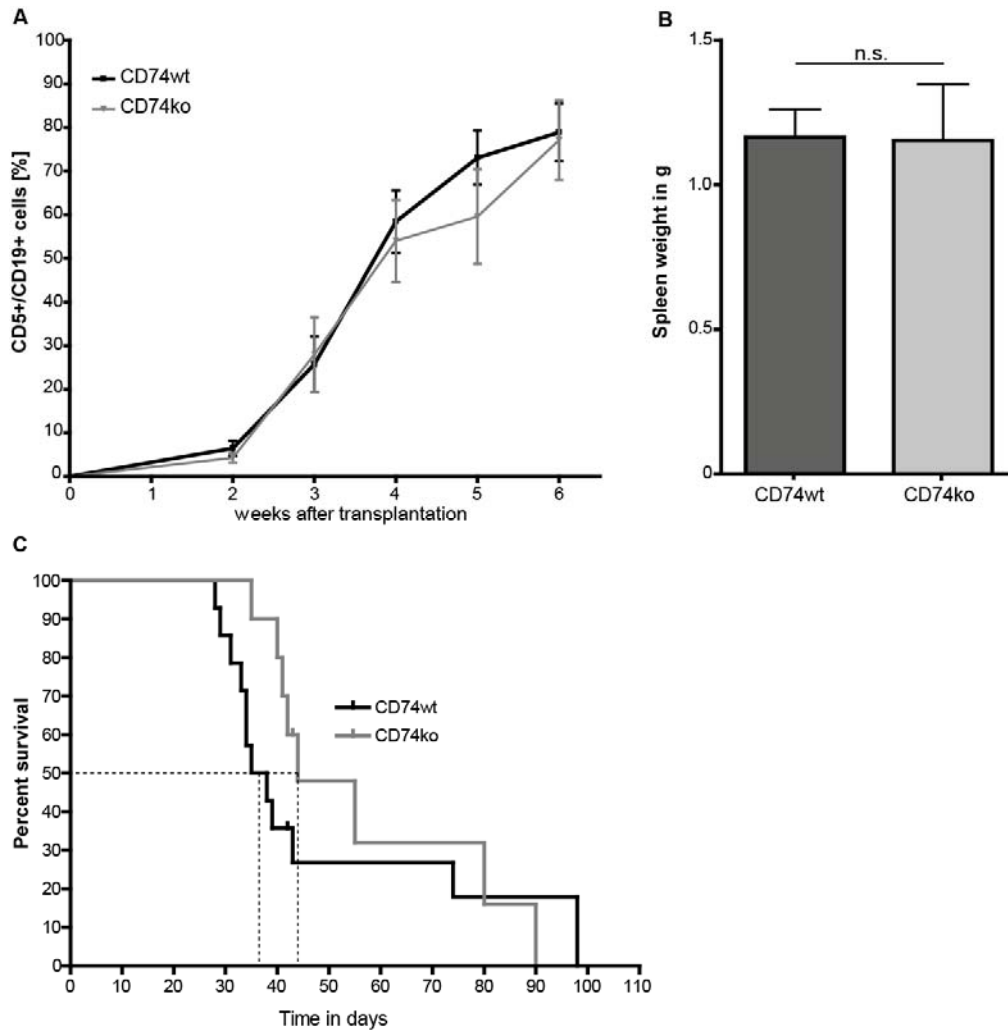


Figure 18: Syngeneic transplantation of malignant TCL1⁺ B cells

Isolated and purified malignant B cells from a leukemic C57BL/6J TCL1⁺ mice were injected i.p. into C57BL/6J CD74^{wt} or CD74^{ko} mice. In this experiment malignant cells obtained from two different mice were used. **A:** Engraftment of the CD5⁺ B cells was examined by taking blood samples from recipient mice every week. CD5⁺ B cells were measured using flow cytometry. [bars show SEM; CD74^{wt} n=12; CD74^{ko} n=13]. **B:** Spleen weight at time of death. [t-test, n.s. p>0.05, bars show SEM; CD74^{wt} n=7, CD74^{ko} n=6] **C:** Overall survival of recipient mice after injection of malignant B cells. [Mantel-Cox test, p>0.05; ticks show censored events; CD74^{wt} n=14, median survival 36.5 days; CD74^{ko} n=10, median survival 44 days]

2.7 CD74-dependent regulation of pro-survival pathways

Based on the available publications, showing CD74 as an important regulator of pro-survival pathways such as PI3K/AKT, MAPK and NF- κ B [94], the signaling in murine TCL1-induced CLL was analyzed. Using the malignant cells from TCL1⁺ CD74^{wt} mice

and comparing them to cells from $TCL1^+ CD74^{ko}$ mice, we aimed to distinguish between CD74-dependent and – independent signaling events.

2.7.1 Activation of pro-survival pathways in unstimulated murine CLL cells

To analyze the activation status of key players in the pro-survival pathways in B cells from $TCL1^+ CD74^{wt}$ and $TCL1^+ CD74^{ko}$ mice, splenocytes of highly leukemic mice were isolated and immediately lysed. Proteinlysates were analyzed by immunoblotting. In order to study the activation of the PI3K/AKT pathway, phosphorylation of AKT (S473) (pAKT) was detected and showed weak activation of AKT with only one mouse per group showing a strong band for pAKT. The phosphorylation of GSK3 β is inhibited by activated AKT. Here, the phosphorylation of GSK3 β (S9) also showed no clear difference between both genotypes. The activation of the MAPK pathway was studied by detecting the phosphorylation of ERK1/2 (T202/Y204) (pERK) and showed strong bands in the majority of the probes suggesting a high basal activation of the MAPK pathway in malignant B cells in both $TCL1^+ CD74^{wt}$ and $TCL1^+ CD74^{ko}$ mice. The activation of the NF- κ B pathway was also studied by detecting phosphorylation of p65 (S536) (pNF- κ B), which showed similar patterns in both groups.

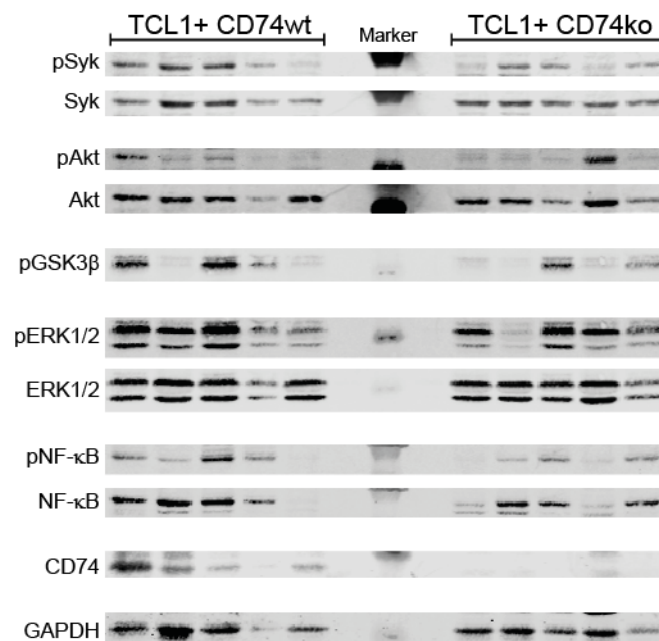


Figure 19: Activation of pro-survival pathways in unstimulated murine CLL cells

Proteinlysates from isolated splenocytes from leukemic $TCL1^+ CD74^{wt}$ and $TCL1^+ CD74^{ko}$ mice ($CD5^+/CD19^+$ -cells >50%) were separated using SDS-PAGE and transferred on to a nitrocellulose membrane. Immunodetection was performed using the Odyssey Imaging system. [one mouse per column; pSyk (Y525/526), pAKT (S473), pGSK3 β (S9), pERK (T202/Y204), pNF- κ B (S536)]

Since the B cell receptor signaling (BCR) is of particular importance for CLL cell survival and proliferation [23, 172], the activation of SYK, a kinase directly downstream of the B cell receptor, was also studied. Phosphorylation of SYK (Y525/Y526) (pSYK) was detected in all samples and was similar between $TCL1^+$ $CD74^{wt}$ and $TCL1^+$ $CD74^{ko}$ mice (Figure 19).

2.7.2 Activation of pro-survival pathways in MIF-stimulated murine CLL cells

$CD74$ -signaling was shown to be activated through binding of the macrophage migration inhibitory factor (MIF) [94], which then leads to the activation of the PI3K/AKT, MAPK and NF- κ B pathway. Here, splenocytes from leukemic $TCL1^+$ $CD74^{wt}$ and $TCL1^+$ $CD74^{ko}$ mice were stimulated with recombinant MIF and activation of pro-survival pathways was analyzed. To avoid B cell isolation, which might stimulate B cells beforehand, only splenocytes from highly leukemic mice with at least 70% malignant B cells ($CD5^+/CD19^+$) in the spleen were used.

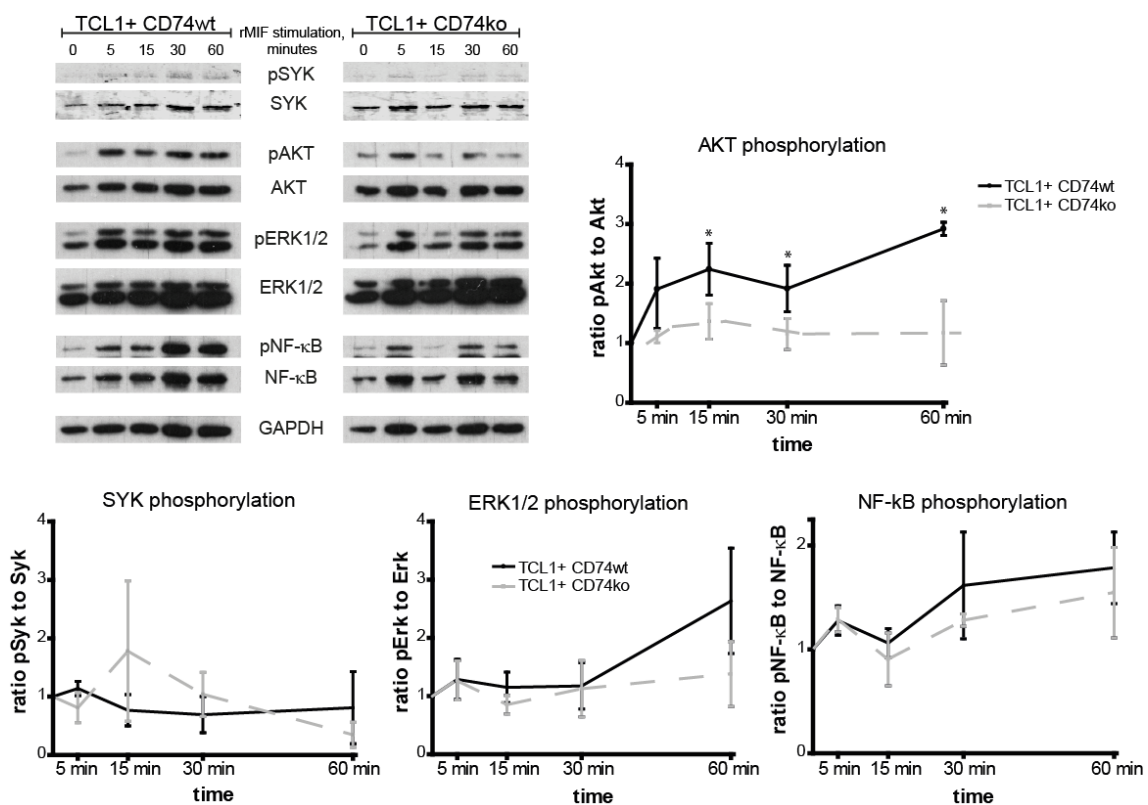


Figure 20: Activation of pro-survival pathways upon MIF stimulation

Splenocytes from leukemic $TCL1^+$ $CD74^{wt}$ and $TCL1^+$ $CD74^{ko}$ mice ($CD5^+/CD19^+$ -cells >70%) were isolated and starved for 4h. Stimulation with recombinant murine MIF (100ng/ml) was carried out for the depicted timepoints. Protein lysates were separated using SDS-PAGE and transferred on to a nitrocellulose membrane. Immunodetection was performed using ECL detection. Top left shows a representative Immunoblot. Densitometry of 4 independent experiments (3 for SYK and NF- κ B phosphorylation) was evaluated using ImageJ software. (pSyk (Y525/526), pAKT (S473), pERK (T202/Y204), pNF- κ B (S536)) [t-test; * $p < 0.05$; bars show SEM]

Proteinlysates were analyzed by immunoblotting for phosphorylation of SYK, AKT, ERK1/2 and NF- κ B. Figure 20 shows a clear AKT activation upon MIF stimulation in splenocytes from TCL1⁺ CD74^{wt} mice (median ratio pAKT to AKT 2 \pm 0.3), which is significantly diminished in leukemic cells from TCL1⁺ CD74^{ko} mice (median ratio pAKT to AKT 1.2 \pm 0.1). Phosphorylation of SYK, ERK1/2 and NF- κ B varied among the tested mice and showed no clear difference between both groups.

2.7.3 Signal transduction upon MIF stimulation in human CLL cells

To confirm the results from MIF stimulation experiments in murine leukemic cells, human CLL samples were also stimulated with recombinant human MIF (see 5.9). Similar to murine TCL1⁺ CD74^{wt} cells, a clear induction of AKT activation through phosphorylation was observed after stimulation with recombinant MIF (median ratio pAKT to AKT 1.47 \pm 0.2) (Figure 21). Activation of NF- κ B was also observed after 5 min of MIF stimulation, whereas ERK phosphorylation slightly decreased after stimulation with recombinant MIF.

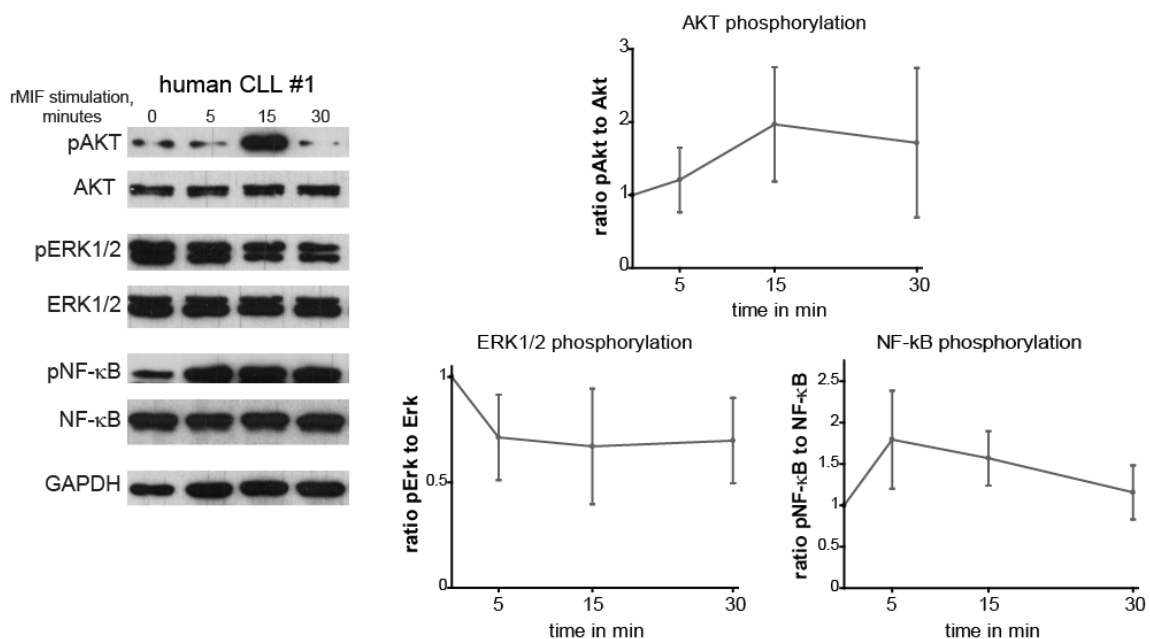


Figure 21: Activation of pro-survival pathways upon MIF stimulation in human CLL

CLL cells were isolated from blood samples and starved overnight. Stimulation with human recombinant MIF (100ng/ml) was carried out for the depicted timepoints. Protein lysates were separated using SDS-PAGE and transferred on to a nitrocellulose membrane. Immunodetection was performed using ECL detection or the Odyssey Imaging system. On the left a representative Immunoblot is shown.

Densitometry of 4 independent experiments was evaluated using ImageJ software. (pAKT (S473), pERK (T202/Y204), pNF- κ B (S536)). Patient status: Raji stage II, Binet stage A-B, IGVH unmutated, untreated, 2 of 4 patients del13q. [bars show SEM]

2.7.4 CD74 receptor stimulation in murine CLL cells

To test whether the signaling events from above (2.7.2) were CD74 receptor specific, splenocytes from leukemic mice were stimulated with an antibody against CD74. As described under 5.9 splenocytes from leukemic $TCL1^+$ $CD74^{wt}$ and $TCL1^+$ $CD74^{ko}$ mice were isolated and stimulated with the CD74 antibody or with an IgG control antibody. As depicted in Figure 22 on the left, both the CD74 antibody and the IgG control induced AKT and ERK1/2 phosphorylation in cells from a $TCL1^+$ $CD74^{wt}$ mouse. In cells from the leukemic $TCL1^+$ $CD74^{ko}$ mouse neither the CD74 antibody nor the IgG control antibody could noticeably induce AKT or ERK1/2 phosphorylation. Further testing of the antibody after removing of sodium azide in the antibody dilution and blocking the FC receptor on the tested cells, to avoid unspecific stimulation of the cells, also did show AKT phosphorylation upon stimulation with IgG control antibody (data not shown).

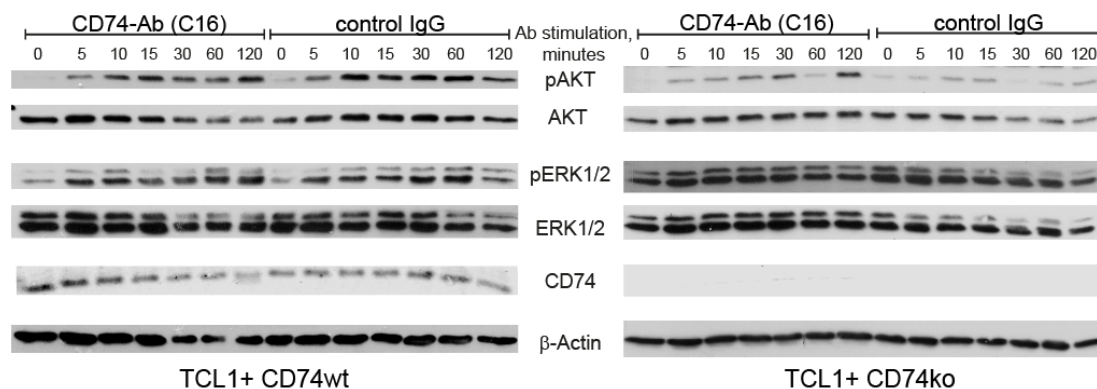


Figure 22: Activation of pro-survival pathways upon CD74 antibody stimulation

Splenocytes from a leukemic $TCL1^+$ $CD74^{wt}$ and $TCL1^+$ $CD74^{ko}$ mouse ($CD5^+/CD19^+$ -cells >70%) were isolated and starved for 4h. Stimulation with CD74 specific antibody or IgG control antibody (5 μ g/ml) was carried out for the depicted timepoints. Protein lysates were separated using SDS-PAGE and transferred on to a nitrocellulose membrane. Immunodetection was performed using ECL detection or the Odyssey Imaging system. [pAKT (S473), pERK (T202/Y204)].

2.7.5 MIF signaling involving CD74 co-receptors CXCR2, CXCR4 and CD44

MIF signaling does not only rely on CD74 receptor binding, but MIF also binds to the chemokine receptors CXCR2 and CXCR4. Both receptors were found to form a receptor complex with CD74 (reviewed in [73]). Next to CXCR2 and CXCR4, is CD44 an integral member of the CD74 receptor complex leading to MIF signal transduction [105]. All three receptors have been shown to work together with CD74 to activate the pro-survival signaling pathways involving PI3K/AKT in B cells [105, 173] (Figure 3).

2.7.5.1 CD74 co-receptor expression levels in $TCL1^+$ $CD74^{ko}$ mice

First the expression level of CD44 and CXCR4 on B cells from $TCL1^+$ $CD74^{ko}$ mice was measured in blood samples using flow cytometry.

CD44 expression is known to increase during leukemogenesis in $TCL1$ -transgenic mice [152]. Therefore surface expression levels of CD44 were measured in preleukemic and leukemic $TCL1^+$ $CD74^{wt}$ and $TCL1^+$ $CD74^{ko}$ mice (Figure 23). CD44 expression was further distinguished between normal B cells ($CD19^+$) and malignant B cells ($CD5^+/CD19^+$) in the tested groups. In correlation with published data, $TCL1^+$ $CD74^{wt}$ mice showed an increase in CD44 expression during leukemia development ($CD19^+$: preleukemic 24.81 ± 3.6 vs leukemic 52.08 ± 6.2 Δ MFI; $CD5^+/CD19^+$: preleukemic 47.17 ± 3.9 vs leukemic 65.67 ± 6.5 Δ MFI). The same increase was observed for CD44 expression in B cells from $TCL1^+$ $CD74^{ko}$ mice ($CD19^+$: preleukemic 44.76 ± 3.9 vs leukemic 91.22 ± 12.6 Δ MFI; $CD5^+/CD19^+$: preleukemic 76.21 ± 2.7 vs leukemic 99.89 ± 14.9 Δ MFI). Noticeably there is a significantly higher surface expression of CD44 overall in $TCL1^+$ $CD74^{ko}$ mice compared to $TCL1^+$ $CD74^{wt}$ mice.

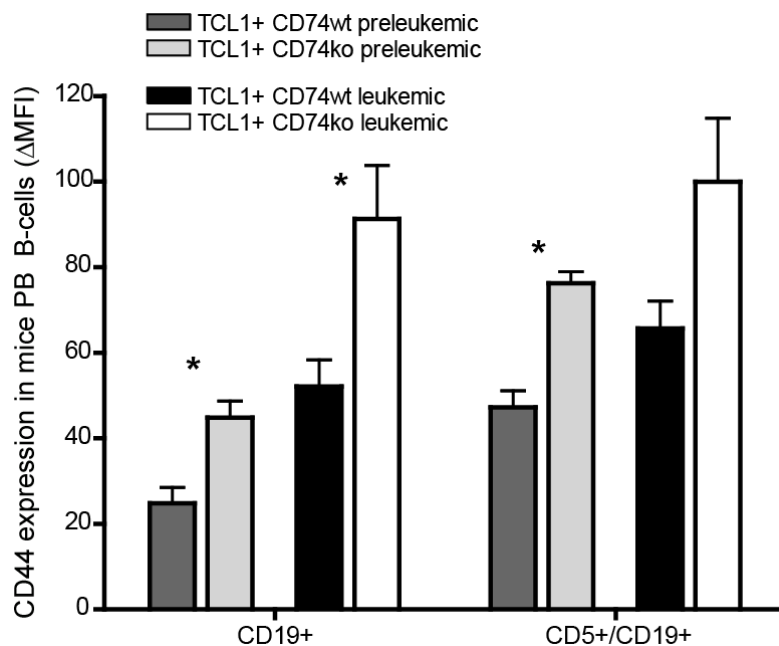


Figure 23: Surface CD44 expression on B cells from pre- and leukemic $TCL1^+$ mice

Blood samples from $TCL1^+$ $CD74^{wt}$ and $TCL1^+$ $CD74^{ko}$ mice were taken at a preleukemic stage (~ 3 months) and at the leukemic stage (~ 12 months). CD44 surface expression was measured using flow cytometry. Using the $CD19^+$ or $CD5^+/CD19^+$ -gate, mean fluorescent intensity (MFI) of the CD44 signal was normalized to the appropriate isotype control (Δ MFI). [Mann Whitney test, * $p < 0.05$, bars show SEM; $n = 4$ per group]

CXCR4 expression was also shown to be up regulated in CLL cells [174] and is known to form a functional receptor complex with CD74 binding MIF [116]. Therefore CXCR4 surface expression was measured in $TCL1^+ CD74^{ko}$ B cells from blood samples and compared to $TCL1^+ CD74^{wt}$, as well as to $TCL1^{wt} CD74^{wt}$ and $TCL1^{wt} CD74^{ko}$ mice (Figure 24). The results show no significant difference of CXCR4 expression in B cells ($CD19^+$) between wild type and TCL1-transgenic mice ($TCL1^{wt} CD74^{wt}$ 2.34 ± 0.8 vs $TCL1^+ CD74^{wt}$ 1.98 ± 0.7 Δ MFI). Additionally, deletion of CD74 did not influence CXCR4 expression on B cells in wild type or TCL1-transgenic background ($TCL1^{wt} CD74^{ko}$ 2.39 ± 0.5 vs $TCL1^+ CD74^{ko}$ 2.67 ± 0.3 Δ MFI).

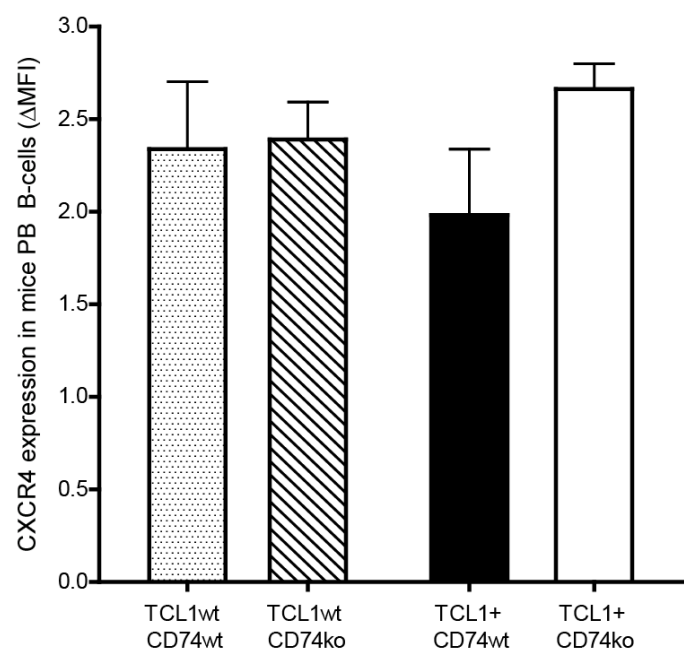


Figure 24: Surface CXCR4 expression on B cells from murine blood samples

Blood samples from $TCL1^{wt} CD74^{wt}$, $TCL1^{wt} CD74^{ko}$ and $TCL1^+ CD74^{wt}$, $TCL1^+ CD74^{ko}$ mice were taken at ~4 months of age. CXCR4 surface expression was measured using flow cytometry. Using the $CD19^+$ -gate, mean fluorescent intensity (MFI) of the CXCR4 signal was normalized to the appropriate isotype control (Δ MFI). [Mann Whitney test, n.s. $p > 0.05$, bars show SEM; $TCL1^{wt} CD74^{wt}$, $TCL1^{wt} CD74^{ko}$ $n=5$; $TCL1^+ CD74^{wt}$, $TCL1^+ CD74^{ko}$ $n=4$]

2.7.5.2 MIF stimulation of murine CLL cells upon CXCR2- and CXCR4- or CD44 inhibition

Since CXCR2, CXCR4 and CD44 are involved in MIF/CD74-dependent signaling the influence of these receptors/co-receptor on the CD74-dependent AKT activation in murine malignant B cells was further studied. Therefore stimulation experiments with recombinant MIF from 2.7.2 were performed using CXCR2- and CXCR4-inhibitors or a CD44 blocking antibody, to exclude MIF signal transduction through those additional

receptors. Figure 25 shows a representative immunoblot of murine leukemic cells stimulated with recombinant MIF (rMIF) under inhibiting conditions. As seen before, cells from the $TCL1^+ CD74^{wt}$ mouse showed an activation of AKT when stimulated with rMIF, which is diminished in cells from a $TCL1^+ CD74^{ko}$ mouse. Addition of CXCR2 and CXCR4 inhibitors led to an increase in the basal pAKT-level compared to cells starved without inhibitors ($TCL1^+ CD74^{wt}$ CXCR 2+4 0min 1.46), while in $TCL1^+ CD74^{ko}$ the basal pAKT-level decreased ($TCL1^+ CD74^{ko}$ CXCR 2+4 0min 0.39). Nonetheless, pAKT levels in both mice slightly increased upon stimulation with rMIF. Inhibition of CD44 also led to a decreased pAKT-level in $TCL1^+ CD74^{ko}$ before stimulation, which couldn't be induced after stimulation with rMIF. In contrary, activation of AKT was unaffected by CD44 antibody treatment in $TCL1^+ CD74^{wt}$ cells.

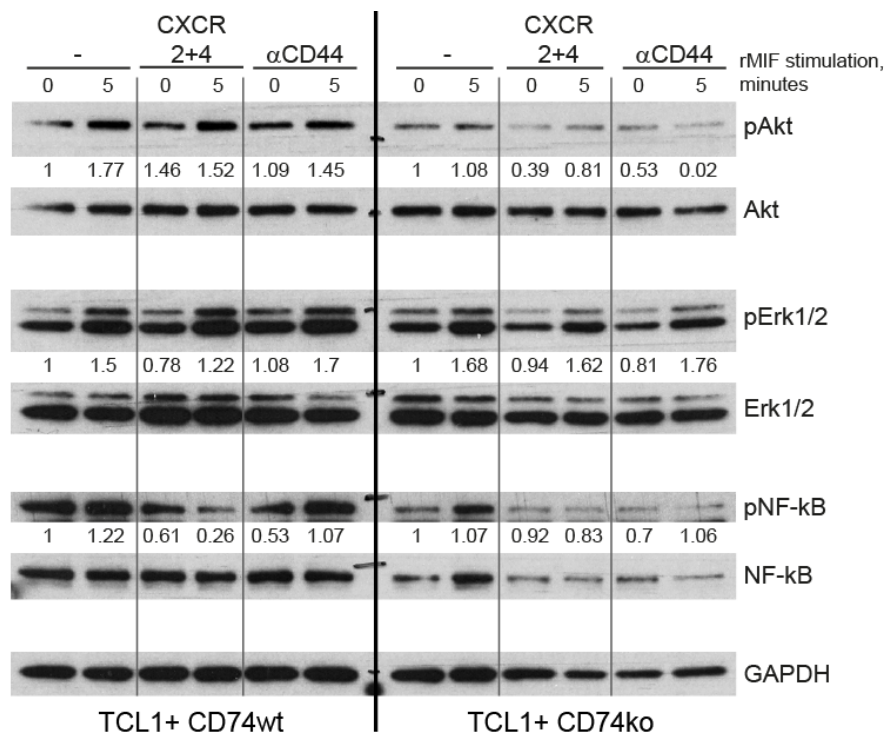


Figure 25: rMIF stimulation under CXCR2 and CXCR4 or CD44 inhibition

Splenocytes from leukemic $TCL1^+ CD74^{wt}$ and $TCL1^+ CD74^{ko}$ mice ($CD5^+/CD19^+$ -cells >70%) were isolated: Cells were serum starved in culture medium containing CXCR2 and CXCR4 inhibitors (SD225002: 45 nmol and AMD31000: 30 nmol respectively) or CD44 inhibiting antibody (IM7: 10 μ g/ml) for 4h. Stimulation with recombinant murine MIF (100ng/ml) was carried out afterwards for the depicted timepoints. Protein lysates were separated using SDS-PAGE and transferred on to a nitrocellulose membrane. Immunodetection was performed using ECL detection. Densitometry was evaluated using ImageJ software. [pAKT (S473), pERK (T202/Y204), pNF- κ B (S536)]

Activation of ERK was induced through stimulation with rMIF in both genotypes and was unaffected by treatment with the inhibitors or the CD44 blocking antibody. Phosphorylation of NF- κ B was slightly induced after stimulation with rMIF and was

unaffected by CD44 antibody treatment in both genotypes. Repetition of the experiment with longer stimulation times showed that inhibition of the chemokine receptors CXCR2 and CXCR4 as well as CD44 did result in similar MIF-induced AKT, ERK1/2 and NF- κ B phosphorylation in TCL1⁺ CD74^{ko} compared to TCL1⁺ CD74^{wt} cells (Figure 26).

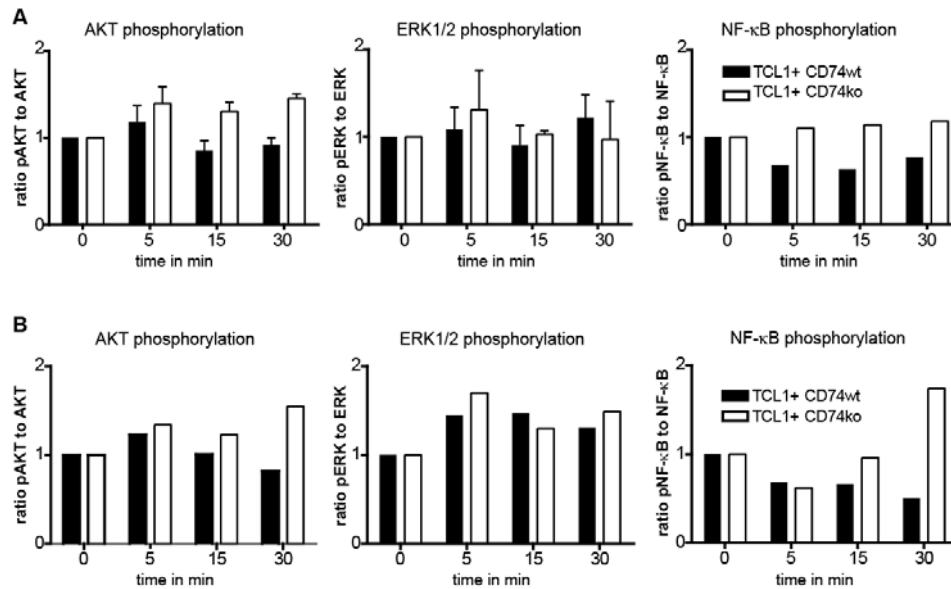


Figure 26: Densitometrical analyses of rMIF stimulation under CXCR2 and CXCR4 or CD44 inhibition

Splenocytes from leukemic TCL1⁺ CD74^{wt} and TCL1⁺ CD74^{ko} mice (CD5⁺/CD19⁺-cells >70%) were isolated. Stimulation with recombinant murine MIF (100ng/ml) was carried out after starvation for the depicted timepoints. Protein lysates were separated using SDS-PAGE and transferred on to a nitrocellulose membrane. Immunodetection was performed using ECL detection. Densitometry was evaluated using ImageJ software. [pAKT (S473), pERK (T202/Y204), pNF- κ B (S536)] **A**: Cells were starved for 4h in culture medium containing CXCR2 and CXCR4 inhibitors (SD225002: 45 nmol and AMD31000: 30 nmol respectively. [n=2 for AKT and ERK phosphorylation, n=1 for NF- κ B phosphorylation; bars show SEM] **B**: Cells were serum starved for 4h in culture medium containing CD44 inhibiting antibody (IM7: 10 μ g/ml). [n=1]

2.8 B cell development in TCL1⁺ CD74^{ko} mice

CD74 has been found to control several aspects of the immune system. One example is its involvement in B cell maturation which leads to an developmental block of CD74^{ko} B cells at the immature stage [121]. Phenotypically, the differentiation block is characterized by an accumulation of marginal zone B cells and a decreased life-span of follicular B cells [123]. Therefore the B cell maturation in TCL1⁺ CD74^{ko} mice was analyzed and compared to TCL1⁺ CD74^{wt} and TCL1^{wt} control mice. Splenic B cells of young (~2 months) and aged (~9 months) mice were analyzed by flow cytometric

analyses using antibodies against CD19, CD21/35, CD45 and IgD, which allowed the determination of different stages of B cell development in the spleen (transitional stage 1, transitional stage 2 and marginal zone B cells) (Figure 27).

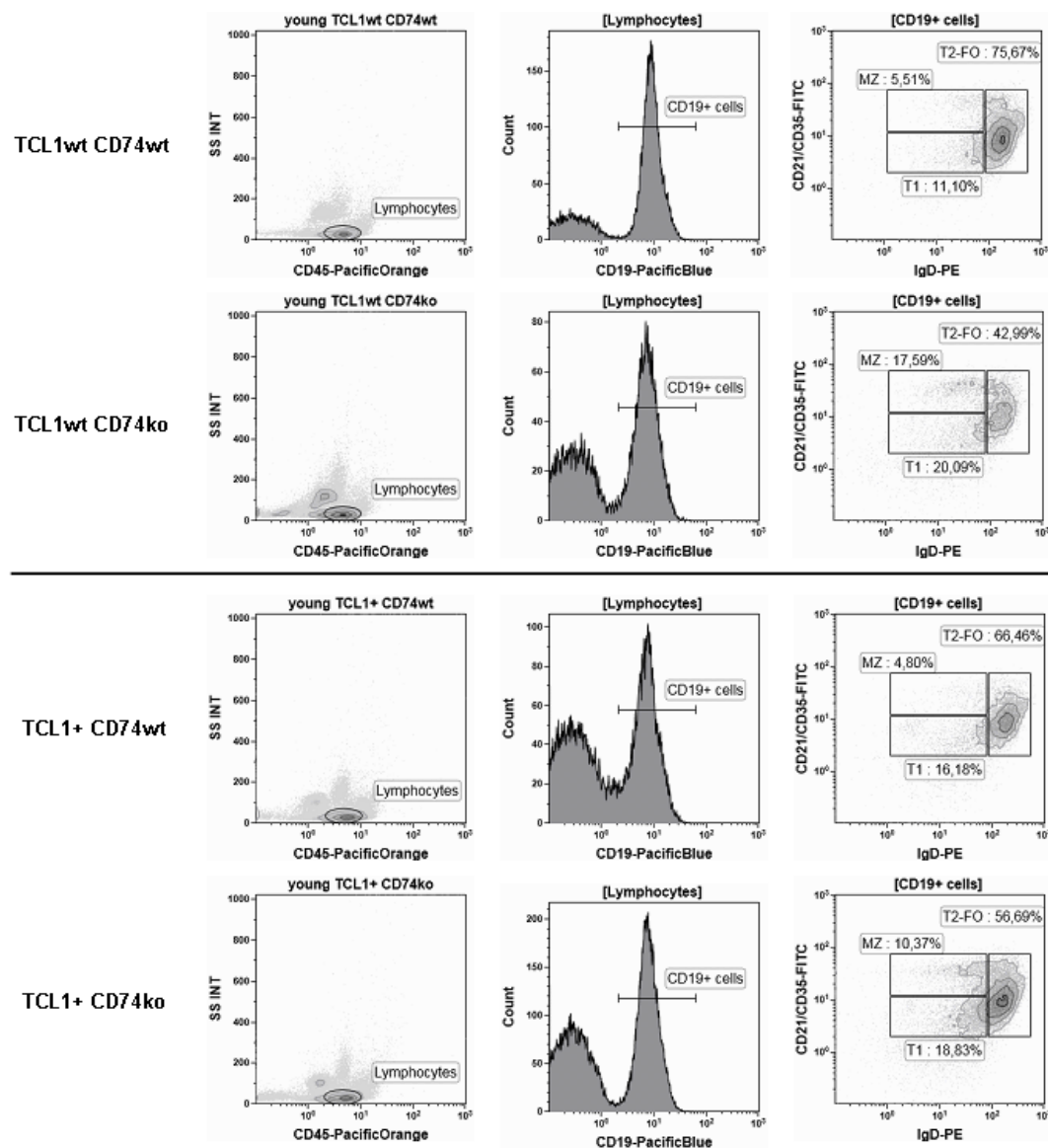


Figure 27: Flow cytometric analyses of B cell maturation in the spleen

Splenocytes were isolated and stained for flow cytometric analyses of B cell subpopulations. Splenocytes were stained with CD19, CD21/CD35, CD45 and IgD. Lymphocytes were clearly distinguishable by CD45 expression and the side scatter. Using the lymphocyte gate, B cells were distinguished by CD19 expression. Gating on CD19⁺ cells, B cells from transitional stage 1 (CD21/35^{low}, IgD^{low}), transitional stage 2 (CD21⁺, IgD^{high}) and marginal zone (CD21^{high}, IgD^{low}) were distinguished.

As published before [121], young TCL1^{wt} CD74^{ko} mice showed a developmental block between the transitional stages 1 and 2 and a significant increase in marginal zone B cells compared to wild type mice (Transitional 1: TCL1^{wt} CD74^{wt} 10.5±0.9 % vs. TCL1^{wt} CD74^{ko} 20.6±1.1 %; Transitional 2: TCL1^{wt} CD74^{wt} 75.9±1.8 % vs. TCL1^{wt}

CD74^{ko} 41.4±1.2 %; Marginal Zone: TCL1^{wt} CD74^{wt} 5.3±0.8 % vs. TCL1^{wt} CD74^{ko} 19±0.6 %) (Figure 28A). This effect was completely abolished in young mice crossed with the E μ -*TCL1*-transgenic mouse. Only an increase in marginal zone B cells was still observed in TCL1⁺ CD74^{ko} compared to TCL1⁺ CD74^{wt} mice (Marginal Zone: TCL1⁺ CD74^{wt} 6.8±0.2 % vs. TCL1⁺ CD74^{ko} 10.3±0.4 %).

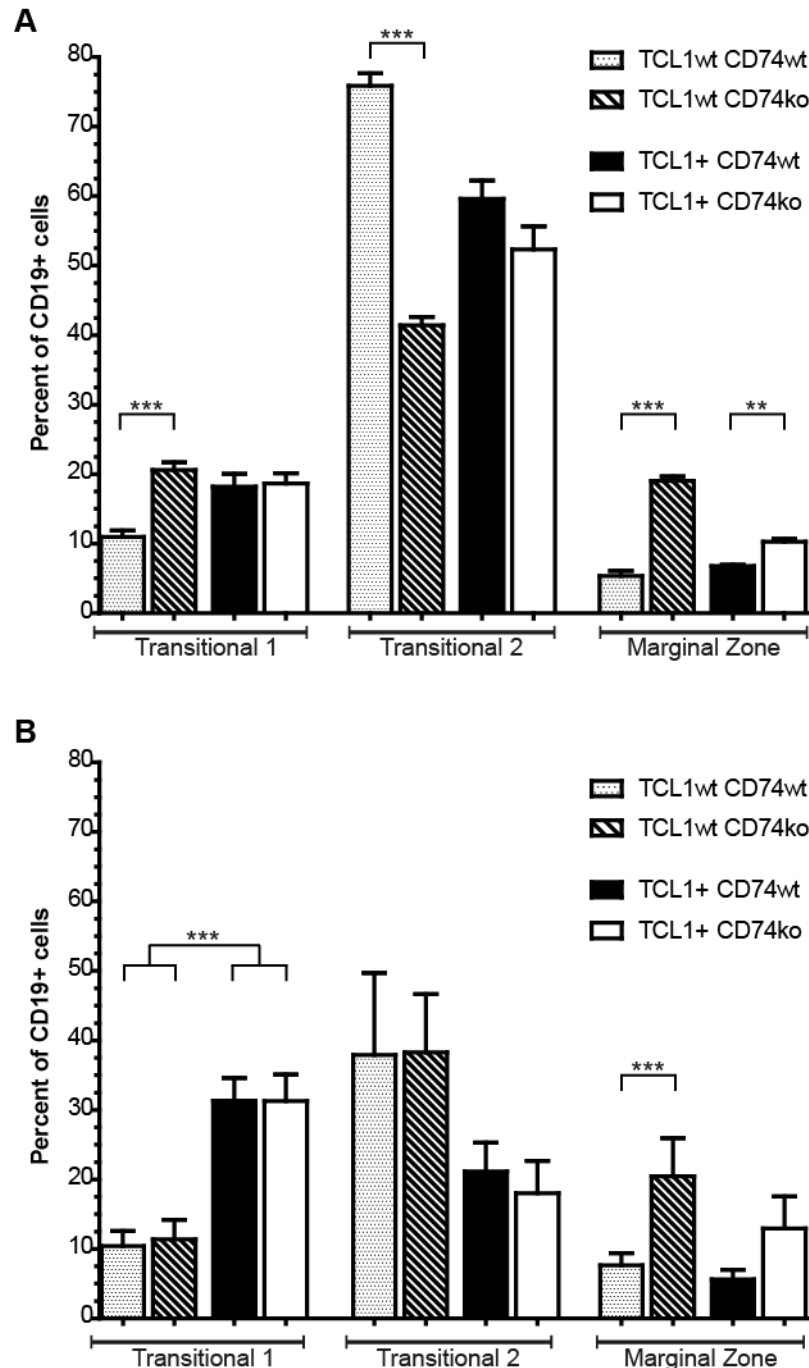


Figure 28: B cell development in young and old TCL1⁺ CD74^{ko} mice

Splenocytes were analyzed by flow cytometric analyses for different B cell subpopulations. **A:** Young mice (~2 months). [n=3 per group; t-test, *** p<0.0005, ** p<0.005; bars show SEM]. **B:** Aged mice (~9 months). [t-test, ** p<0.005, *** p<0.0005, bars show SEM; TCL1^{wt} CD74^{wt} and TCL1^{wt} CD74^{ko} n=6, TCL1⁺ CD74^{wt} n=9, TCL1⁺ CD74^{ko} n=8;] (B cell subpopulations from transitional stage 1 (CD21/35^{low}, IgD^{low}), transitional stage 2 (CD21⁺, IgD^{high}) and marginal zone (CD21^{high}, IgD^{low})).

To further analyze B cell development upon CD74 deletion in a leukemic background, splenocytes from aged mice were also measured via flow cytometry (Figure 28B). While there was still a significant accumulation of marginal zone B cells in aged $TCL1^{wt} CD74^{ko}$ mice compared to $TCL1^{wt} CD74^{wt}$ mice (Marginal Zone: $TCL1^{wt} CD74^{wt}$ 7.6±1.8 % vs. $TCL1^{wt} CD74^{ko}$ 20.5±5.5 %), there was a similar amount of transitional stage 1 and 2 B cells in the spleen. In leukemic $E\mu-TCLI$ -transgenic mice, the amount of the three tested B cell subpopulations was similar between CD74-wild type and -knock out mice. Interestingly, leukemic mice, $TCL1^+ CD74^{wt}$ and $TCL1^+ CD74^{ko}$, showed a significant increase in B cells of the transitional stage 1 compared to $TCL1^{wt} CD74^{wt}$ and $TCL1^{wt} CD74^{ko}$ mice.

3 Discussion

This project aimed to clarify the influence of the CD74 receptor during B cell lymphomagenesis and the mechanisms underlying CD74-dependent signaling in B cells using the CLL mouse model.

After studies within our group showed the importance of the chemokine MIF and the surface protein CD44 in the pathogenesis of TCL1-induced CLL [44, 152], both involved in CD74 signaling pathways, a central role for CD74 in CLL development and CLL survival signaling was postulated.

This study shows, that targeted genetic deletion of *Cd74* does not influence the development of CLL in the E μ -*TCL1*-transgenic mice.

3.1 CD74 expression is upregulated in E μ -*TCL1*-transgenic mice

This study used the commonly utilized E μ -*TCL1*-transgenic mouse model. At around 8-12 months these mice develop a CLL-like disease resembling the aggressive form of the disease [54].

To test the validity of the E μ -*TCL1* mouse model for the analysis of CD74, expression of CD74 was measured during leukemia development. Results show that the expression of CD74 is upregulated in CD5-positive B cells from the peripheral blood, whereas it stays similar to wild type B cells in the spleen. While results of CD74 overexpression in malignant cells from the peripheral blood are in line with the literature showing an increase of CD74 expression in human CLL cells from patient blood samples [142], uniform expression of CD74 in malignant B cells from the spleen has not been described before. The differential regulation of CD74 expression between varying compartments is hinting to a correlation between the microenvironment and the CD74 expression in malignant B cells. Analyses of CD74 expression in human CLL cells from proliferative centers such as the lymph node could provide further insight.

3.2 CD74 deletion does not influence development in TCL1-induced CLL

E μ -*TCL1*-transgenic mice were crossed with the CD74^{ko} mice and resulting TCL1⁺ CD74^{ko} mice then were compared to the well described TCL1⁺ CD74^{wt} mice [175]. Although CD74 expression is over expressed in CLL cells, monitoring of the mice during disease development showed that overall survival of E μ -TCL1-transgenic mice was not influenced by CD74 deletion.

Accordingly, $TCL1^+ CD74^{ko}$ mice showed similar increase in the leukocyte count and number of malignant B cells in the course of disease development. Proliferation and the apoptosis rate of the malignant cells in the $TCL1^+ CD74^{ko}$ model also show similar results to $TCL1^+ CD74^{wt}$ mice. Additionally, infiltration of malignant cells into lymphoid tissue is independent from CD74 expression leading to similar enlargement of liver and spleen at time of death. Taken together the results show that CD74 deletion does not influence disease development in TCL1-induced CLL.

These results are unexpected since CD74 has been shown to be an important factor in pro-survival signaling in B cells [111] and is suggested as a target for B cell neoplasia therapy [130]. Previous studies on CD74 in B cell survival were using primary human CLL cells from blood samples or B lymphoma cell lines [46, 105] excluding the microenvironment, an important factor for CLL survival (reviewed in [36]). Here the role of the microenvironment was taken into consideration by using the CLL mouse model. CLL cells actively shape their microenvironment by producing cytokines, chemokines and by subverting normal accessory cells to promote leukemia cell survival [43]. This dynamic process might compensate the loss of CD74 signaling in B cells and lead to “normal” CLL development.

Another factor plays the proto-oncogene *TCL1*, which is overexpressed in the B cells of the mouse model. TCL1 itself has been shown to interact with AKT and to enhance its kinase activity leading to the transduction of anti-apoptotic and proliferative signals [65], which itself could be a strong supporter for CLL cells.

Despite the microenvironment and the *TCL1* overexpression, deletion of the CD74-ligand MIF or the CD74-co-receptor CD44 is sufficient to delay CLL development in the $E\mu$ -*TCL1* mouse model [44, 152]. MIF is a ubiquitously expressed proinflammatory and immunoregulatory cytokine involved in inflammation by promoting the release of pro-inflammatory mediators, such as $TNF\alpha$ and interleukins (IL-1 β , IL-6, IL-8) [176], which themselves have been implicated to support CLL cell survival [39]. Additionally, MIF does not bind to CD74 exclusively. The chemokine receptors CXCR2 and CXCR4 also are high-affinity receptors for MIF, triggering cell responses [101]. Next to binding to surface receptors, MIF is endocytosed into the cells leading to endosomal signaling responses [173]. Reinart *et al.* suggested that MIF supports the expansion of the malignant clone via the accumulation of tumor associated macrophages (TAMs) to the leukemia homing organs [44], but it remains to be explored if MIF secreted by B cells or macrophages is the main source.

Nonetheless the process of MIF-induced TAM accumulation into leukemia homing organs might be independent of CD74 signaling. Indeed, screening for myeloid cells and macrophages in the spleen of leukemic mice shows that infiltration of macrophages and dendritic cells is comparable between $TCL1^+ CD74^{wt}$ and $TCL1^+ CD74^{ko}$ mice, supporting the hypothesis that MIF regulated migration of TAMs is CD74 independent. In the case of the CD74-co-receptor CD44, Fedorchenko *et al.* showed that stimulation of the CD44 receptor by its natural ligands hyaluronic acid and chondroitin sulfate promotes CLL survival *in vitro* [152], supporting the possibility that CD44 promotes CLL survival by a mechanism independent of MIF/CD74 signaling.

In another attempt, the role of CD74 in the tumor microenvironment was tested. While TCL1 expression is restricted to B cells, deletion of *Cd74* is ubiquitously expressed in the tested mouse model. To dissect the influence of CD74 in cells from the CLL microenvironment, e.g. dendritic cells or monocytes, syngeneic transplantation experiments were established in the laboratory. Results display similar engraftment of established TCL1 B cell clones ($C57Bl/6J TCL1^{+/+}$) in $CD74^{ko}$ mice ($C57Bl/6J CD74^{-/-}$) and $CD74^{wt}$ mice ($C57Bl/6J CD74^{wt/wt}$), showing that engraftment of a B cell clone was independent from CD74 expression in the microenvironment.

To elucidate the role of CD74 in the B cell clone, transplantation of an established $TCL1^+ CD74^{ko}$ B cell clone ($B6C3H E\mu-TCL^{wt/+} CD74^{-/-}$) was carried out but was not successful (data not shown). The syngeneic genetic background of experiment mice is crucial for successful transplantation [171]. Therefore transplantation within the $C57Bl/6J$ background is working, while the transplantation within the undefined and mixed background of the $B6C3H E\mu-TCL1$ -transgenic mice was unsuccessful in this study.

3.3 AKT kinase activation upon MIF stimulation is CD74-dependent

The established $TCL1^+ CD74^{ko}$ mouse model provides a good tool to further analyze the mechanisms underlying MIF/CD74-dependent signaling in B cells.

First, the activation of signaling pathways in unstimulated B cells of both $TCL1^+ CD74^{wt}$ and $TCL1^+ CD74^{ko}$ mice was analyzed, showing the same status between both genotypes.

MIF stimulation experiments show that only AKT activation is CD74-dependent, while the other tested pro-survival pathways involving SYK, ERK1/2 and NF- κ B are unaffected. In concurrence, published data show that binding of MIF to CD74 leads to

transmission of survival signals through the AKT pathway [94]. Nonetheless, it has also been shown that ERK1/2 and NF- κ B pathways are activated by MIF binding to CD74 in cell lines, macrophages, monocytes and Raji B cells [111, 113], which cannot be observed in the here tested murine B cells.

Data from the literature using the CD74 antibody (C-16) to analyze CD74 specific activation could not be reproduced [46, 111, 139]. Here stimulation with the isotype control led to similar signaling events in cells stimulated with the CD74 antibody.

To verify the results from the murine samples, primary CLL cells from patient samples were also stimulated with recombinant MIF and analyzed for the activation of the pro-survival signaling. Similarly, AKT activation upon MIF stimulation is observed. Phosphorylation of ERK1/2 remained unaffected, while NF- κ B activation was induced. Overall these results show that AKT activation is induced upon MIF stimulation in the murine and the human system, but these signaling events are not efficient to induce proliferation or cell survival in B cells.

Since MIF signaling responses are also transmitted through the chemokine receptors CXCR2 and CXCR4 and the CD74 co-receptor CD44 [45, 101], their influence on MIF stimulated signaling activation was addressed. First the expression of CXCR4 and CD44 has been measured in the mouse models showing that deletion of CD74 in E μ -*TCL1*-transgenic mice increases the surface expression of CD44 in B cells. CXCR4 expression remained similar between both mouse models although CXCR4 as well as CD44 expression are known to increase during CLL development [152, 174]. Taking into consideration that CXCR4 expression had been measured in young mice with not fully manifested leukemia, differential CXCR4 expression is possible in highly leukemic mice. The chemokine receptor CXCR2 has been described not to be expressed on splenic B cells [177] and therefore has not been measured.

Nonetheless inhibitors for both chemokine receptors have been included in experiments to exclude the possibility of MIF signaling via CXCR2 or CXCR4. Stimulation experiments with CXCR2 and CXCR4 inhibition before MIF addition show a skewed AKT activation profile suggesting unspecific activation of the cells by these inhibitors before MIF stimulation. Although both inhibitors have been shown to be highly specific receptor antagonist for human cells [177-179], it is possible that the murine system reacts differently. Moreover, MIF might activate other pathways, which have not been described before.

Similarly, AKT activation upon MIF stimulation seems to be unaffected by CD44 antibody treatment. CD44 is known to mainly transmit MIF/CD74-induced ERK1/2 activation [105], but in this experiment treatment with the CD44 antibody could not inhibit MIF-dependent ERK1/2 activation. The CD44 antibody IM7, used in the experiments, does not block the binding of hyaluronic acid to CD44 [180] but has been shown to efficiently block CD44 transmitted cellular functions [181]. Additionally, the CD44 antibody induces cell death in malignant B cells from E μ -*TCL1*-transgenic mice *in vitro* [152]. The question whether the CD44 antibody IM7 is sufficiently blocking MIF/CD74-transmitted signaling through CD44 has not been analyzed yet. Further analyses with genetically deleted CXCR2, CXCR4 and especially CD44 could provide additional insights into MIF-dependent signaling events.

To gain further insight into CD74 dependent signaling, gene array analyses with RNA samples from splenic B cells of young pre-leukemic $TCL1^+$ $CD74^{wt}$ and $TCL1^+$ $CD74^{ko}$ mice has been screened (data not shown). Pathway analyses and manually viewing of differential expressed genes between $TCL1^+$ $CD74^{wt}$ and $TCL1^+$ $CD74^{ko}$ mice did not reveal differential expression of genes involved in B cell signaling events. Gene array analyses with samples from aged leukemic mice could provide further insight into the gene expression profile of malignant B cells from $TCL1^+$ $CD74^{ko}$ mice.

3.4 *TCL1* overexpression alters B cell development in $CD74^{ko}$ mice

Overexpression of *TCL1* in B cells of $CD74^{ko}$ mice diminishes the B cell differentiation block phenotypically found in young $CD74^{ko}$ mice. Studies have shown that CD74 is an essential cofactor for B cell maturation by mediating activation of the NF- κ B transcription program [113]. Mice deficient for CD74 show accumulation of immature B cells in the transitional stage 1 (T1) and the marginal zone (MZ) B cells in the spleen, while follicular, transitional stage 2 (T2) B cells are decreased [123]. Here those findings are reproduced in young $TCL1^{wt}$ $CD74^{wt}$ and $TCL1^{wt}$ $CD74^{ko}$ mice.

However, in young mice transgenic for *TCL1*, levels of T1 B cells and T2 B cells are similar independently from CD74 deletion. Only MZ B cells are still significantly accumulated in $TCL1^+$ $CD74^{ko}$ splenocytes. Therefore, *TCL1* seems to play an important role in B cell differentiation that might compensate for the lack of CD74 signaling. In fact, *TCL1* has been implicated to cooperate with the NF- κ B pathway [182]. More specifically, Ropars *et al.* showed direct bind of *TCL1* to I κ B, the inhibitor of NF- κ B transcription factors, which may increase the concentration of free NF- κ B

molecules [67]. Our results suggest a higher NF- κ B activation in $TCL1^+$ $CD74^{ko}$ mice which is able to overcome diminished CD74-dependent NF- κ B signaling. To test this hypothesis, several attempts to analyze NF- κ B activation in B cells from wild type and $E\mu$ -*TCLI*-transgenic mice using the electrophoretic mobility shift assay (EMSA) have been done showing varying results between the tested mice (data not shown). So far, the hypothesis could not be verified and could be addressed in future experiments.

To have a complete picture of the B cell development in the mouse models from this project, aged or leukemic mice have been analyzed as well. Aged mice show similar amounts of B cell subpopulations independent of the CD74 status. In all tested genotypes the amount of immature B cells is comparable between CD74 wild type and knock out mice. Only MZ B cells are still significantly increased upon CD74 deletion. It seems that defective B cell development in $CD74^{ko}$ mice only becomes apparent in young mice, while older $CD74^{ko}$ mice only shown an increase in MZ B cells.

Interestingly, leukemic $E\mu$ -*TCLI*-transgenic mice show a significant increase in T1 B cells regardless of CD74 deletion compared to wild type mice. Published data shows that CLL cells from $E\mu$ -*TCLI*-transgenic mice show a $CD5^+$, $CD19^+$, $CD21^{low}$, IgD^{low} phenotype [183], so that malignant B cells from the mice tested here fall in the category of transitional stage 1 B cells (characterized as $CD19^+/CD21/35^{low}$, IgD^{low}).

3.5 Conclusion and Outlook

For the first time, this study analyzed the role of CD74 in B cell lymphomagenesis *in vivo* by using the E μ -*TCL1*-transgenic CLL mouse model.

Previous studies on MIF, the high affinity ligand of CD74, and the CD74 co-receptor CD44, have shown that both molecules promote disease development in the CLL mouse model, postulating a central role for CD74 in CLL development and CLL survival signaling.

In this study we could show that like in human CLL, CD74 expression is upregulated in malignant B cells of E μ -*TCL1*-transgenic mice. Furthermore, targeted genetic deletion of *Cd74* in this CLL model does not influence the development of CLL, the proliferation and apoptosis of the malignant B cells or the overall survival of the animals. While MIF induced AKT activation, a kinase involved in B cell pro-survival signaling, it failed to stimulate a number of additional pathways through CD74, such as MAPK/ ERK1/2 and NF- κ B.

Additionally, we found that TCL1 overexpression diminishes the CD74-related B cell maturation block in mice showing the impact of TCL1 on B cell signaling. Although we could not show the effect of TCL1 on AKT and NF- κ B signaling in this study, published data show that TCL1 activates both pathways. Therefore future studies could focus on the role of TCL1 onto B cell development and B cell survival signaling.

Taken together this study showed that targeted gene deletion of *Cd74* - other than its ligand MIF and its co-receptor CD44 - does not influence the development of CLL in E μ -*TCL1*-transgenic mice and suggested that the pathways mediated by MIF through CD74 are not sufficiently potent to promote growth of CLL cells.

4 Materials

4.1 Instruments

Device and Type	Company
4°C Fridge; -20°C and -80°C Freezer	AEG, Stockholm, Schweden
ABI 3130 sequencer	Applied Biosystems, Darmstadt
Centrifuge 5415 R, 5415 D, 5810 R	Eppendorf, Hamburg
Counting chamber Typ: Neubauer	Marienfeld, Lauda Königshofen
Elisa-Reader µQuant	BioTek, Bad Friedrichshall
Film processor Curix 60	AGFA, Köln
Gallios™ 10/3 flow cytometer	Beckmann Coulter, Krefeld
Incubator	Heraeus, Hanau
Incubator C200	Labotec, Göttingen
Lab water purification system Elix Advantage 15	Millipore, Schwalbach/Ts
Laminar flow hood Laminar Air HA2448	Heraeus, Hanau
Lasergene software	DNASar; Madison, WI, USA
Medical X-Ray film	Fujifilm, Düsseldorf
Microscope	Axiophot Zeiss, Göttingen
Mini centrifuge Rotilabo®	Carl Roth GmbH & Co. KG, Karlsruhe
NanoDrop 1000	PEQLAB Biotechnologie, Erlangen
Nitrogen tank	Thermo Fisher Scientific, Bonn
Odyssey® Imaging system	Li-Cor Bioscience, Lincoln, USA
PCR-machine Mastercycler EPgradient S	Eppendorf, Hamburg
pH meter	Mettler-Toledo, Schwerzenbach
Power supply peqPower 300	PEQLAB Biotechnologie, Erlangen
Protein electrophoresis system	BioRad Laboratories, München
QuadroMACS™ separator	Miltenyi Biotech, Bergisch Gladbach
Radiographic cassette	AGFA, Köln
Scanner Pannoramic 250 Flash	3DHISTECH Kft., Budapest, Ungarn
Scanner Perfection 3490 Photo	Epson, Meerbusch
Single channel pipettes Research® variabel	Eppendorf, Hamburg
Special accuracy weighing machine Navigator™	OHAUS, Parsippany, NJ, USA
ThermoMixer	Eppendorf, Hamburg
Trans-Blot DS Semi Dry	BioRad Laboratories, München

UV-Camera system	LTF Labortechnik, Wasserburg
Vortex	VWR, Darmstadt
Water pump jet	Brand, Wertheim
Waterbath1003	Heidolph, Schwabach
Welding equipment	TEW, Reseda, USA
XE-5000 hematology-analyzer	SysmexEurope GmbH, Norderstedt

4.2 Chemicals and reagents

Chemicals and reagents	Company
2-mercaptoethanol	Carl Roth GmbH & Co. KG, Karlsruhe
5x <i>Green GoTaq® Reaction Buffer</i>	Promega, Mannheim
Acetic acid	Carl Roth GmbH & Co. KG, Karlsruhe
Acrylamide 30%	Carl Roth GmbH & Co. KG, Karlsruhe
Agarose	Biozym, Hess, Oldendorf
Ammonium chloride (NH ₄ Cl)	Carl Roth GmbH & Co. KG, Karlsruhe
Ammonium persulfate (APS)	Carl Roth GmbH & Co. KG, Karlsruhe
<i>Bovine Serum Albumin</i> (BSA)	PAA, Pasching, Österreich
Bromphenol blue	Carl Roth GmbH & Co. KG, Karlsruhe
Calcium chloride (CaCl ₂)	Carl Roth GmbH & Co. KG, Karlsruhe
CellPack	BD Pharmingen™, Heidelberg
<i>Complete mini</i> (Protease inhibitor)	Roche, Mannheim
DABCO	Carl Roth GmbH & Co. KG, Karlsruhe
Disodium hydrogen phosphate (Na ₂ HPO ₄)	Carl Roth GmbH & Co. KG, Karlsruhe
dNTP's	Fermentas GmbH, St. Leon-Rot
DTT	AppliChem GmbH, Darmstadt
Ethanol	Carl Roth GmbH & Co. KG, Karlsruhe
Ethidium bromide	Carl Roth GmbH & Co. KG, Karlsruhe
Ethylenediaminetetraacetic acid (EDTA)	Carl Roth GmbH & Co. KG, Karlsruhe
Fetal Calf Serum (FCS)	PAA, Pasching, Österreich
Formaldehyde 4%	Merck, Darmstadt
Glycerol	Carl Roth GmbH & Co. KG, Karlsruhe
HEPES	Gibco, Darmstadt
Isopropanol	Carl Roth GmbH & Co. KG, Karlsruhe

LSM 1077	PAA, Pasching, Österreich
Lymphoprep	STEMCELL Technologies SARL, Köln
Methanol	Carl Roth GmbH & Co. KG, Karlsruhe
Milk powder	Carl Roth GmbH & Co. KG, Karlsruhe
Monopotassium phosphate (KH ₂ PO ₄)	Carl Roth GmbH & Co. KG, Karlsruhe
Mowiol 4-88	Carl Roth GmbH & Co. KG, Karlsruhe
n-Butanol	Sigma-Aldrich, Steinheim
Nonidet P-40 (NP-40)	Gibco, Darmstadt
Penicillin/Streptomycin-Solution	Sigma-Aldrich, Steinheim
<i>PhosStop</i> (Phosphatase inhibitor)	Roche Diagnostics, Mannheim
Poly (dI/dC)	Thermo Fischer Scientific, Bonn
Ponceau S	Sigma-Aldrich, Steinheim
Potassium bicarbonate	Carl Roth GmbH & Co. KG, Karlsruhe
<i>Power SYBR® Green</i>	Applied Biosystems, Darmstadt
RosetteSep [®] Human B cell enrichment cocktail	STEMCELL Technologies SARL, Köln
RPMI-1640	PAA, Pasching, Österreich
Sodium azide (NaN ₃)	Carl Roth GmbH & Co. KG, Karlsruhe
Sodium chloride (NaCl)	Carl Roth GmbH & Co. KG, Karlsruhe
Sodium dodecyl sulfate (SDS)	Carl Roth GmbH & Co. KG, Karlsruhe
Taq-polymerase	Fermentas GmbH, St. Leon-Rot
Tetramethylethylenediamine (TEMED)	Carl Roth GmbH & Co. KG, Karlsruhe
Tri-sodium citrate	Carl Roth GmbH & Co. KG, Karlsruhe
Trilogy	Cell Marque Corp., CA, USA
Tris	Merck, Darmstadt
<i>Trypan Blue Stain 0,4%</i>	Gibco, Darmstadt
Tween-20	Carl Roth GmbH & Co. KG, Karlsruhe
Xylene	Carl Roth GmbH & Co. KG, Karlsruhe

4.3 Substances

Substance	company
AMD 3100 (CXCR4 inhibitor)	Sigma-Aldrich, Steinheim
Recombinant mouse MIF	R&D systems
Recombinant human MIF	Kindly provided by Dr. Richard Bucala
SD225002 (CXCR2 inhibitor)	Cayman Chemical

4.4 Antibodies

4.4.1 Antibodies for Immunoblotting

Antibody specificity	Clone	Source	Company
β -Actin	C-11	goat	SantaCruz Technologies, CA, USA
Akt (pan)	40D4	mouse	CellSignaling Technology, MA, USA
BCL-2	Poly6119	rabbit	BioLegend [®] , CA, USA
CD74	In-1	rat	BD Pharmingen [™] , Heidelberg
p42/44 MAPK (ERK1/2)	Polyclonal	rabbit	CellSignaling Technology, MA, USA
p42/44 MAPK (ERK1/2)	3A7	rabbit	CellSignaling Technology, MA, USA
GAPDH	FL-335	rabbit	SantaCruz Technologies, CA, USA
NF- κ B (p65)	D14E2	rabbit	CellSignaling Technology, MA, USA
phospho-AKT (S473)	D9E	rabbit	CellSignaling Technology, MA, USA
Phosphor-GSK3 β	D85E12	rabbit	CellSignaling Technology, MA, USA
phospho-p42/44 MAPK (ERK1/2) (T202/Y204)	D13.14.4E	rabbit	CellSignaling Technology, MA, USA
phospho-NF- κ B (p65) (S536)	93H1	rabbit	CellSignaling Technology, MA, USA
phospho-Syk (Y525/526)	Polyclonal	rabbit	CellSignaling Technology, MA, USA
Syk	Polyclonal	rabbit	CellSignaling Technology, MA, USA
TCL1	Polyclonal	rabbit	CellSignaling Technology, MA, USA
Goat IgG	Polyclonal	donkey	SantaCruz Technologies, CA, USA
Mouse IgG HRP-linked	Polyclonal	horse	CellSignaling Technology, MA, USA
Rabbit IgG HRP-linked	Polyclonal	goat	CellSignaling Technology, MA, USA
Rat IgG	Poly 4054	goat	BioLegend [®] , CA, USA

4.4.2 Antibodies for cell culture

Antibody specificity	Clone	company
mouse IgM F(ab) ₂ μ chain LE/AF		SouthernBiotech, AL, USA
CD44 LE/AF	IM7	BioLegend [®] , CA, USA
CD74	C-16	SantaCruz Technologies, CA, USA
human IgG	P-17	SantaCruz Technologies, CA, USA

4.4.3 Antibodies for flow cytometry

Antibody specificity	Clone	Fluorochrome	Company
CD3	17A2	APC-Cy7	BioLegend [®] , CA, USA
CD5	53-7.3	PE	BioLegend [®] , CA, USA
CD5	53-7.3	PerCP	BioLegend [®] , CA, USA
CD5	53-7.3	PerCP-Cy5.5	eBioscience, Inc, CA, USA
CD11b	M1/70	PE-Cy7	BioLegend [®] , CA, USA
CD11c	N418	APC-Cy7	BioLegend [®] , CA, USA
CD18	M18/2	AlexaFluor 647	BioLegend [®] , CA, USA
CD19	6D5	PacificBlue	BioLegend [®] , CA, USA
CD21/CD35	7E9	FITC	BioLegend [®] , CA, USA
CD23	B3B4	PE-Cy7	BioLegend [®] , CA, USA
CD44	IM7	PE	BD Pharmingen [™] , Heidelberg
CD45	30-F11	PacificOrange	Life technologies [™] , Darmstadt
CD74	In-1	FITC	BD Pharmingen [™] , Heidelberg
CXCR4	REA107	APC	Miltenyi Biotec, Bergisch Gladbach
F4/80	BM8	AlexaFluor 488	BioLegend [®] , CA, USA
Gr-1	RB6-8C5	PE	BioLegend [®] , CA, USA
IgD	11-26c.2a	PE	BioLegend [®] , CA, USA
IgM	RMM-1	APC	BioLegend [®] , CA, USA
Isotype control rat IgG _{2b}	A95-1	FITC	BD Pharmingen [™] , Heidelberg
Isotype control rat IgG _{2b}	A95-1	PE	BD Pharmingen [™] , Heidelberg
Isotype control REA	REA293	APC	Miltenyi Biotec, Bergisch Gladbach

4.5 Mouse strains

TCL1 ⁺ mouse	Heterozygous transgenic overexpression of human <i>TCL1</i> in B cells (B6C3H E μ - <i>TCL1</i>)	[54]
CD74 ^{ko} mouse	Homozygous knockout of the <i>Cd74</i> gene (C57Bl/6J CD74 ^{-/-})	[117]
TCL1 ^{+/+} mouse	Homozygous transgenic overexpression of human <i>TCL1</i> in B cells (C57Bl/6J E μ - <i>TCL1</i>)	

4.6 Oligonukleotides

Primer	sequence	amplicon
CD74 wt 1	5'-CGA CCT CAT CTC TAA CCA TGA ACA G-3'	
CD74 wt 2	5'-TCA CTC AAG GCA ACC TTC CTG C-3'	165 bp
CD74 neo 1	5'-CTT GGG TGG AGA GGC TAT TC-3'	
CD74 neo 2	5'-AGG TGA GAT GAC AGG AGA TC-3'	260 bp
TCL1 universal	5'-GCC GAG TGC CCG ACA CTC-3'	
TCL1 reverse	5'-CAT CTG GCA GCA GCT CGA-3'	300 bp
β -Actin forward	5'-GAC AAA ACT CCT GAG GCC ATA-3'	
β -Actin reverse	5'-TTG CTG ATC CAC ATC TGC TG-3'	490 bp
NF- κ B sense	5'-AGT TGA GGG GAC TTT CCC AGG C-3'	
NF- κ B antisense	5'-G CCT GGG AAA GTC CCC TCA ACT-3'	

4.7 Special reagents and Kits

Reagent or Kit	Manufacturer
5x Green Go Tag reaction buffer	Promega, Mannheim
ApopTag [®] Plus peroxidase In Situ Apoptosis Detection Kit	Millipore, Schalbach/Ts.
CD19 microbeads, mouse	Miltenyi Biotec, Bergisch Gladbach
Complete Mini	Roche Diagnostics, Mannheim
FITC AnnexinV Apoptosis Detection Kit I	BD Pharmingen [™] , Heidelberg
FITC BrdU Flow Kit	BD Pharmingen [™] , Heidelberg
Microvette [®] 100 LH	Sarstedt, Nümbrecht

NE-PER [®] Nuclear and Cytoplasmic Reagents	Extraction	Thermo Fischer Scientific, Bonn
Pan B cell Isolation Kit II		Miltenyi Biotec, Bergisch Gladbach
PhosSTOP		Roche Diagnostics, Mannheim
Pierce ECL Western Blotting Substrate		Thermo Fischer Scientific, Bonn
RNeasy Plus Mini Kit		Qiagen, Hilden
Roti [®] Quant		Carl Roth GmbH & Co. KG, Karlsruhe
UltraVision LP Kit		Thermo Fischer Scientific, Bonn

4.8 Primary patient material

All CLL patients in this study had a confirmed diagnosis according to standard criteria [Cheson et al. 1996]. Patients represented different Binet stages and have been untreated. All patients provided written informed consent and the study was in accordance with the declaration of Helsinki and approved by the internal review board of the University Hospital Cologne.

The study was supported by the Biobank of the Center of Integrated Oncology Cologne Bonn funded by the German Cancer Aid, with special references to Lukas C. Heukamp and Thomas Landwehr.

4.9 Software

Adobe Illustrator

Adobe Photoshop

Endnote

FlowJo

GraphPad Prism

Image J

Image Studio Lite

Kaluza[®] Flow Analysis Software

Microsoft Office

Pannoramic Viewer

5 Methods

5.1 Breeding

Breeding of E μ -*TCL1* transgenic mice with CD74-knockout animals (CD74^{ko}) were done in the animal facility of the Experimental Medicine at the University Hospital of Cologne. Crossing of both strains led to F2 generations of E μ -*TCL1* mice with CD74 in wildtype (TCL1⁺ CD74^{wt}) or knockout (TCL1⁺ CD74^{ko}) configuration. The animals were kept under a controlled atmosphere with semi-annual health checks in individually ventilated cages at groups of maximum 5 mice. They were allowed to feed and drink *ad libitum*. Breeding was done on a one to one basis and pups were weaned after 21 days. Experiments were approved by the state of North Rhine Westphalia, Germany, under #9.93.2.10.31.07.098.

5.2 Genotyping

To assess the correct genotype in experimental mice a piece of the tail is cut at the time of weaning. Genomic DNA is prepared and the region of interest is amplified in a polymerase chain reaction (PCR).

5.2.1 DNA-Preparation

A piece of tail is put into a tube and lysed for an hour in 100 μ l of lysis buffer in a thermomixer at 95°C. The probes were cooled of at 4°C for 30 min and then 100 μ l neutralisation buffer is added. After mixing the samples are used for the following PCR or stored at 4°C.

DNA Lysis buffer:

10 M NaOH	2.5 ml
0,5 M EDTA	1 ml
add H ₂ O	1 l

Neutralisation buffer:

1 M Tris-HCl	40 ml
add H ₂ O	1 l

5.2.2 Polymerase-Chain-Reaction (PCR)

Amplification of DNA fragments is done by polymerase-chain-reaction (PCR). A piece of DNA is amplified with specific primers binding to the gene of interest. The amplification is done with Taq (named after the thermophilic bacterium *Thermus aquaticus*) -polymerase by *in vitro* enzymatic replication.

PCR reaction mix TCL1-Genotyping

PCR reaction components	concentration	Amount for n=1
Green Go Taq Reaction Buffer	5x	5 μ l
dNTP's	10 mM	0.5 μ l
Primer TCL1 universal	10 pmol	1 μ l
Primer TCL1 reverse	10 pmol	1 μ l
Primer \square -Actin forward	10 pmol	0.75 μ l
Primer \square -Actin reverse	10 pmol	0.75 μ l
Taq-Polymerase		0.2 μ l
H ₂ O		14.8 μ l
Template		1 μ l
		25 μ l

Cycler -Program

PCR reaction components	temperature	time	
Initiation	95°C	10 min	
Denaturation	95°C	30 sec	30 cycles
Annealing	62°C	30 sec	
Elongation	72°C	1 min	
Final elongation	72°C	5 min	

PCR reaction mix TCL1-Genotyping

PCR reaction components	concentration	Amount for n=1
Green Go Taq Reaction Buffer	5x	5 μ l
dNTP's	10 mM	0.5 μ l
Primer CD74 wt 1	10 pmol	1 μ l
Primer CD74 wt 2	10 pmol	1 μ l
Primer CD74 neo 1	10 pmol	1 μ l
Primer CD74 neo 2	10 pmol	1 μ l
Taq-Polymerase		0.2 μ l
H ₂ O		14.8 μ l
Template		1 μ l
		25 μ l

Cycler -Program

PCR reaction components	temperature	time	
Initiation	95°C	10 min	
Denaturation	95°C	1 min	36 cycles
Annealing	59°C	45 sec	
Elongation	72°C	1 min	
Final elongation	72°C	7 min	

5.2.3 Agarose gel electrophoresis

Horizontal agarose gel electrophoresis is carried out to separate DNA fragments according to size. Agarose gel is made by dissolving agarose in 1x TAE buffer through boiling. Gels contain 1.5 % to 2 % agarose, depending on the size of the DNA fragments. Adding 0.5µg/ml ethidium bromide (EtBr) to the gels, allowed visualization of DNA under UV-light. After setting of the gels at room temperature, 12.5 µl of PCR product is loaded on to the gel. The Green Go Taq Reaction Buffer used for PCR (see 5.2.2) already provided gel loading buffer to avoid leakage of the samples from the wells. Agarose gels are run in 1x TAE buffer for approximately 30 min at 100V. DNA bands then are visualized by UV light (366 nm) exposure.

50x TAE buffer:

Tris	242 g
0.5 M Na ₂ EDTA (pH=8,0)	100 ml
add H ₂ O	1 l

5.3 Blood analysis

5.3.1 Blood sampling

For the analysis of leukemia, blood of the experimental mice is taken from the lateral tail vein. Mice are warmed up under red-light to dilate the blood vessel. An incision at the tail vein is done by a scalpel and the blood is collected in a heparin coated microvette. A total volume of approximately 40-50 µl blood is taken for each mouse and then further used for differential blood cell count and flow cytometry.

5.3.2 Differential blood count

To determine the complete blood count, blood is diluted 1:10 with CellPack and measured on a Sysmex XE-2100. Characteristics of the cells are measured by flow cytometry where the blood is separated by a semiconductor into a number of channels. The XE-2100 has got five different

channels, differentiating the white blood count, the differential leukocyte count as well as reticulocyte count and fluorescence platelet count.

5.4 Extraction of organs

If an animal died or was euthanized because of severe disease, organs including spleen, bone marrow, liver and lymph nodes were taken out and fixed in a 4 % formalin solution and stored in the dark at 4°C until embedding in paraffin. Before fixation, parts of the spleen were prepared for further *ex vivo* analysis by FACS, for detection of the malignant clone or apoptosis and proliferation.

5.5 Cell culture

5.5.1 Culture conditions

Primary cells were cultured at 37 °C, a relative humidity of 90 % and 5 % CO₂. RPMI cell culture medium is supplemented with 10 % (v/v) FCS, 1 % HEPES-buffer and 1 % penicillin / streptomycin.

5.5.2 Counting

Cells were diluted with Trypan Blue, which is a vital stain selectively staining dead cells. Approximately 10 µl of dilution were transferred into a “Neubauer” chamber. Four squares were counted and an average was calculated. The number of cells (n) in one square equals $n \times 10^4$ per ml divided through dilution factor of Trypan Blue.

5.5.3 Freezing and thawing of cells

Cells were harvested at 300 g for 5 min. The pelleted cells were then resuspended in freezing medium at 1×10^7 cells / ml. Aliquots were pipetted into cryotubes and frozen at -80°C in freezing containers. For long term storage cryotubes were transferred into liquid nitrogen storage tanks.

For thawing of the cells, frozen vials were taken out of the liquid nitrogen tank, carefully thawed at 37 °C in the water bath and immediately transferred into a 15 ml tube containing 10 ml of prewarmed culture medium. Pelleting the cells by centrifugation at 300 g for 5 min removed the toxic DMSO. Cells were then resuspended in fresh culture medium.

Freezing medium:

RPMI	500 ml
DMSO	10 %
FCS	40 %

5.6 Isolation of primary murine cells

5.6.1 Isolation of primary murine splenocytes

Animals were killed by cervical dislocation and the abdominal cavity opened after sterilisation of the surface with 70 % ethanol. After localisation of the spleen the organ was taken out with tweezers and transferred into ice-cold PBS. A single cell suspension was obtained by homogenizing the tissue and filtering cells through a 100 µm nylon cell strainer (BD Pharming) into PBS on ice. After rinsing the mesh with 5-10 ml PBS, cells were harvested by centrifugation (300g 5 min). Red blood cells were lysed by 1x AcK buffer for 3 min at room temperature. After washing the cells with PBS, cells were counted and used for further experiments.

10 x PBS:

NaCl	80 g
KCl	2 g
Na ₂ HPO ₄ -2H ₂ O	17.8 g
KH ₂ PO ₄	2.4 g
add H ₂ O	1 l
pH 7,4	

10 x AcK:

NH ₄ Cl	82.9 g
KHCO ₃	10 g
EDTA	0.37 g
add H ₂ O	1 l

5.6.2 Isolation of primary murine B cells

Isolation of B cells from murine splenocytes was carried out by using the MACS[®]-technology from Miltenyi Biotec. In principle cells are magnetically labelled with MACS MicroBeads and then the sample is applied to a MACS column placed in a MACS separator. While unlabelled cells pass through the magnetic field of the separator, magnetically labelled cells are retained within the column. Afterwards the column is removed from the separator and the magnetically labelled cells are eluted from the column. With this technology both labelled and unlabelled cells can easily be isolated with high purity and recovery. The efficiency of the B cell isolation was subsequently tested by flow cytometry.

5.6.2.1 Positive B cell selection

For positive selection of B cells the CD19 MicroBeads for mouse were used (Miltenyi Biotec) according to manufacturer's instructions. CD19 MicroBeads bind to CD19 expressing B cells and lead to the retention of labelled B cells in the magnetic field. After washing of the column, labelled B cells were eluted by removing the column from the separator.

5.6.2.2 Negative B cell selection

To avoid stimulation of B cells through labelling with CD19 MicroBeads, negative selection was carried out. The Pan B cell II isolation kit for mouse (Miltenyi Biotec) provided a cocktail of biotinylated CD3ε, CD4, CD8a, CD49b, Gr-1, and Ter119 antibodies labelling non B cells. These cells are subsequently labelled with anti-biotin MicroBeads. With this method unlabeled B cells flow through the magnetic field, leaving magnetically labeled non B cells in the column.

5.7 Isolation of primary human CLL cells

Primary human CLL cells were kindly provided by Thomas Landwehr from the CLL Biobank of the Center of Integrated Oncology Cologne Bonn. Blood samples were taken from patients into S-Monovette® with EDTA K3E (Sarstedt). Then 50 µl RosetteSep human B cell enrichment cocktail was added to 1 ml blood and incubated for 20 min at room temperature. An equal amount of wash buffer was added. This mixture then was carefully pipetted to the side of a SepMate™-50 tube filled with 15 ml Lymphoprep™ (STEMCELL Technologies). Centrifugation at 1200 g for 10 min separated the B cell phase from the other cells. The B cell phase was filled into a new tube, where cells were washed with wash buffer and centrifuged at 300g for 10 min. The supernatant was discarded and the B cell pellet resuspended in culture medium.

Wash buffer:

DPBS	500 ml
FBS Good (heat inactivated)	50 ml

Culture medium:

RPMI 1640 GlutaMAX™	500 ml
FBS Good (heat inactivated)	50 ml
Penicillin (10.000 Units) /Streptomycin (10 mg/ml))	5 ml

5.8 Flow cytometry

Fluorescence activated cell sorting (FACS) provides a method to study cells based on the specific light scattering and fluorescent characteristics of each cell. Expression of either surface or intracellular proteins can further be detected by staining the cells with fluorochrome-conjugated antibodies (see 4.4.3), whereas cells expressing endogenous fluorescent proteins can be detected directly. For flow cytometry single cell suspensions were prepared beforehand.

5.8.1 Staining of surface proteins

Up to 1×10^7 cells in 100 μ l PBS were stained with 1 μ l antibody solution for 20 min in the dark at room temperature. After staining cells were washed with PBS and centrifuged (300 g 5 min). For blood samples, red blood cells were lysed using AcK buffer (see 5.6.1) and then washed with PBS. Cell pellets then were resuspended in 100- 200 μ l PBS and measured using the Gallios™ 10/3 flow cytometer (Beckman Coulter).

5.8.2 Staining of intracellular proteins

For staining of intracellular proteins permeabilization reagent IntraPrep™ from Beckman Coulter was used. First, surface staining was carried out as described above. After washing of the cells, pelleted cells were resuspended in 50 μ l reagent I and mixed well by vortexing. After 15 min incubation in the dark at room temperature cells were washed with ~ 4 ml PBS (centrifugation 300 g 5 min). Then cells were resuspended in 50 μ l reagent II without vortexing. After 5 min incubation in the dark at room temperature 1 μ l of conjugated antibody for intracellular staining was added. Staining was carried out for 10 min in the dark at room temperature. After washing with ~ 4ml PBS (centrifugation 300 g 5 min), pelleted cells were resuspended in 100- 200 μ l PBS and measured using the Gallios™ 10/3 flow cytometer.

5.9 Stimulation experiments

Stimulation of primary murine splenocytes and human CLL cells was carried out in RPMI medium containing 1 % penicillin / streptomycin but no FCS (RPMI+). 1.5×10^7 cells were used per time point and condition.

Single cell suspensions were washed with RPMI+ and further processed under a sterile laminar flow hood to avoid contamination. Cells were then resuspended in RPMI+ to 1.5×10^7 cells per 800 μ l medium. 800 μ l cell suspension was then pipetted into 24-well plates. Human CLL samples were starved overnight and murine cells were starved for 4 h under culture conditions. Then cells were stimulated with 100 ng/ml recombinant MIF (diluted into 200 μ l RPMI+), 5 μ g/ml CD74 antibody (C-16) or 5 μ g/ml IgG (P-17) for 0, 5, 15, 30 or 60 min. During the time periods cells were kept under culture conditions at 37°C. Stimulation was stopped by quickly transferring cell suspensions into 1.5 ml tubes and spinning off at max speed for 30 sec. The

supernatant was taken off carefully and cell pellets diluted into 75 μ l protein lysis buffer. Lysis of cells was carried out as described under 5.10.1. The CD44 inhibiting antibody (IM7 LE/AF 10 μ g/ml) or CXCR2- (SD225002 45 nmol) and CXCR4-inhibitor (AMD3100 30 nmol) were added before starvation for 4h.

5.10 Protein biochemistry

5.10.1 Preparation of cell lysates

In order to access the protein status of the cell, the cell membrane needs to be ruptured. Therefore cell lysis is carried out. All following steps were carried out on ice to avoid degradation of proteins.

Up to 1×10^7 cells were resuspended in 50 μ l protein lysis buffer containing protease and phosphatase inhibitors, and lysed on ice for 30–60 min. Cell debris, DNA and insoluble proteins were spun off by centrifugation at 13.000 rpm for 15 min at 4°C. The supernatant containing the soluble protein lysate was taken and pipetted into a fresh tube. Protein lysates were either used directly or stored at -80°C until further use.

Protein lysis buffer:

1 M Tris (pH 7,5)	5 ml
0,5 M EDTA (pH 8,0)	400 μ l
5 M NaCl	3 ml
NP-40	0.2 ml
add H ₂ O	100 ml

PhosphoSTOP and complete mini from Roche were added freshly to the protein lysis buffer 1:10.

5.10.2 Protein quantification

Protein concentrations in protein lysates were measured using the Roti[®] Quant from Carl Roth, which is based on the method described by Bradford in 1976 [184]. Measurement was carried out after manufacturers' instructions. In short a BSA standard ranging from 0-100 μ g was prepared and protein lysates were diluted 1:40 till 1:50 with protein lysis buffer to stay within the measurable range. 200 μ l diluted Roti[®] Quant solution was added to 50 μ l protein sample and incubated for 5 min at room temperature. Afterwards the optical density was measured at 595 nm. Protein concentrations in the samples were calculated based on the BSA standard curve. BSA standards were measured in duplicates und samples in triplicates.

5.10.3 SDS Polyacrylamide gel electrophoresis (PAGE)

SDS-PAGE is used to separate denatured proteins according to their molecular weight. Therefore two sequential gels were cast, the bottom gel, so called separation gel, is basic (pH 8.8) and has a high polyacrylamide content (usually 12 %) which allows the separation of proteins according to their molecular size. On top, the so called stacking gel is cast which is slightly acidic (pH 6.8) and has a lower polyacrylamide concentration (5%), where proteins are poorly separated but form a slim defined band. Sample loading buffer containing SDS and β -mercaptoethanol was added to the protein samples (~ 30 μ g protein) which were then cooked for 5 min at 95°C. *Sodium Dodecyl Sulfat* (SDS) is an anionic detergent applied to protein samples to linearize proteins and impart a negative charge, so that they run towards the positive pole during electrophoresis. β -mercaptoethanol, a hybrid of ethylene glycol, further denatures the proteins by reducing disulfide bonds in the proteins. After cooling off, samples were transferred to the gel. Electrophoresis was carried out using a vertical apparatus Mini Protean II (BioRad). Equal amounts of protein samples and the molecular weight marker (PageRuler™ Prestained, Fermentas) were loaded in the slots of the stacking gel. Gels were run at 120 V, until the blue running front has travelled to the bottom of the separating gel.

Solutions	Stacking gel	Separation gel
	5%	12 %
H ₂ O	3.4 ml	6.6 ml
Tris (1 M, pH 6.8)	630 μ l	-
Tris (1,5 M, pH 8.8)	-	5 ml
10 % SDS	50 μ l	200 μ l
10 % APS	50 μ l	200 μ l
30 % Acrylamide	830 μ l	8 ml
TEMED	5 μ l	20 μ l

10 x Electrophoresis buffer:

Tris	30.28 g
Glycine	144.12 g
SDS	10 g
add H ₂ O	1 l

4 x Sample buffer:	
1 M Tris (pH 6.8)	5 ml
Glycerol	2 ml
SDS	4 g
β -Mercaptoethanol	200 μ l
add H ₂ O	10 ml

5.10.4 Protein transfer

For the detection of the protein of interest, the separated protein bands from the SDS-PAGE are transferred on to a membrane by an electrical field. The so called blotting process was achieved by using the Semi-Dry-Blot system from BioRad. Proteins were transferred onto nitrocellulose membranes. Membranes, filter paper and fibre pads were all pre-soaked in transfer buffer.

Transfer buffer:	
Glycine	7.21 g
Tris	1.52 g
Methanol	100 ml
add H ₂ O	500 ml

After assembling of the blot and carefully removing air bubbles, transfer of the proteins were carried out 45 mA per blot for 1.5 – 2 h. To proof blotting efficiency membranes were stained with PonceauS red solution after transfer. PonceauS visualizes proteins by reversibly binding positively charged amino groups. Washing with ddH₂O removes the dye completely.

5.10.5 Immunoblotting

To visualize proteins of interest specific antibodies were used. First membranes were blocked with Blotto buffer at room temperature for 1 h to avoid unspecific binding of the antibodies. After washing off residual blocking buffer with TBS-T (3 x 10 min), membranes were incubated with the specific primary antibody, diluted in antibody diluent, overnight at 4°C. In the next day membranes were washed with TBS-T (3 x 10 min) and incubated with the appropriate secondary antibody diluted in Blotto buffer at room temperature for at least 1 h. Depending on the detection system secondary antibodies were labeled with horse radish peroxidase (HRP) or a fluorochrome. After incubation with the secondary antibody, membranes were washed with TBS-T (3 x 10 min) and detection was carried out.

Blotto buffer:

Milk powder	25 g
1 M Tris (pH 8.0)	25 ml
5 M NaCl	8 ml
NP-40	1 ml
1.5 M CaCl ₂	0.4 ml
add H ₂ O	500 ml

10 x TBS-T:

NaCl	87 g
Tris	12.11 g
Tween- 20	10 ml
add H ₂ O	1 l
pH 7.6	

Antibody diluent:

1 M HEPES (pH 7.4)	2.5 ml
5 M NaCl	25 ml
BSA	2.5 g
Tween-20	0.5 ml
10 % NaN ₃	1.5 ml
add H ₂ O	250 ml

5.10.5.1 Detection by chemiluminescence

Visualization of HRP-labeled antibodies was carried out by using the enhanced chemiluminescent (ECL) detection system. Pierce ECL-reagents A and B (ThermoFischer Scientific) were freshly mixed 1:1 and membranes were incubated in ECL-mix for 2 minutes. Membranes were briefly freed from excessive liquid and put between two clean clear foils in a light protected film cassette. Kodak X-ray films were exposed to membranes between 10 sec and 1 h, dependent on antibody and protein load. Exposed films were developed using an automated photo developing machine (Kodak).

5.10.5.2 Detection by fluorescence

To visualize fluorochrome-labeled secondary antibodies (IRDye[®] 800CW or IRDye[®] 680) membranes were scanned on the Odyssey imaging system from Li-Cor at 700 nm or 800 nm.

5.11 Syngeneic transplantation of TCL1-CLL cells

Massively enlarged spleens from C57BL/6 E μ -*TCL1* (*TCL1*^{+/+}) mice were removed and single cells were obtained by homogenizing the tissue and filtering the cells through a 100 μ m nylon cell strainer. Lymphocyte separation was carried out using LSM 1077 (PAA) according to manufacturer's instruction. Isolated lymphocytes were counted and diluted to 1×10^7 cells per 200 μ l into PBS. Parallel lymphocytes were analyzed for purity and percentage of malignant B cells via flow cytometry. If more than 90% of isolated lymphocytes were malignant B cells (expressing CD5 and CD19), cells were stored by freezing or transplanted immediately into young recipient mice (~ 3 months) via intraperitoneal injection. The engraftment of the malignant cells was observed by measuring blood samples. If recipient mice became highly leukemic (over 90 % malignant cells in the blood) or showed signs of suffering, mice were sacrificed and lymphocytes isolated as mentioned above. These malignant B cells were further stored by freezing or injected into new recipient mice. Malignant cells were transferred into up to three different recipient generations. In this study malignant cells were passaged through 1 recipient generation before transferred to experimental mice, leading to a fast growing and aggressive clone.

5.12 Quantification of proliferating cells

To analyze the proliferation capacity of murine malignant cells *in vivo*, BrdU incorporation was measured. Bromodeoxyuridine (BrdU) is an analog of the DNA precursor thymidine and incorporated into newly synthesized DNA by cells entering and progressing through the S phase of the cell cycle [169]. The incorporated BrdU then can be stained with specific anti-BrdU antibodies.

In this study the FITC BrdU Flow Kit from BD Pharming was used. Leukemic mice (~ 9 months) were injected with 2 mg BrdU i.p and sacrificed after 24 h to isolate primary splenocytes (see 5.6.1). Splenocytes then were stained according to manufacturer's instruction. Shortly, cells were stained for surface marker and further permeabilized to allow intracellular staining. Then cells were treated with DNase in order to expose BrdU epitopes before they were stained with a specific FITC-labelled BrdU antibody. After staining cells were measured via flow cytometry.

5.13 Quantification of apoptosis

In order to measure the apoptotic capacity of murine malignant B cells the FITC Annexin V Apoptosis Detection Kit from BD Pharming was used. Cells undergoing apoptosis are characterized by certain morphologic features including loss of plasma membrane asymmetry and attachment, condensation of the cytoplasm and nucleus, and internucleosomal cleavage of DNA. One of the early steps involves the exposure of phosphatidylserine (PS) to the extracellular environment. Annexin V is a phospholipid-binding protein that has a high affinity for PS and thus serves as a sensitive probe for cells that are undergoing apoptosis. A vital dye like 7-AAD (7-Amino-Actinomycin), which is a fluorescent intercalator that undergoes a spectral shift upon association with DNA, helps to distinguish vital cells from late apoptotic (Annexin V and 7-AAD positive) or necrotic cells (only 7-AAD positive).

To measure apoptosis in murine malignant B cells, mice were sacrificed at leukemic stage (~9months) and primary splenocytes were isolated. Then cells were kept under cell culture conditions (see 5.5.1) for 24 h. Depending on the experiment Fludarabin, an purine analog interfering with DNA synthesis was added to the culture medium at a concentration of 50 μ M. Staining for Annexin V and 7-AAD was carried out after manufacturer's instructions and cells measured via flow cytometry.

5.14 IGVH status

The IGVH status of samples was kindly carried out by the group of Manuel Montesinos-Rongen (Institute for Pathology; UKK Cologne). Shortly, Trizol based RNA extraction from murine splenocytes was followed by gene sequence analysis on an ABI3130 sequencer using the Lasergene software. Sequence comparison was performed with mouse germline gene sequences using the IMGT database.

5.15 Immunohistochemistry

For immunohistochemistry staining organs were first fixed in 4% paraformaldehyde to preserve tissue from degradation, and to maintain the structure of the cell and of sub-cellular components. Fixed organs were then embedded into paraffin wax. Afterwards, using a steel knife mounted in a microtome 4 μ m thick tissue sections were cut which then were mounted on a glass microscope slide. For staining sections were deparaffinized and rehydrated:

Incubate sections in Xylene two times for 10 min

Incubate sections in decreasing Ethanol for 1 min each; 100% \rightarrow 100%
 \rightarrow 96% \rightarrow 96% \rightarrow 70%

Incubate sections in ddH₂O for 5 min

Next antigen retrieval was carried out to break the methylene bridge, which were formed during fixation, and expose the antigenic sites in order to allow the antibodies to bind. Therefore

sections were either boiled (heat induced epitope retrieval) or incubated in acidic buffer for 20 min. The next steps, blocking and staining, were carried out using the UltraVision LP Kit (Thermo Scientific). After washing of the sections (wash buffer 1x TBS-T; see 5.10.5), UltraV Block was applied for 5 min and followed by primary antibody incubation.

Antibody	Antigen retrieval	Dilution	Incubation time and temperature
CD68	30 min 95°C in Trilogy buffer	1:50	60 min, room temperature
cCaspase3	20 min 10mM sodium citrate pH 6,0	1:100	30 min room temperature
Ki-67	20 min 10mM sodium citrate pH 6,0	1:50	30 min room temperature

After another washing step sections were incubated in Enhancer for 15 min, followed by another washing step and incubation in AP polymer for 15 min. Then slides were washed three times and stained with FastRed solution for ~10 min. During FastRed staining sections need to be watched under a microscope to avoid background staining. Staining was stopped by washing the slides. Counterstain was carried out using Hemalaun solution for 1 min. Sections were embedded in Mowiol.

References

1. Rozman, C. and E. Montserrat, *Chronic lymphocytic leukemia*. N Engl J Med, 1995. **333**(16): p. 1052-7.
2. Santanam, U., N. Zanesi, A. Efanov, S. Costinean, A. Palamarchuk, J.P. Hagan, . . . Y. Pekarsky, *Chronic lymphocytic leukemia modeled in mouse by targeted miR-29 expression*. Proc Natl Acad Sci U S A, 2010. **107**(27): p. 12210-5.
3. Müller-Hermelink HK, M.E., Catovsky D, Harris NL, *Chronic lymphocytic leukemia/ small lymphocytic leukemia*, in *World Health Organization Classification of Tumours: Pathology and Genetics of Tumours or Haematopoietic and Lymphoid Tissues*, E.S. Jaffe, Harris NL, Stein H, Vardiman JW, eds., Editor 2001, IARC Press: Lyon, France. p. 195-196.
4. Dighiero, G. and T.J. Hamblin, *Chronic lymphocytic leukaemia*. Lancet, 2008. **371**(9617): p. 1017-29.
5. Panovska, A., M. Doubek, Y. Brychtova, and J. Mayer, *Chronic lymphocytic leukemia and focusing on epidemiology and management in everyday hematologic practice: recent data from the Czech Leukemia Study Group for Life (CELL)*. Clin Lymphoma Myeloma Leuk, 2010. **10**(4): p. 297-300.
6. Goldin, L.R. and S.L. Slager, *Familial CLL: genes and environment*. Hematology Am Soc Hematol Educ Program, 2007: p. 339-45.
7. Cuttner, J., *Increased incidence of hematologic malignancies in first-degree relatives of patients with chronic lymphocytic leukemia*. Cancer Invest, 1992. **10**(2): p. 103-9.
8. Sellick, G.S., D. Catovsky, and R.S. Houlston, *Familial chronic lymphocytic leukemia*. Semin Oncol, 2006. **33**(2): p. 195-201.
9. Cimino, P.J., Jr., D.W. Bahler, and E.J. Duncavage, *Detection of Merkel cell polyomavirus in chronic lymphocytic leukemia T-cells*. Exp Mol Pathol, 2013. **94**(1): p. 40-4.
10. Rego, E.M., H.T. Kim, G.J. Ruiz-Arguelles, R. Uriarte Mdel, R.H. Jacomo, H. Gutierrez-Aguirre, . . . M.A. Sanz, *The impact of medical education and networking on the outcome of leukemia treatment in developing countries. The experience of International Consortium on Acute Promyelocytic Leukemia (IC-APL)*. Hematology, 2012. **17 Suppl 1**: p. 36-8.
11. Hallek, M., B.D. Cheson, D. Catovsky, F. Caligaris-Cappio, G. Dighiero, H. Dohner, . . . T.J. Kipps, *Guidelines for the diagnosis and treatment of chronic lymphocytic leukemia: a report from the International Workshop on Chronic Lymphocytic Leukemia updating the National Cancer Institute-Working Group 1996 guidelines*. Blood, 2008. **111**(12): p. 5446-56.
12. Butler, T. and J.G. Gribben, *Biologic and clinical significance of molecular profiling in Chronic Lymphocytic Leukemia*. Blood Rev, 2010. **24**(3): p. 135-41.
13. Mauro, F.R., R. Foa, D. Giannarelli, I. Cordone, S. Crescenzi, E. Pescarmona, . . . F. Mandelli, *Clinical characteristics and outcome of young chronic lymphocytic leukemia patients: a single institution study of 204 cases*. Blood, 1999. **94**(2): p. 448-54.

14. Hallek, M., M. Bergmann, and B. Emmerich, *Chronic lymphocytic leukaemia: up-dated recommendations on diagnosis and treatment*. *Onkologie*, 2004. **27**(1): p. 97-104.
15. Boggs, D.R., S.A. Sofferan, M.M. Wintrobe, and G.E. Cartwright, *Factors influencing the duration of survival of patients with chronic lymphocytic leukemia*. *Am J Med*, 1966. **40**(2): p. 243-54.
16. Galton, D.A., *The pathogenesis of chronic lymphocytic leukemia*. *Can Med Assoc J*, 1966. **94**(19): p. 1005-10.
17. Rai, K.R., A. Sawitsky, E.P. Cronkite, A.D. Chanana, R.N. Levy, and B.S. Pasternack, *Clinical staging of chronic lymphocytic leukemia*. *Blood*, 1975. **46**(2): p. 219-34.
18. Binet, J.L., A. Auquier, G. Dighiero, C. Chastang, H. Piguët, J. Goasguen, . . . F. Gremy, *A new prognostic classification of chronic lymphocytic leukemia derived from a multivariate survival analysis*. *Cancer*, 1981. **48**(1): p. 198-206.
19. Watson, L., P. Wyld, and D. Catovsky, *Disease burden of chronic lymphocytic leukaemia within the European Union*. *Eur J Haematol*, 2008. **81**(4): p. 253-8.
20. Sagatys, E.M. and L. Zhang, *Clinical and laboratory prognostic indicators in chronic lymphocytic leukemia*. *Cancer Control*, 2012. **19**(1): p. 18-25.
21. Vuillier, F., G. Dumas, C. Magnac, M.-C. Prevost, A.I. Lalanne, P. Oppedazzo, . . . B. Payelle-Brogard, *Lower levels of surface B-cell-receptor expression in chronic lymphocytic leukemia are associated with glycosylation and folding defects of the μ and CD79a chains*. *Blood*, 2005. **105**(7): p. 2933-2940.
22. Niiro, H. and E.A. Clark, *Regulation of B-cell fate by antigen-receptor signals*. *Nat Rev Immunol*, 2002. **2**(12): p. 945-56.
23. Stevenson, F.K., S. Krysov, A.J. Davies, A.J. Steele, and G. Packham, *B-cell receptor signaling in chronic lymphocytic leukemia*. *Blood*, 2011. **118**(16): p. 4313-20.
24. Hamblin, T.J., Z. Davis, A. Gardiner, D.G. Oscier, and F.K. Stevenson, *Unmutated Ig V(H) genes are associated with a more aggressive form of chronic lymphocytic leukemia*. *Blood*, 1999. **94**(6): p. 1848-54.
25. Dohner, H., S. Stilgenbauer, A. Benner, E. Leupolt, A. Krober, L. Bullinger, . . . P. Lichter, *Genomic aberrations and survival in chronic lymphocytic leukemia*. *N Engl J Med*, 2000. **343**(26): p. 1910-6.
26. de Viron, E., L. Michaux, N. Put, F. Bontemps, and E. van den Neste, *Present status and perspectives in functional analysis of p53 in chronic lymphocytic leukemia*. *Leuk Lymphoma*, 2012. **53**(8): p. 1445-51.
27. Bullrich, F., D. Rasio, S. Kitada, P. Starostik, T. Kipps, M. Keating, . . . C.M. Croce, *ATM mutations in B-cell chronic lymphocytic leukemia*. *Cancer Res*, 1999. **59**(1): p. 24-7.
28. Schaffner, C., S. Stilgenbauer, G.A. Rappold, H. Dohner, and P. Lichter, *Somatic ATM mutations indicate a pathogenic role of ATM in B-cell chronic lymphocytic leukemia*. *Blood*, 1999. **94**(2): p. 748-53.
29. Calin, G.A., C.D. Dumitru, M. Shimizu, R. Bichi, S. Zupo, E. Noch, . . . C.M. Croce, *Frequent deletions and down-regulation of micro- RNA genes miR15 and miR16 at*

- 13q14 in chronic lymphocytic leukemia.* Proc Natl Acad Sci U S A, 2002. **99**(24): p. 15524-9.
30. Cimmino, A., G.A. Calin, M. Fabbri, M.V. Iorio, M. Ferracin, M. Shimizu, . . . C.M. Croce, *miR-15 and miR-16 induce apoptosis by targeting BCL2.* Proc Natl Acad Sci U S A, 2005. **102**(39): p. 13944-9.
 31. Klein, U., Y. Tu, G.A. Stolovitzky, M. Mattioli, G. Cattoretti, H. Husson, . . . R. Dalla-Favera, *Gene expression profiling of B cell chronic lymphocytic leukemia reveals a homogeneous phenotype related to memory B cells.* J Exp Med, 2001. **194**(11): p. 1625-38.
 32. Rosenwald, A., A.A. Alizadeh, G. Widhopf, R. Simon, R.E. Davis, X. Yu, . . . L.M. Staudt, *Relation of gene expression phenotype to immunoglobulin mutation genotype in B cell chronic lymphocytic leukemia.* J Exp Med, 2001. **194**(11): p. 1639-47.
 33. Seifert, M., L. Sellmann, J. Bloehdorn, F. Wein, S. Stilgenbauer, J. Dürig, and R. Küppers, *Cellular origin and pathophysiology of chronic lymphocytic leukemia.* J Exp Med, 2012. **209**(12): p. 2183-98.
 34. O'Brien, S., H. Kantarjian, M. Beran, L.E. Robertson, C. Koller, S. Lerner, and M.J. Keating, *Interferon maintenance therapy for patients with chronic lymphocytic leukemia in remission after fludarabine therapy.* Blood, 1995. **86**(4): p. 1298-300.
 35. Kitada, S., I.M. Pedersen, A.D. Schimmer, and J.C. Reed, *Dysregulation of apoptosis genes in hematopoietic malignancies.* Oncogene, 2002. **21**(21): p. 3459-74.
 36. Caligaris-Cappio, F., *Role of the microenvironment in chronic lymphocytic leukaemia.* Br J Haematol, 2003. **123**(3): p. 380-8.
 37. Granziero, L., P. Ghia, P. Circosta, D. Gottardi, G. Strola, M. Geuna, . . . F. Caligaris-Cappio, *Survivin is expressed on CD40 stimulation and interfaces proliferation and apoptosis in B-cell chronic lymphocytic leukemia.* Blood, 2001. **97**(9): p. 2777-83.
 38. Schattner, E.J., *CD40 ligand in CLL pathogenesis and therapy.* Leuk Lymphoma, 2000. **37**(5-6): p. 461-72.
 39. Munk Pedersen, I. and J. Reed, *Microenvironmental interactions and survival of CLL B-cells.* Leuk Lymphoma, 2004. **45**(12): p. 2365-72.
 40. Endo, T., M. Nishio, T. Enzler, H.B. Cottam, T. Fukuda, D.F. James, . . . T.J. Kipps, *BAFF and APRIL support chronic lymphocytic leukemia B-cell survival through activation of the canonical NF- κ B pathway.* Blood, 2007. **109**(2): p. 703-710.
 41. Burger, J.A. and T.J. Kipps, *Chemokine Receptors and Stromal Cells in the Homing and Homeostasis of Chronic Lymphocytic Leukemia B Cells.* Leuk Lymphoma, 2002. **43**(3): p. 461-466.
 42. Tsukada, N., J.A. Burger, N.J. Zvaifler, and T.J. Kipps, *Distinctive features of "nurselike" cells that differentiate in the context of chronic lymphocytic leukemia.* Blood, 2002. **99**(3): p. 1030-7.
 43. Fecteau, J.F. and T.J. Kipps, *Structure and function of the hematopoietic cancer niche: focus on chronic lymphocytic leukemia.* Front Biosci (Schol Ed), 2012. **4**: p. 61-73.

44. Reinart, N., P.H. Nguyen, J. Boucas, N. Rosen, H.M. Kvasnicka, L. Heukamp, . . . G. Fingerle-Rowson, *Delayed development of chronic lymphocytic leukemia in the absence of macrophage migration inhibitory factor*. Blood, 2013. **121**(5): p. 812-21.
45. Gore, Y., D. Starlets, N. Maharshak, S. Becker-Herman, U. Kaneyuki, L. Leng, . . . I. Shachar, *Macrophage migration inhibitory factor induces B cell survival by activation of a CD74-CD44 receptor complex*. J Biol Chem, 2008. **283**(5): p. 2784-92.
46. Binsky, I., M. Haran, D. Starlets, Y. Gore, F. Lantner, N. Harpaz, . . . I. Shachar, *IL-8 secreted in a macrophage migration-inhibitory factor- and CD74-dependent manner regulates B cell chronic lymphocytic leukemia survival*. Proc Natl Acad Sci U S A, 2007. **104**(33): p. 13408-13.
47. Dreger, P., P. Corradini, E. Kimby, M. Michallet, D. Milligan, J. Schetelig, . . . E. Montserrat, *Indications for allogeneic stem cell transplantation in chronic lymphocytic leukemia: the EBMT transplant consensus*. Leukemia, 2007. **21**(1): p. 12-7.
48. Ghia, P. and M. Hallek, *Management of chronic lymphocytic leukemia*. Haematologica, 2014. **99**(6): p. 965-72.
49. Grever, M.R., D.M. Lucas, G.W. Dewald, D.S. Neuberg, J.C. Reed, S. Kitada, . . . J.C. Byrd, *Comprehensive assessment of genetic and molecular features predicting outcome in patients with chronic lymphocytic leukemia: results from the US Intergroup Phase III Trial E2997*. J Clin Oncol, 2007. **25**(7): p. 799-804.
50. Pettitt, A.R., R. Jackson, S. Carruthers, J. Dodd, S. Dodd, M. Oates, . . . P. Hillmen, *Alemtuzumab in combination with methylprednisolone is a highly effective induction regimen for patients with chronic lymphocytic leukemia and deletion of TP53: final results of the national cancer research institute CLL206 trial*. J Clin Oncol, 2012. **30**(14): p. 1647-55.
51. Advani, R.H., J.J. Buggy, J.P. Sharman, S.M. Smith, T.E. Boyd, B. Grant, . . . N.H. Fowler, *Bruton tyrosine kinase inhibitor ibrutinib (PCI-32765) has significant activity in patients with relapsed/refractory B-cell malignancies*. J Clin Oncol, 2013. **31**(1): p. 88-94.
52. Castillo, J.J., M. Furman, and E.S. Winer, *CAL-101: a phosphatidylinositol-3-kinase p110-delta inhibitor for the treatment of lymphoid malignancies*. Expert Opin Investig Drugs, 2012. **21**(1): p. 15-22.
53. Simonetti, G., M.T. Bertilaccio, P. Ghia, and U. Klein, *Mouse models in the study of chronic lymphocytic leukemia pathogenesis and therapy*. Blood, 2014. **124**(7): p. 1010-9.
54. Bichi, R., S.A. Shinton, E.S. Martin, A. Koval, G.A. Calin, R. Cesari, . . . C.M. Croce, *Human chronic lymphocytic leukemia modeled in mouse by targeted TCL1 expression*. Proc Natl Acad Sci U S A, 2002. **99**(10): p. 6955-60.
55. Planelles, L., C.E. Carvalho-Pinto, G. Hardenberg, S. Smaniotto, W. Savino, R. Gomez-Caro, . . . M. Hahne, *APRIL promotes B-1 cell-associated neoplasm*. Cancer Cell, 2004. **6**(4): p. 399-408.
56. Zapata, J.M., M. Krajewska, H.C. Morse, 3rd, Y. Choi, and J.C. Reed, *TNF receptor-associated factor (TRAF) domain and Bcl-2 cooperate to induce small B cell lymphoma/chronic lymphocytic leukemia in transgenic mice*. Proc Natl Acad Sci U S A, 2004. **101**(47): p. 16600-5.

57. Lin, Y., J. Ryan, J. Lewis, M.A. Wani, J.B. Lingrel, and Z.G. Liu, *TRAF2 exerts its antiapoptotic effect by regulating the expression of Kruppel-like factor LKLF*. Mol Cell Biol, 2003. **23**(16): p. 5849-56.
58. Klein, U., M. Lia, M. Crespo, R. Siegel, Q. Shen, T. Mo, . . . R. Dalla-Favera, *The DLEU2/miR-15a/16-1 cluster controls B cell proliferation and its deletion leads to chronic lymphocytic leukemia*. Cancer Cell, 2010. **17**(1): p. 28-40.
59. Herling, M., K.A. Patel, J. Khalili, E. Schlette, R. Kobayashi, L.J. Medeiros, and D. Jones, *TCL1 shows a regulated expression pattern in chronic lymphocytic leukemia that correlates with molecular subtypes and proliferative state*. Leukemia, 2006. **20**(2): p. 280-5.
60. Herling, M., K.A. Patel, M.A. Teitell, M. Konopleva, F. Ravandi, R. Kobayashi, and D. Jones, *High TCL1 expression and intact T-cell receptor signaling define a hyperproliferative subset of T-cell prolymphocytic leukemia*. Blood, 2008. **111**(1): p. 328-37.
61. Herling, M., K.A. Patel, E.D. Hsi, K.C. Chang, G.Z. Rassidakis, R. Ford, and D. Jones, *TCL1 in B-cell tumors retains its normal b-cell pattern of regulation and is a marker of differentiation stage*. Am J Surg Pathol, 2007. **31**(7): p. 1123-9.
62. Teitell, M.A., *The TCL1 family of oncoproteins: co-activators of transformation*. Nat Rev Cancer, 2005. **5**(8): p. 640-8.
63. Narducci, M.G., L. Virgilio, J.B. Engiles, A.M. Buchberg, L. Billips, A. Facchiano, . . . J.L. Rothstein, *The murine Tc11 oncogene: embryonic and lymphoid cell expression*. Oncogene, 1997. **15**(8): p. 919-26.
64. Yan, X.J., E. Albesiano, N. Zanasi, S. Yancopoulos, A. Sawyer, E. Romano, . . . N. Chiorazzi, *B cell receptors in TCL1 transgenic mice resemble those of aggressive, treatment-resistant human chronic lymphocytic leukemia*. Proc Natl Acad Sci U S A, 2006. **103**(31): p. 11713-8.
65. Pekarsky, Y., A. Koval, C. Hallas, R. Bichi, M. Tresini, S. Malstrom, . . . C.M. Croce, *Tc11 enhances Akt kinase activity and mediates its nuclear translocation*. Proc Natl Acad Sci U S A, 2000. **97**(7): p. 3028-33.
66. Suzuki, A., T. Kaisho, M. Ohishi, M. Tsukio-Yamaguchi, T. Tsubata, P.A. Koni, . . . T. Nakano, *Critical roles of Pten in B cell homeostasis and immunoglobulin class switch recombination*. J Exp Med, 2003. **197**(5): p. 657-67.
67. Ropars, V., G. Despouy, M.H. Stern, S. Benichou, C. Roumestand, and S.T. Arold, *The TCL1A oncoprotein interacts directly with the NF-kappaB inhibitor IkappaB*. PLoS ONE, 2009. **4**(8): p. 6567.
68. Pekarsky, Y., N. Zanasi, R.I. Aqeilan, and C.M. Croce, *Animal models for chronic lymphocytic leukemia*. J Cell Biochem, 2007. **100**(5): p. 1109-18.
69. Pekarsky, Y., A. Palamarchuk, V. Maximov, A. Efanov, N. Nazaryan, U. Santanam, . . . C.M. Croce, *Tc11 functions as a transcriptional regulator and is directly involved in the pathogenesis of CLL*. Proceedings of the National Academy of Sciences, 2008. **105**(50): p. 19643-19648.
70. Borghese, F.C., F. IL, *CD74: an emerging opportunity as a therapeutic target in cancer and autoimmune disease*. Expert Opin. Ther. Targets, 2011: p. 1472-8222.

71. Pyrz, M., B. Wang, M. Wabl, and F.S. Pedersen, *A retroviral mutagenesis screen identifies Cd74 as a common insertion site in murine B-lymphomas and reveals the existence of a novel IFN γ -inducible Cd74 isoform*. Mol Cancer, 2010. **9**: p. 86.
72. Warmerdam, P.A., E.O. Long, and P.A. Roche, *Isoforms of the invariant chain regulate transport of MHC class II molecules to antigen processing compartments*. J Cell Biol, 1996. **133**(2): p. 281-91.
73. Sanchez-Niño, M.D., A.B. Sanz, O. Ruiz-Andres, J. Poveda, M.C. Izquierdo, R. Selgas, . . . A. Ortiz, *MIF, CD74 and other partners in kidney disease: Tales of a promiscuous couple*. Cytokine & Growth Factor Reviews, 2013. **24**(1): p. 23-40.
74. Strubin, M., C. Berte, and B. Mach, *Alternative splicing and alternative initiation of translation explain the four forms of the Ia antigen-associated invariant chain*. EMBO J, 1986. **5**(13): p. 3483-8.
75. Koch, N., W. Lauer, J. Habicht, and B. Dobberstein, *Primary structure of the gene for the murine Ia antigen-associated invariant chains (Ii). An alternatively spliced exon encodes a cysteine-rich domain highly homologous to a repetitive sequence of thyroglobulin*. EMBO J, 1987. **6**(6): p. 1677-83.
76. Bikoff, E.K.H., L.; Episkopou, V.; van Meerwijk, J.; Germain, R.N. and Robertson, E.J., *Defective Major Histocompatibility Complex Class II Assembly, Transport, Peptide Acquisition, and CD4 + T Cell Selection in Mice Lacking Invariant Chain Expression*. The Journal of Experimental Medicine, 1993. **177**: p. 1699-1712.
77. Elliott, E.A.D., J.R.; Amigorena, S.; Elsemore, J.; Webster, P.; Mellman, I. and Flavell, R.A., *The Invariant Chain Is Required for Intracellular Transport and Function of Major Histocompatibility Complex Class II Molecules*. J. Exp. Med., 1994. **179**: p. 681-694.
78. Cresswell, P., *Assembly, transport, and function of MHC class II molecules*. Annu Rev Immunol, 1994. **12**: p. 259-93.
79. Stumptner-Cuvelette, P. and P. Benaroch, *Multiple roles of the invariant chain in MHC class II function*. Biochim Biophys Acta, 2002. **1542**(1-3): p. 1-13.
80. Peterson, M. and J. Miller, *Invariant chain influences the immunological recognition of MHC class II molecules*. Nature, 1990. **345**(6271): p. 172-4.
81. Layet, C. and R.N. Germain, *Invariant chain promotes egress of poorly expressed, haplotype-mismatched class II major histocompatibility complex A alpha A beta dimers from the endoplasmic reticulum/cis-Golgi compartment*. Proc Natl Acad Sci U S A, 1991. **88**(6): p. 2346-50.
82. Anderson, M.S. and J. Miller, *Invariant chain can function as a chaperone protein for class II major histocompatibility complex molecules*. Proc Natl Acad Sci U S A, 1992. **89**(6): p. 2282-6.
83. Hofmann, M.W., S. Honing, D. Rodionov, B. Dobberstein, K. von Figura, and O. Bakke, *The leucine-based sorting motifs in the cytoplasmic domain of the invariant chain are recognized by the clathrin adaptors AP1 and AP2 and their medium chains*. J Biol Chem, 1999. **274**(51): p. 36153-8.
84. Roche, P.A. and P. Cresswell, *Invariant chain association with HLA-DR molecules inhibits immunogenic peptide binding*. Nature, 1990. **345**(6276): p. 615-8.

85. Basha, G., K. Omilusik, A. Chavez-Steenbock, A.T. Reinicke, N. Lack, K.B. Choi, and W.A. Jefferies, *A CD74-dependent MHC class I endolysosomal cross-presentation pathway*. Nat Immunol, 2012. **13**(3): p. 237-245.
86. Wraight, C.J., P. van Endert, P. Moller, J. Lipp, N.R. Ling, I.C. MacLennan, . . . G. Moldenhauer, *Human major histocompatibility complex class II invariant chain is expressed on the cell surface*. J Biol Chem, 1990. **265**(10): p. 5787-92.
87. Fernandez, N. and A. Klididis, *Molecular profiles of the cell membrane bound and cytoplasmic forms of the human MHC class-II associated invariant polypeptides*. Electrophoresis, 1991. **12**(7-8): p. 523-6.
88. Arneson, L.S. and J. Miller, *The chondroitin sulfate form of invariant chain trimerizes with conventional invariant chain and these complexes are rapidly transported from the trans-Golgi network to the cell surface*. Biochem J, 2007. **406**(1): p. 97-103.
89. Roche, P.A., C.L. Teletski, E. Stang, O. Bakke, and E.O. Long, *Cell surface HLA-DR-invariant chain complexes are targeted to endosomes by rapid internalization*. Proceedings of the National Academy of Sciences, 1993. **90**(18): p. 8581-8585.
90. Wilson, K.M., M.O. Labeta, G. Pawelec, and N. Fernandez, *Cell-surface expression of human histocompatibility leucocyte antigen (HLA) class II-associated invariant chain (CD74) does not always correlate with cell-surface expression of HLA class II molecules*. Immunology, 1993. **79**: p. 331-335.
91. Henne, C., F. Schwenk, N. Koch, and P. Möller, *Surface expression of the invariant chain (CD74) is independent of concomitant expression of major histocompatibility complex class II antigens*. Immunology, 1994. **84**: p. 177-182.
92. Badve, S., C. Deshpande, Z. Hua, and L. Logdberg, *Expression of invariant chain (CD 74) and major histocompatibility complex (MHC) class II antigens in the human fetus*. J Histochem Cytochem, 2002. **50**(4): p. 473-82.
93. Momburg, F., N. Koch, P. Moller, G. Moldenhauer, G.W. Butcher, and G.J. Hammerling, *Differential expression of Ia and Ia-associated invariant chain in mouse tissues after in vivo treatment with IFN-gamma*. J Immunol, 1986. **136**(3): p. 940-8.
94. Leng, L., C.N. Metz, Y. Fang, J. Xu, S. Donnelly, J. Baugh, . . . R. Bucala, *MIF signal transduction initiated by binding to CD74*. J Exp Med, 2003. **197**(11): p. 1467-76.
95. Merk, M., S. Zierow, L. Leng, R. Das, X. Du, W. Schulte, . . . R. Bucala, *The D-dopachrome tautomerase (DDT) gene product is a cytokine and functional homolog of macrophage migration inhibitory factor (MIF)*. Proc Natl Acad Sci U S A, 2011. **108**(34): p. E577-85.
96. Beswick, E.J., D.A. Bland, G. Suarez, C.A. Barrera, X. Fan, and V.E. Reyes, *Helicobacter pylori binds to CD74 on gastric epithelial cells and stimulates interleukin-8 production*. Infect Immun, 2005. **73**(5): p. 2736-43.
97. Beswick, E.J., S. Das, I.V. Pinchuk, P. Adegboyega, G. Suarez, Y. Yamaoka, and V.E. Reyes, *Helicobacter pylori-induced IL-8 production by gastric epithelial cells up-regulates CD74 expression*. J Immunol, 2005. **175**(1): p. 171-6.
98. Beswick, E.J., I.V. Pinchuk, K. Minch, G. Suarez, J.C. Sierra, Y. Yamaoka, and V.E. Reyes, *The Helicobacter pylori urease B subunit binds to CD74 on gastric epithelial cells and induces NF-kappaB activation and interleukin-8 production*. Infect Immun, 2006. **74**(2): p. 1148-55.

99. Bland, D.A., G. Suarez, E.J. Beswick, J.C. Sierra, and V.E. Reyes, *H. pylori receptor MHC class II contributes to the dynamic gastric epithelial apoptotic response*. World J Gastroenterol, 2006. **12**(33): p. 5306-10.
100. Calandra, T. and T. Roger, *Macrophage migration inhibitory factor: a regulator of innate immunity*. Nat Rev Immunol, 2003. **3**(10): p. 791-800.
101. Bernhagen, J., R. Krohn, H. Lue, J.L. Gregory, A. Zernecke, R.R. Koenen, . . . C. Weber, *MIF is a noncognate ligand of CXC chemokine receptors in inflammatory and atherogenic cell recruitment*. Nat Med, 2007. **13**(5): p. 587-596.
102. Lue, H., M. Thiele, J. Franz, E. Dahl, S. Speckgens, L. Leng, . . . J. Bernhagen, *Macrophage migration inhibitory factor (MIF) promotes cell survival by activation of the Akt pathway and role for CSN5/JAB1 in the control of autocrine MIF activity*. Oncogene, 2007. **26**(35): p. 5046-59.
103. Mitchell, R.A., C.N. Metz, T. Peng, and R. Bucala, *Sustained Mitogen-activated Protein Kinase (MAPK) and Cytoplasmic Phospholipase A2 Activation by Macrophage Migration Inhibitory Factor (MIF)*. Journal of Biological Chemistry, 1999. **274**(25): p. 18100-18106.
104. Anderson, H.A.B., D.T.; Kawamura,T.; Blauvelt,A. and Roche,P.A., *Trafficking to Antigen-Processing Protein Kinase C Regulates MHC Class II Phosphorylation of the Invariant Chain by Compartments*. The Journal of Immunology, 1999. **163**: p. 5435-5443.
105. Shi, X., L. Leng, T. Wang, W. Wang, X. Du, J. Li, . . . R. Bucala, *CD44 is the signaling component of the macrophage migration inhibitory factor-CD74 receptor complex*. Immunity, 2006. **25**(4): p. 595-606.
106. Toole, B.P., *Hyaluronan-CD44 Interactions in Cancer: Paradoxes and Possibilities*. Clin Cancer Res, 2009. **15**(24): p. 7462-7468.
107. Becker-Herman, S., G. Arie, H. Medvedovsky, A. Kerem, and I. Shachar, *CD74 Is a Member of the Regulated Intramembrane Proteolysis-processed Protein Family*. Mol. Biol. Cell, 2005. **16**(11): p. 5061-5069.
108. Lipp, J. and B. Dobberstein, *The membrane-spanning segment of invariant chain (I gamma) contains a potentially cleavable signal sequence*. Cell, 1986. **46**(7): p. 1103-12.
109. Ehrmann, M. and T. Clausen, *Proteolysis as a regulatory mechanism*. Annu Rev Genet, 2004. **38**: p. 709-24.
110. Brown, M.S., J. Ye, R.B. Rawson, and J.L. Goldstein, *Regulated intramembrane proteolysis: a control mechanism conserved from bacteria to humans*. Cell, 2000. **100**(4): p. 391-8.
111. Starlets, D.G., Y.; Binsky,I.; Haran,M.; Harpaz,N.; Shvidel,L.; Becker-Herman,S.; Berrebi,A. and Shachar,I., *Cell-surface CD74 initiates a signaling cascade leading to cell proliferation and survival*. Blood, 2006. **107**(12): p. 4807-4816.
112. Becker-Herman, S., G. Arie, H. Medvedovsky, A. Kerem, and I. Shachar, *CD74 is a member of the regulated intramembrane proteolysis-processed protein family*. Mol Biol Cell, 2005. **16**(11): p. 5061-9.

113. Matza, D., O. Wolstein, R. Dikstein, and I. Shachar, *Invariant chain induces B cell maturation by activating a TAF(II)105-NF-kappaB-dependent transcription program*. J Biol Chem, 2001. **276**(29): p. 27203-6.
114. Vera, P.L., K.A. Iczkowski, X. Wang, and K.L. Meyer-Siegler, *Cyclophosphamide-induced cystitis increases bladder CXCR4 expression and CXCR4-macrophage migration inhibitory factor association*. PLoS ONE, 2008. **3**(12): p. e3898.
115. Moser, B. and P. Loetscher, *Lymphocyte traffic control by chemokines*. Nat Immunol, 2001. **2**(2): p. 123-8.
116. Schwartz, V., H. Lue, S. Kraemer, J. Korbiel, R. Krohn, K. Ohl, . . . J. Bernhagen, *A functional heteromeric MIF receptor formed by CD74 and CXCR4*. FEBS Letters, 2009. **583**(17): p. 2749-2757.
117. Viville, S., Neefjes, J., Lotteau, V., Dierich, A., Lemeur, M., Pioegh, H., Benoist, C. and Diane Mathis, *Mice Lacking the MHC Class II-Associated Invariant Chain*. Cell, 1993. **72**: p. 635-648.
118. Grusby, M.J., R.S. Johnson, V.E. Papaioannou, and L.H. Glimcher, *Depletion of CD4+ T cells in major histocompatibility complex class II-deficient mice*. Science, 1991. **253**(5026): p. 1417-20.
119. Faure-André, G.V., P.; Yuseff, M.; Heuzé, M.; Diaz, J.; Lankar, D.; Steri, V.; Manry, J.; Hugues, S.; Vascotto, F.; Boulanger, J.; Raposo, G.; Bono, M.; Roseblatt, M.; Piel, M.; Lennon-Duménil, A., *Regulation of Dendritic Cell Migration by CD74, the MHC Class II-Associated Invariant Chain*. Science, 2008. **322**(5908): p. 1705-1710.
120. Vascotto, F., D. Lankar, G. Faure-Andre, P. Vargas, J. Diaz, D. Le Roux, . . . A.M. Lennon-Dumenil, *The actin-based motor protein myosin II regulates MHC class II trafficking and BCR-driven antigen presentation*. J Cell Biol, 2007. **176**(7): p. 1007-19.
121. Shachar, I. and R.A. Flavell, *Requirement for Invariant Chain in B Cell Maturation and Function*. Science, 1996. **274**(5284): p. 106-8.
122. LeBien, T.W.a.T., T.F., *B lymphocytes: how they develop and function*. Blood, 2008. **112**: p. 1570-1580.
123. Benlagha, K., S. Park, R. Guinamard, C. Forestier, L. Karlsson, C. Chang, and A. Bendelac, *Mechanisms Governing B Cell Developmental Defects in Invariant Chain-Deficient Mice*. The Journal of Immunology, 2004. **172**: p. 2076-2083.
124. Beisner, D.R., P. Langerak, A.E. Parker, C. Dahlberg, F.J. Otero, S.E. Sutton, . . . M.P. Cooke, *The intramembrane protease Sppl2a is required for B cell and DC development and survival via cleavage of the invariant chain*. J Exp Med, 2012. **210**(1): p. 23-30.
125. Matza, D., F. Lantner, Y. Bogoch, L. Flaishon, R. Hershkovich, and I. Shachar, *Invariant chain induces B cell maturation in a process that is independent of its chaperonic activity*. Proc Natl Acad Sci U S A, 2002. **99**(5): p. 3018-23.
126. Lawrance, I.C., C. Fiocchi, and S. Chakravarti, *Ulcerative colitis and Crohn's disease: distinctive gene expression profiles and novel susceptibility candidate genes*. Hum Mol Genet, 2001. **10**(5): p. 445-56.
127. Miller, E.J., J. Li, L. Leng, C. McDonald, T. Atsumi, R. Bucala, and L.H. Young, *Macrophage migration inhibitory factor stimulates AMP-activated protein kinase in the ischaemic heart*. Nature, 2008. **451**(7178): p. 578-82.

128. Heinrichs, D., M. Knauel, C. Offermanns, M.L. Berres, A. Nellen, L. Leng, . . . H.E. Wasmuth, *Macrophage migration inhibitory factor (MIF) exerts antifibrotic effects in experimental liver fibrosis via CD74*. Proc Natl Acad Sci U S A, 2011. **108**(42): p. 17444-9.
129. Martin-Ventura, J.L., J. Madrigal-Matute, B. Munoz-Garcia, L.M. Blanco-Colio, M. Van Oostrom, G. Zalba, . . . J. Egido, *Increased CD74 expression in human atherosclerotic plaques: contribution to inflammatory responses in vascular cells*. Cardiovasc Res, 2009. **83**(3): p. 586-94.
130. Burton, J.D.S., R.; Ely,S.; Cardillo,T.M.; Reddy,P.K.; Gold,D.V. and Goldenberg,D.M., *CD74 Is Expressed by Multiple Myeloma and Is a Promising Target for Therapy*. Clinical Cancer Research, 2004. **10**: p. 6606-6011.
131. Young, A.N., M.B. Amin, C.S. Moreno, S.D. Lim, C. Cohen, J.A. Petros, . . . A.S. Neish, *Expression profiling of renal epithelial neoplasms: a method for tumor classification and discovery of diagnostic molecular markers*. Am J Pathol, 2001. **158**(5): p. 1639-51.
132. Cuthbert, R.J., J.M. Wilson, N. Scott, P.L. Coletta, and M.A. Hull, *Differential CD74 (major histocompatibility complex Class II invariant chain) expression in mouse and human intestinal adenomas*. Eur J Cancer, 2009. **45**(9): p. 1654-63.
133. Ioachim, H.L., S.E. Pambuccian, M. Hekimgil, F.R. Giancotti, and B.H. Dorsett, *Lymphoid monoclonal antibodies reactive with lung tumors. Diagnostic applications*. Am J Surg Pathol, 1996. **20**(1): p. 64-71.
134. Porter, D., J. Lahti-Domenici, A. Keshaviah, Y.K. Bae, P. Argani, J. Marks, . . . K. Polyak, *Molecular markers in ductal carcinoma in situ of the breast*. Mol Cancer Res, 2003. **1**(5): p. 362-75.
135. Beswick, E.J. and V.E. Reyes, *CD74 in antigen presentation, inflammation, and cancers of the gastrointestinal tract*. World J Gastroenterol, 2009. **15**(23): p. 2855-61.
136. Lue, H., A. Kapurniotu, G. Fingerle-Rowson, T. Roger, L. Leng, M. Thiele, . . . J. Bernhagen, *Rapid and transient activation of the ERK MAPK signalling pathway by macrophage migration inhibitory factor (MIF) and dependence on JAB1/CSN5 and Src kinase activity*. Cell Signal, 2006. **18**(5): p. 688-703.
137. Stein, R., Z. Qu, T.M. Cardillo, S. Chen, A. Rosario, I.D. Horak, . . . D.M. Goldenberg, *Antiproliferative activity of a humanized anti-CD74 monoclonal antibody, hLL1, on B-cell malignancies*. Blood, 2004. **104**(12): p. 3705-11.
138. Gordin, M., M. Tesio, S. Cohen, Y. Gore, F. Lantner, L. Leng, . . . I. Shachar, *c-Met and its ligand hepatocyte growth factor/scatter factor regulate mature B cell survival in a pathway induced by CD74*. J Immunol, 2010. **185**(4): p. 2020-31.
139. Lantner, F.S., D.; Gore,Y.; Flaishon,L.; Yamit-Hezi,A.; Dikstein,R; Leng,L.; Bucala,R.; Machluf,Y.; Oren,M. and Shachar,I., *CD74 induces TAp63 expression leading to B-cell survival*. Blood, 2007. **110**: p. 4303-4311.
140. Yang, A., M. Kaghad, Y. Wang, E. Gillett, M.D. Fleming, V. Dotsch, . . . F. McKeon, *p63, a p53 homolog at 3q27-29, encodes multiple products with transactivating, death-inducing, and dominant-negative activities*. Mol Cell, 1998. **2**(3): p. 305-16.

141. Yang, A., R. Schweitzer, D. Sun, M. Kaghad, N. Walker, R.T. Bronson, . . . F. McKeon, *p63 is essential for regenerative proliferation in limb, craniofacial and epithelial development*. Nature, 1999. **398**(6729): p. 714-8.
142. Shachar, I. and M. Haran, *The secret second life of an innocent chaperone: the story of CD74 and B cell/chronic lymphocytic leukemia cell survival*. Leuk Lymphoma, 2011. **52**(8): p. 1446-54.
143. Harada, A., N. Sekido, T. Akahoshi, T. Wada, N. Mukaida, and K. Matsushima, *Essential involvement of interleukin-8 (IL-8) in acute inflammation*. J Leukoc Biol, 1994. **56**(5): p. 559-64.
144. Koch, A.E., P.J. Polverini, S.L. Kunkel, L.A. Harlow, L.A. DiPietro, V.M. Elner, . . . R.M. Strieter, *Interleukin-8 as a macrophage-derived mediator of angiogenesis*. Science, 1992. **258**(5089): p. 1798-801.
145. Smyth, M.J., C.O. Zachariae, Y. Norihisa, J.R. Ortaldo, A. Hishinuma, and K. Matsushima, *IL-8 gene expression and production in human peripheral blood lymphocyte subsets*. J Immunol, 1991. **146**(11): p. 3815-23.
146. Brat, D.J., A.C. Bellail, and E.G. Van Meir, *The role of interleukin-8 and its receptors in gliomagenesis and tumoral angiogenesis*. Neuro Oncol, 2005. **7**(2): p. 122-33.
147. Wierda, W.G., M.M. Johnson, K.A. Do, T. Manshouri, A. Dey, S. O'Brien, . . . M. Albitar, *Plasma interleukin 8 level predicts for survival in chronic lymphocytic leukaemia*. Br J Haematol, 2003. **120**(3): p. 452-6.
148. Sapozhnikov, A., Y. Pewzner-Jung, V. Kalchenko, R. Krauthgamer, I. Shachar, and S. Jung, *Perivascular clusters of dendritic cells provide critical survival signals to B cells in bone marrow niches*. Nat Immunol, 2008. **9**(4): p. 388-95.
149. Chappell, C.P. and E.A. Clark, *Survival niches: B cells get MIFed as well as BAFFled by dendritic cells*. Immunol Cell Biol, 2008. **86**(6): p. 487-8.
150. Binsky, I., F. Lantner, V. Grabovsky, N. Harpaz, L. Shvidel, A. Berrebi, . . . I. Shachar, *TAp63 regulates VLA-4 expression and chronic lymphocytic leukemia cell migration to the bone marrow in a CD74-dependent manner*. J Immunol, 2010. **184**(9): p. 4761-9.
151. Gattei, V., P. Bulian, M.I. Del Principe, A. Zucchetto, L. Maurillo, F. Buccisano, . . . G. Del Poeta, *Relevance of CD49d protein expression as overall survival and progressive disease prognosticator in chronic lymphocytic leukemia*. Blood, 2008. **111**(2): p. 865-73.
152. Fedorchenko, O., M. Stiefelhagen, A.A. Peer Zada, R. Barthel, P. Mayer, L. Ecker, . . . M. Herling, *CD44 regulates the apoptotic response and promotes disease development in chronic lymphocytic leukemia*. Blood, 2013. **121**(20): p. 4126-36.
153. Ochakovskaya, R.O., L.; Goldenberg,D.M. and Mattes,M.J., *Therapy of Disseminated B-Cell Lymphoma Xenografts in Severe Combined Immunodeficient Mice with an Anti-CD74 Antibody Conjugated with 111Indium, 67Gallium, or 90Yttrium*. Clinical Cancer Research, 2001. **7**: p. 1505-1510.
154. Griffiths, G.L.S., R.; Horak,I.D.; Mattes,M.J.; Govindan,S.V.; Hansen,H.J. and Goldenberg,D.M., *Cure of SCID Mice Bearing Human B-Lymphoma Xenografts by an Anti-CD74 Antibody-Anthracycline Drug Conjugate*. Clin Cancer Res, 2003. **9**: p. 6567-6571.

155. Stein, R., M.J. Mattes, T.M. Cardillo, H.J. Hansen, C.H. Chang, J. Burton, . . . D.M. Goldenberg, *CD74: a new candidate target for the immunotherapy of B-cell neoplasms*. Clin Cancer Res, 2007. **13**(18 Pt 2): p. 5556s-5563s.
156. Lundberg, B.B., G. Griffiths, and H.J. Hansen, *Cellular association and cytotoxicity of doxorubicin-loaded immunoliposomes targeted via Fab' fragments of an anti-CD74 antibody*. Drug Deliv, 2007. **14**(3): p. 171-5.
157. Michel, R.B., A.V. Rosario, P.M. Andrews, D.M. Goldenberg, and M.J. Mattes, *Therapy of small subcutaneous B-lymphoma xenografts with antibodies conjugated to radionuclides emitting low-energy electrons*. Clin Cancer Res, 2005. **11**(2 Pt 1): p. 777-86.
158. Burger, J.A., P. Ghia, A. Rosenwald, and F. Caligaris-Cappio, *The microenvironment in mature B-cell malignancies: a target for new treatment strategies*. Blood, 2009. **114**(16): p. 3367-75.
159. Deaglio, S. and F. Malavasi, *Chronic lymphocytic leukemia microenvironment: shifting the balance from apoptosis to proliferation*. Haematologica, 2009. **94**(6): p. 752-6.
160. Maehr, R., M. Kraus, and H.L. Ploegh, *Mice deficient in invariant-chain and MHC class II exhibit a normal mature B2 cell compartment*. Eur J Immunol, 2004. **34**(8): p. 2230-6.
161. Arnaout, M.A., *Structure and function of the leukocyte adhesion molecules CD11/CD18*. Blood, 1990. **75**(5): p. 1037-50.
162. Shortman, K. and Y.J. Liu, *Mouse and human dendritic cell subtypes*. Nat Rev Immunol, 2002. **2**(3): p. 151-61.
163. Fleming, T.J., M.L. Fleming, and T.R. Malek, *Selective expression of Ly-6G on myeloid lineage cells in mouse bone marrow. RB6-8C5 mAb to granulocyte-differentiation antigen (Gr-1) detects members of the Ly-6 family*. The Journal of Immunology, 1993. **151**(5): p. 2399-408.
164. Fernandes-Alnemri, T., G. Litwack, and E.S. Alnemri, *CPP32, a novel human apoptotic protein with homology to Caenorhabditis elegans cell death protein Ced-3 and mammalian interleukin-1 beta-converting enzyme*. J Biol Chem, 1994. **269**(49): p. 30761-4.
165. Keating, M.J., H. Kantarjian, M. Talpaz, J. Redman, C. Koller, B. Barlogie, . . . K.B. McCredie, *Fludarabine: a new agent with major activity against chronic lymphocytic leukemia*. Blood, 1989. **74**(1): p. 19-25.
166. Elter, T., M. Hallek, and A. Engert, *Fludarabine in chronic lymphocytic leukaemia*. Expert Opinion on Pharmacotherapy, 2006. **7**(12): p. 1641-1651.
167. Galmarini, C.M., J.R. Mackey, and C. Dumontet, *Nucleoside analogues and nucleobases in cancer treatment*. Lancet Oncol, 2002. **3**(7): p. 415-24.
168. Plunkett, W. and P.P. Saunders, *Metabolism and action of purine nucleoside analogs*. Pharmacol Ther, 1991. **49**(3): p. 239-68.
169. Rothausler, K. and N. Baumgarth, *Assessment of cell proliferation by 5-bromodeoxyuridine (BrdU) labeling for multicolor flow cytometry*. Curr Protoc Cytom, 2007. **Chapter 7**: p. Unit7 31.

170. Gerdes, J., U. Schwab, H. Lemke, and H. Stein, *Production of a mouse monoclonal antibody reactive with a human nuclear antigen associated with cell proliferation*. *Int J Cancer*, 1983. **31**(1): p. 13-20.
171. Hofbauer, J.P., C. Heyder, U. Denk, T. Kocher, C. Holler, D. Trapin, . . . A. Egle, *Development of CLL in the TCL1 transgenic mouse model is associated with severe skewing of the T-cell compartment homologous to human CLL*. *Leukemia*, 2011. **25**(9): p. 1452-8.
172. Oppezzo, P. and G. Dighiero, *"Role of the B-cell receptor and the microenvironment in chronic lymphocytic leukemia"*. *Blood Cancer J*, 2013. **3**: p. e149.
173. Schwartz, V., A. Kruttgen, J. Weis, C. Weber, T. Ostendorf, H. Lue, and J. Bernhagen, *Role for CD74 and CXCR4 in clathrin-dependent endocytosis of the cytokine MIF*. *Eur J Cell Biol*, 2011. **91**(6-7): p. 435-49.
174. Burger, J.A., M. Burger, and T.J. Kipps, *Chronic Lymphocytic Leukemia B Cells Express Functional CXCR4 Chemokine Receptors That Mediate Spontaneous Migration Beneath Bone Marrow Stromal Cells*. *Blood*, 1999. **94**(11): p. 3658-3667.
175. Hamblin, T.J., *The TCL1 mouse as a model for chronic lymphocytic leukemia*. *Leuk Res*, 2010. **34**(2): p. 135-6.
176. Onodera, S., J. Nishihira, Y. Koyama, T. Majima, Y. Aoki, H. Ichiyama, . . . A. Minami, *Macrophage migration inhibitory factor up-regulates the expression of interleukin-8 messenger RNA in synovial fibroblasts of rheumatoid arthritis patients: common transcriptional regulatory mechanism between interleukin-8 and interleukin-1beta*. *Arthritis Rheum*, 2004. **50**(5): p. 1437-47.
177. Klasen, C., K. Ohl, M. Sternkopf, I. Shachar, C. Schmitz, N. Heussen, . . . O. El Bounkari, *MIF promotes B cell chemotaxis through the receptors CXCR4 and CD74 and ZAP-70 signaling*. *J Immunol*, 2014. **192**(11): p. 5273-84.
178. Fricker, S.P., V. Anastassov, J. Cox, M.C. Darkes, O. Grujic, S.R. Idzan, . . . R.S. Wong, *Characterization of the molecular pharmacology of AMD3100: a specific antagonist of the G-protein coupled chemokine receptor, CXCR4*. *Biochem Pharmacol*, 2006. **72**(5): p. 588-96.
179. Catusse, J., A. Liotard, B. Loillier, D. Pruneau, and J.L. Paquet, *Characterization of the molecular interactions of interleukin-8 (CXCL8), growth related oncogen alpha (CXCL1) and a non-peptide antagonist (SB 225002) with the human CXCR2*. *Biochem Pharmacol*, 2003. **65**(5): p. 813-21.
180. Zheng, Z., S. Katoh, Q. He, K. Oritani, K. Miyake, J. Lesley, . . . P.W. Kincade, *Monoclonal antibodies to CD44 and their influence on hyaluronan recognition*. *J Cell Biol*, 1995. **130**(2): p. 485-95.
181. Weiss, J.M., J. Sleeman, A.C. Renkl, H. Dittmar, C.C. Termeer, S. Taxis, . . . J.C. Simon, *An essential role for CD44 variant isoforms in epidermal Langerhans cell and blood dendritic cell function*. *J Cell Biol*, 1997. **137**(5): p. 1137-47.
182. Zanesi, N., V. Balatti, J. Riordan, A. Burch, L. Rizzotto, A. Palamarchuk, . . . Y. Pekarsky, *A Sleeping Beauty screen reveals NF-kB activation in CLL mouse model*. *Blood*, 2013. **121**(21): p. 4355-8.

183. Dilillo, D.J., J.B. Weinberg, A. Yoshizaki, M. Horikawa, J.M. Bryant, Y. Iwata, . . . T.F. Tedder, *Chronic lymphocytic leukemia and regulatory B cells share IL-10 competence and immunosuppressive function*. *Leukemia*, 2013. **27**(1): p. 170-82.
184. Bradford, M.M., *A rapid and sensitive method for the quantitation of microgram quantities of protein utilizing the principle of protein-dye binding*. *Anal Biochem*, 1976. **72**: p. 248-54.

Abbreviations

%	percent	ECL	enhanced chemiluminescent
°C	degree Celsius		
μ	micro	ECM	extracellular matrix
7-AAD	7-Amino-Actinomycin	EDTA	ethylenediaminetetraacetic acid
A	Ampere	e.g.	<i>exempli gratia</i> ; for example
ACK	Ammoniumchlorid-Kaliumchlorid	EM	extracellular matrix
Ab	Antibody	ER	endoplasmic reticulum
AKT	protein kinase B	ERK 1/2	extracellular signal-regulated kinase 1 and 2
APC	adenomatous polyposis coli	<i>et al.</i>	<i>et alii</i> ; and others
ATM	Ataxia telangiectasia mutated kinase	FACS	fluorescence activated cell sorting
BAD	BCL-2-associated death promoter homologue	Fc region	crystallisable fragment
Bcl2	B-cell lymphoma 2	FCS	fetal calf serum
BclXL	B-cell lymphoma extra large	Fig.	Figure
BCR	B cell receptor	FISH	fluorescent <i>in situ</i> hybridization
bp	Basepair	FITC	Fluorescein isothiocyanate
BM	bone marrow	FSC	forward scatter
BrdU	Bromodeoxyuridine	g	gram
BSA	bovine serum albumin	GSK3β	glycogen synthase kinase β
c	concentration	h	hour(s)
CaCl ₂	calcium chloride	HCl	hydrogen chloride
CD	cluster of differentiation	HEPES	4-(2-hydroxyethyl)-1-piperazineethanesulfonic acid
cDNA	complementary DNA		
CLL	chronic lymphocytic leukemia	HLA	human leukocyte antigen
CO ₂	carbon dioxide	HRP	horse radish peroxidase
Da	Dalton	Ig	immunoglobulin
DABCO	1,4-diazabicyclo [2.2.2]octane, triethylenediamine	I _G V _H	immunoglobulin heavy chain
ddH ₂ O	double distilled water	IHC	Immunohistochemistry
DMSO	dimethyl sulfoxid	IL	interleukin
DNA	deoxyribonucleic acid	i.p.	intraperitoneal
dNTP	deoxyribonucleotide triphosphate (dATP, dCTP, dTTP, dGTP)	kg	kilogram
		l	liter
		mm	millimeter
		M	molar (mol/liter)

mAb	monoclonal antibody	rpm	revolutions per minute
MAPK	mitogen activated protein kinase	RPMI	Roswell Park Memorial Park
MBL	monoclonal B-cell lymphocytosis	RNA	ribonucleic acid
MCL	mantel cell lymphoma	RT	room temperature
MHC	major histocompatibility complex	RTKs	receptor tyrosine kinases
MIF	macrophage migration inhibitory factor	RT-PCR	reverse transcription-PCR
		RTQ-PCR	real time quantitative-PCR
		SDS	sodium dodecyl sulphate
min	minute(s)	sec	second(s)
MM	multiple myeloma	SEM	standard error of the mean
MZ B cells	marginal zone B cells	SLL	small lymphocytic leukemia
n	nano		
n	number	Sppl2a	Signal peptide peptidase-like 2a
NaCl	sodium chloride	T1 B cells	transitional stage 1 B cells
NaN3	sodium azide	T2 B cells	transitional stage 2 B cells
NaOH	sodium hydroxide	TAE	Tris-acetate-EDTA-buffer
NF- κ B	nuclear factor 'kappa-light-chain-enhancer' of activated B-cells	TAMs	tumor associated macrophages
NP-40	Nonidet™ P-40 (octyl phenoxy polyethoxyle thanol)	<i>Taq</i>	<i>Thermus aquaticus</i>
p53	proapoptotic protein 53	TBS	Tris buffered saline
pAb	polyclonal antibody	TCL1	T cell leukemia-1
PAGE	Polyacrylamide gel electrophoresis	TEME	Tetramethyl-ethylenediamine
pAKT	phosphorylated AKT	tg/wt	heterozygote transgenic
PB	peripheral blood	Tris	tris(hydroxymethyl) aminomethane
PBMC	peripheral blood mononuclear cells	Tween-20	Polysorbate 20
PBS	phosphate buffered saline	U	unit
PCR	polymerase chain reaction	UV	ultraviolet
PE	Phycoerythrin	V	Volt
pH	negative logarithm of the hydrogen ion concentration	V _H / V _L	variable region of the heavy (H) and light (L) Ig-chain
Pi3K	phosphatidyl inositole -3 kinase	v/v	volume/volume
PLC	phospho lipase C	w/v	weight/volume
rMIF	recombinant MIF	wt/wt	homozygote wildtyp
		ZAP-70	zeta associated protein kinase 70
		σ	standard deviation

List of Figures

Figure 1: Study of novel pathogenic mechanisms in the E μ - <i>TCL1</i> -transgenic mouse model	8
Figure 2: CD74 structure.....	10
Figure 3: CD74- dependent MIF signaling	12
Figure 4: CD74 expression in splenic B cells from wild type and <i>TCL1</i> ⁺ mice	18
Figure 5: Flow cytometric analyses of CD74 expression in malignant B cells from murine blood samples.....	19
Figure 6: Breeding strategy for <i>TCL1</i> ⁺ with <i>CD74</i> ^{ko} mice	20
Figure 7: Genotyping PCR for CD74 status.....	21
Figure 8: White blood cell count in <i>TCL1</i> ⁺ <i>CD74</i> ^{wt} and <i>TCL1</i> ⁺ <i>CD74</i> ^{ko} mice	22
Figure 9: Absolute numbers of CD5-expressing B cells in <i>TCL1</i> ⁺ <i>CD74</i> ^{wt} and <i>TCL1</i> ⁺ <i>CD74</i> ^{ko} mice.....	23
Figure 10: Hepatosplenomegaly in <i>TCL1</i> ⁺ <i>CD74</i> ^{wt} and <i>TCL1</i> ⁺ <i>CD74</i> ^{ko} mice.....	24
Figure 11: Flow cytometric analyses of myeloid cells in the spleen of <i>TCL1</i> ⁺ <i>CD74</i> ^{ko} mice.....	26
Figure 12: Macrophages in the spleen of <i>TCL1</i> ⁺ <i>CD74</i> ^{ko} mice.....	27
Figure 13: Apoptosis rate in the spleens of <i>TCL1</i> ⁺ <i>CD74</i> ^{wt} and <i>TCL1</i> ⁺ <i>CD74</i> ^{ko} mice.....	28
Figure 14: In vitro apoptosis analyses of leukemic mice	29
Figure 15: Proliferation capacity of lymphocytes from <i>TCL1</i> ⁺ <i>CD74</i> ^{wt} and <i>TCL1</i> ⁺ <i>CD74</i> ^{ko} mice	30
Figure 16: Proliferation in the spleen of <i>TCL1</i> ⁺ <i>CD74</i> ^{wt} and <i>TCL1</i> ⁺ <i>CD74</i> ^{ko} mice	31
Figure 17: Overall survival of <i>TCL1</i> ⁺ <i>CD74</i> ^{ko} mice	32
Figure 18: Syngeneic transplantation of malignant <i>TCL1</i> ⁺ B cells.....	33
Figure 19: Activation of pro-survival pathways in unstimulated murine CLL cells.....	34
Figure 20: Activation of pro-survival pathways upon MIF stimulation.....	35
Figure 21: Activation of pro-survival pathways upon MIF stimulation in human CLL	36
Figure 22: Activation of pro-survival pathways upon CD74 antibody stimulation	37
Figure 23: Surface CD44 expression on B cells from pre- and leukemic <i>TCL1</i> ⁺ mice	38
Figure 24: Surface CXCR4 expression on B cells from murine blood samples	39
Figure 25: rMIF stimulation under CXCR2 and CXCR4 or CD44 inhibition.....	40
Figure 26: Densitometrical analyses of rMIF stimulation under CXCR2 and CXCR4 or CD44 inhibition	41
Figure 27: Flow cytometric analyses of B cell maturation in the spleen	42
Figure 28: B cell development in young and old <i>TCL1</i> ⁺ <i>CD74</i> ^{ko} mice.....	43

Danksagung

Mein besonderer Dank gilt Prof. Hallek für die Möglichkeit dieses interessante Thema in seinem Institut zu erforschen. Auch möchte ich mich für die Hilfestellungen und vielen interessanten Diskussionen während der gesamten Zeit bedanken.

Prof. Wunderlich danke ich für die Bereitschaft meine Doktorarbeit extern zu betreuen und diese so zu ermöglichen. Meinen Tutoren Prof. Wunderlich und Prof. Büning möchte ich für die jährlichen Treffen und anregenden Diskussionen danken. Vielen Dank auch an Prof. Hoppe für die Übernahme des Zweitgutachtens und Prof. Kloppenburg für die Übernahme des Vorsitzes.

Dr. Fingerle-Rowson möchte ich für die Überlassung des Themas und die freundliche und kompetente Betreuung in den ersten Jahren danken.

Ein großer Dank gilt meiner Arbeitsgruppe, Hien, Natascha, Oleg und Nina, für die gute Arbeitsatmosphäre und die seelische und wissenschaftliche Unterstützung während der ganzen Zeit. Oleg und Nina danke ich für die stets offene Tür und Hilfe in allen Arbeitsphasen. Natascha danke ich für die stetige Versorgung mit Nervennahrung und der Unterstützung bei den Versuchen. Bei Hien möchte ich mich für ihr immer offenes Ohr und ihren Beistand bedanken.

Edward O'Brien und Martin Roth und dem restlichen Team danke ich für die Versorgung der Tiere.

Bei den Kollegen aus dem LFI und den „neuen“ Kollegen im CECAD-Gebäude möchte ich mich für die nette Arbeitsatmosphäre, die wissenschaftlichen Hilfestellung und vor allem für die lustigen Stunden bei Ausflügen, Weihnachtsfeiern und netten Mittagspausen bedanken.

Meinen Eltern möchte ich herzlich für Ihre Unterstützung und ihren Glauben an mich danken. Vielen Dank für eure Hilfen in allen Lebenslagen!

Tobias, ich danke dir für deine Unterstützung und Geduld. Besonderer Dank auch dafür, dass du mich immer wieder mit deinen leckeren Kochkünsten verwöhnt hast.

Ein großer Dank geht auch an meine „große“ Schwester Franziska, die mich mit ihren Erfahrungen und Optimismus immer wieder aufgebaut hat. Vielen Dank Franzi, ich könnte mir keine bessere Schwester vorstellen!

Erklärung

Ich versichere, dass ich die von mir vorgelegte Dissertation selbständig angefertigt, die benutzten Quellen und Hilfsmittel vollständig angegeben und die Stellen der Arbeit – einschließlich Tabellen, Karten und Abbildungen –, die anderen Werken im Wortlaut oder dem Sinn nach entnommen sind, in jedem Einzelfall als Entlehnung kenntlich gemacht habe; dass diese Dissertation noch keiner anderen Fakultät oder Universität zur Prüfung vorgelegen hat; dass sie – abgesehen von unten angegebenen Teilpublikationen – noch nicht veröffentlicht worden ist, sowie, dass ich eine solche Veröffentlichung vor Abschluss des Promotionsverfahrens nicht vornehmen werde. Die Bestimmungen der Promotionsordnung sind mir bekannt. Die von mir vorgelegte Dissertation ist von Herrn Prof. Dr. med. Michael Hallek betreut worden.

Köln, den